U.PORTO
FEUP FACULDADE DE ENGENHARIA
UNIVERSIDADE DO PORTO

MULTI-SENSOR DIGITAL SURVEYING FOR OPEN-SOURCE SCAN-TO-BIM

JUAN JOSÉ GAVILANES BOWEN

Dissertação submetida para satisfação parcial dos requisitos do grau de

MESTRE EM PROJETO INTEGRADO NA CONSTRUÇÃO DE EDIFÍCIOS

Orientador: Professor Doutor João Pedro Da Silva Poças Martins

JULHO DE 2025

Mestrado em Projeto Integrado na Construção de Edifícios 2024/2025

Departamento de Engenharia Civil e Georrecursos

Tel. +351-22-508 1901

✉ mprince@fe.up.pt

Editado por

Faculdade de Engenharia da Universidade do Porto

Rua Dr. Roberto Frias

4200-465 PORTO

Portugal

Tel. +351-22-508 1400

✉ feup@fe.up.pt

http://www.fe.up.pt

A mis Padres

A possibilidade de realizarmos um sonho é o que torna a vida interessante.

Paulo Coelho

Acknowledgments

To my advisors, Professor Dr. João Poças Martins, and engineer Diogo Parracho, for their time and guidance, for sharing their expertise throughout the different developmental stages of this dissertation, and for leading the flight operations.

To my classmates, who worked alongside me during the last two years, particularly to Ludmila De Leo, for her quick and helpful responses to my various doubts.

To the Department of Civil and Georesources Engineering, for facilitating the access to the UAV employed in this research.

To FEUP's Technical Services for Maintenance and Environment team, for granting me authorized and rapid access to the faculty's facilities and permitting me to carry out the multiple surveys.

To the Johnson Family, for taking me in and providing the hardware support needed to carry out this study, as well as their hospitality and patience.

To my parents, Francisco Gavilanes and Lorena Bowen, and my brother Francisco Xavier Gavilanes: although we have not been able to be together as much as we wanted, their support and motivation were never absent, always showing me the right path to follow and whose love and support I can always count on.

Resumo

A utilização de programas de código aberto (open-source), no contexto da engenharia civil, pode facilmente fomentar a inovação e acessibilidade no setor, ao disponibilizar ferramentas economicamente viáveis de desenho e análise, graças à sua natureza acessível. Por outro lado, Scan-to-BIM refere-se ao processo de usar dados capturados com tecnologias de digitalização 3D, para criar modelos BIM (Building Information Models) detalhados e precisos, facilitando tarefas como renovação, manutenção, e gestão de ativos ao longo do ciclo de vida de uma infraestrutura. Atualmente, a literatura existente sobre Scan-to-BIM realça avanços significativos na integração de várias tecnologias de deteção para melhorar a documentação dos edifícios. Não obstante, muitos estudos focam-se em soluções de software proprietários, os quais restringem seu acesso e escalabilidade a projetos menores. Para abordar este problema, este trabalho tem como objetivo desenvolver una metodologia open-source Scan-to-BIM, baseada em levantamentos com diversos tipos de sensor.

Com este propósito, este estudo utiliza o software open-source Blender, aliado ao add-on Bonsai, para criar um modelo BIM a partir de dados recolhidos por vários levantamentos aéreos e manuais realizados na Faculdade de Engenharia da Universidade do Porto (FEUP). Estes levantamentos integram em simultâneo três das maiores tecnologias de deteção para conseguir captar dados do exterior e do interior de um edifício: fotogrametria e termografia com recurso a uma aeronave não tripulada (UAV), e um equipamento iOS com tecnologia LiDAR. Os resultados da fotogrametria e do LiDAR são processados e otimizados para depois ser alinhados e usados como guia para a modelação Open-BIM (BIM em formato aberto). Por sua vez, as imagens captadas pela camara térmica são usadas como uma textura que é projetada no modelo Open-BIM, seguindo assim uma metodologia Image-to-BIM, de forma a possibilitar uma análise térmica.

As principais conclusões deste estudo provam que uma metodologia open-source Scan-to-BIM é completamente conseguível. Isto significa que entidades como instituições de ensino, pequenas empresas, entusiastas e projetos com recursos limitados podem ter acesso a documentação 3D de alta qualidade e capacidades de diagnóstico. Além disso, ao alinhar os diferentes conjuntos de dados dos levantamentos com múltiplos sensores, a fotogrametria demonstrou uma precisão de nível milimétrico em relação ao edifício real. No caso do LiDAR, pouca ou nenhuma necessidade de ajuste de escala foi necessária para que os dados pudessem ser alinhados, indicando que a integração de dados de diversas fontes dentro da metodologia é confiável e é capaz de produzir modelos 3D coerentes e espacialmente precisos. Por fim, durante a integração BIM, o software open-source Blender, com o add-on Bonsai, demonstrou ser uma plataforma completa e versátil, capaz de gerir processos Scan-to-BIM complexos de forma eficiente, mostrando que as ferramentas open-source podem efetivamente suportar tarefas BIM avançadas, oferecendo uma alternativa pratica e económica às soluções de software proprietárias.

PALAVRAS-CHAVE: Open-source Scan-to-BIM, UAVs, Fotogrametria, LiDAR, Termografia.

Abstract

Open-source software, within the civil engineering field, can easily foster innovation and accessibility by providing cost-effective tools for design and analysis, because of its accessible nature. Meanwhile Scan-to-BIM refers to the process of using captured data from 3D scanning technologies, to create accurate, detailed as-built Building Information Models (BIM), facilitating tasks such as renovation, maintenance, and management throughout the infrastructure lifecycle. Currently, the existing literature on Scan-to-BIM highlights significant advances in integrating various sensing technologies to improve building documentation. Nevertheless, a lot of research focuses on proprietary software solutions, which restricts smaller projects' access and scalability. To address this problem, this study aims to develop an open-source Scan-to-BIM workflow, based on multi-sensor surveying.

For this purpose, the study employs the open-source software Blender, paired with the Bonsai add-on, to create a BIM model from the data gathered by various aerial and hand-held surveys taking place at the Faculty of Engineering of the University of Porto (FEUP). At the same time, these surveys are used to integrate three major spatial sensing technologies to capture exterior and interior data: Unmanned Aerial Vehicle (UAV) based photogrammetry and thermography, and an iOS device equipped with Light Detection and Ranging (LiDAR). The photogrammetry and LiDAR results are processed and optimized to then be aligned and used as a guide for Open-BIM (open-source BIM) modelling. Meanwhile, the images gathered from the thermal camera are used as a texture that is projected on top of the Open-BIM model, following an Image-to-BIM workflow, allowing for comprehensive thermal data analysis.

The main findings of the study prove that an affordable open-source Scan-to-BIM workflow is fully achievable. That means that entities such as educational institutions, small businesses, enthusiasts and projects with limited resources, can have access to high-quality 3D documentation and diagnostic capabilities. Additionally, when aligning the different datasets from the multi-sensor surveys, the photogrammetry demonstrated millimetric-level accuracy relative to the real building, and with LiDAR's case, little to no requirement for scale adjustment was needed to match and align them, indicating that the integration of diverse data sources within the workflow is reliable and produces coherent, spatially accurate 3D models. Finally, during the BIM data integration, the open-source software Blender, with the Bonsai add-on, established itself as a complete and versatile platform capable of managing complex Scan-to-BIM processes efficiently, demonstrating that open-source tools can effectively support advanced BIM tasks, offering a practical and cost-effective alternative to proprietary software solutions.

KEYWORDS: Open-source Scan-to-BIM, UAV, Photogrammetry, LiDAR scanning, Thermal imaging

TABLE OF CONTENTS

LIST OF FIGURES

List of Tables

Symbols, Acronyms, and Abbreviations

AAN – Autoridade Aeronáutica Nacional

AEC – Architectural, Engineering, and Construction

AECO – Architecture, Engineering, Construction, and Operations

AGA – Aktiebolaget Gas Accumulator

ANAC – Autoridade Nacional da Aviação Civil

API – Application Programming Interface

AR – Augmented Reality

BA – Bundle Adjustment

BEM – Building Energy Models

BIM – Building Information Modeling

BLS – Backpack Laser Scanning

CC – ContextCapture

CE – Conformité Européenne

CIA – Central Intelligence Agency

CMOS – Complementary Metal-Oxide-Semiconductor

CNN – Convolutional Neural Networks

COTS – Commercial Off-the-Shelf

CV – Computer Vision

CW – Continuous Wave

DECG – Departamento de Engenharia Civil e Georrecursos

DFSG – Debian Free Software Guidelines

EASA – European Union Aviation Safety Agency

EU – European Union

FAA – Federal Aviation Administration

FBX – Filmbox

FEUP – Faculty of Engineering of the University of Porto

FFC – Flat Field Correction

FLIR – Forward-Looking Infrared

FOV – Field of View

FPAs – Focal Plane Arrays

GB – Gigabyte

GCPs – Ground Control Points

GHz – Gigahertz

GIS – Geographic Information Systems

GNSS – Global Navigation Satellite System

GPL – General Public License

GPS – Global Positioning System

GZ – Geographical Zone

HBIM – Heritage Building Information Modeling

HFOV – Horizontal Field of View

HVAC – Heating, Ventilation, and Air Conditioning

ICP – Iterative Closest Point

IFC – Industry Foundation Classes

IMU – Inertial Measurement Unit

iOS – iPhone Operating System

IR – Infrared

IRT – Infrared Thermal

JRC – Joint Research Centre

LCD – Liquid Crystal Display

LEDs – Light Emitting Diodes

LiDAR – Light Detection and Ranging

LOD – Level of Detail

LWIR – Long-Wave Infrared

M2E – Mavic 2 Enterprise

MEMS – Micro-Electro-Mechanical Systems

MLS – Mobile Laser Scanning

MM – MicMac

MP – Megapixel

MTOM – Maximum Take-Off Mass

MVS – Multi-View Stereo

OBJ – Object File

OcuSync – DJI’s Wireless Video Transmission System

OpenGL – Open Graphics Library

OSArch – Open-Source Architecture

OSS – Open-Source Software

PLY – Polygon File Format

PRT – Portugal

PS – Photoscan Professional

PTAs – Pilotless Target Aircraft

RCA – Radio Corporation of America

RFML – Random Forest Machine Learning

RGB – Red, Green, Blue

RTH – Return to Home

SDK – Software Development Kit

SfM – Structure-From-Motion

SVM – Support Vector Machine

TLS – Terrestrial Laser Scanners

TRANARG – Transportes Aéreos de la Región Guayana

UA – Unmanned Aircraft

UAS – Unmanned Aircraft Systems

UAV – Unmanned Aerial Vehicle

US – United States

USB – Universal Serial Bus

USDZ – Universal Scene Description Zip

UV – U (horizontal) and V (vertical) Coordinates

VLOS – Visual Line of Sight

VSFM – VisualSFM

VTOL – Vertical Takeoff and Landing

WebGL – Web Graphics Library

Wi-Fi – Wireless Fidelity

WWI – World War I

WWII – World War II

1
INTRODUCTION

1.1. CONTEXT

Digital 3D reconstruction currently represents an important point of interest within the civil engineering field, overall, in activities such as the preservation of existing conditions, which is critical for the documentation of historical or culturally important buildings, or as a reference for future restoration or renovation projects. Additionally, as-is models allow architects and engineers to design more accurately within the real constraints of a structure, simulate changes or additions before physical intervention, and promptly detect design conflicts or structural problems. Its applications can also extend to maintenance and facility management, where these models facilitate the planning and managing of maintenance activities, they also help track the condition of building elements over time.

The principal contribution of this study is to create a Scan-to-BIM workflow to process and integrate collected spatial data by employing the open-source software (OSS) Blender, with the Bonsai add-on. Enhancing the capability to integrate the datasets acquired and develop an easily scalable and replicable workflow. Due to its vast and diverse applications, streamlining the process of integrating the results of these technologies into a single environment. Furthermore, the proposed technologies can be complemented by UAVs, aiding them in reaching areas that could be dangerous or problematic for other techniques.

This methodology relies on advanced sensing technologies, which capture detailed spatial information about the built environment. This study aims to explore in-depth three of the most predominant technologies presently used: photogrammetry, LiDAR, and thermography. To assess their strengths, especially how photogrammetry can capture high-resolution color imagery that can be used to generate detailed and textured 3D models, how LiDAR provides highly accurate and dense 3D point clouds, even in low-light or complex environments, and how thermography detects temperature variations on surfaces, enabling the identification of hidden defects like insulation failures or moisture intrusion. Along with examining their limitations and investigating how their combined use can enhance the accuracy and comprehensiveness of building inspections.

To support this theoretical framework, this work includes a case study focused on digitally recreating the B001-B003 rooms at the Faculty of Engineering of the University of Porto (FEUP), carrying out various surveys conducted with handheld LiDAR methods, and an UAV equipped with RGB and thermal cameras. It is a perfect example of how digital reconstruction can aid in facility management, retrofitting, or energy analysis, as it is a functional building. Its varied surfaces and materials make it a strong subject where thermography, LiDAR, and photogrammetry can show their strengths and limitations. Moreover, the author, as a student at FEUP, has easy physical access to the building, which simplifies data collection with UAVs and sensors.

1.2. MOTIVATION

This research is driven by the need to make Scan-to-BIM processes more accessible, proposing a methodology based entirely on open-source software. In this context, UAVs have become more and more popular for use in building documentation and inspection thanks to their ability to access difficult-to-reach areas and collect data efficiently. However, the technologies included in this study, photogrammetry, LiDAR, and thermal imaging have shown great promise in capturing various aspects of buildings, including their geometry, visual detail, and thermal performance. Nevertheless, there is still a dearth of research on how these technologies can be successfully integrated into a single, cohesive workflow for Scan-to-BIM reconstruction.

Most of the existing research explores one or two of these techniques, frequently utilizing highly specialized set-ups and commercial software that restrict accessibility and reproducibility. As a result, the full potential of a multi-sensor approach remains underutilized, particularly in academic or low-cost professional contexts. To guarantee wider applicability approaches that not only integrate data from several sensors but also rely on open-source tools are needed.

This dissertation was motivated by the opportunity to bridge that gap. The goal of this project is to create a scalable and compatible open-source Scan-to-BIM workflow using LiDAR, and UAV-mounted photogrammetry and thermal cameras. The data will be processed using open-source software like Blender with the Bonsai add-on. The goal is to contribute a practical methodology that can support building diagnostics, energy analysis, and heritage conservation while promoting accessibility and integration across disciplines.

1.3. STUDY OBJECTIVES

By combining UAV-based photogrammetry, LiDAR, and thermal imaging, this dissertation aims to create and validate a workflow for 3D reconstruction. Open-source tools, like Blender with the Bonsai add-on, are used for data processing, visualization, fusion and BIM modelling. Photogrammetry provides visual and spatial detail, LiDAR provides geometric accuracy and depth, and thermal imaging identifies temperature anomalies and hidden pathologies such as moisture presence or insulation flaws. The objective is to evaluate the contributions of each sensing technology to different aspects of façade and interior surface documentation. The presented study explores how their combination can overcome the drawbacks of each technology when used separately, creating a more comprehensive, accurate, and diagnostically meaningful digital representation of buildings by identifying their outputs and aligning them within a shared spatial framework. Specifically, the dissertation aims to:

- Develop a Scan-to-BIM workflow compatible with the open-source methodology, by using the available equipment and software.
- Produce a methodology for data acquisition using UAV-mounted sensors and manual methods in a real case study.
- Test and document a data integration workflow using open-access software, primarily Blender with the Bonsai add-on.
- Identify the main challenges of combining heterogeneous datasets in terms of scale, resolution, and spatial alignment.
- Propose a scalable and replicable approach that can support future applications in civil engineering, energy diagnostics, and building conservation.

By achieving these goals, the study fills a gap in literature and provides a workable, approachable solution for the integration of multi-sensor data in façade analysis.

1.4. METHODOLOGY

In conducting this dissertation, first, a bibliographic data collection to examine the existing literature was carried out, establishing a technical foundation through an exploration of the historical development and operational principles of each of the three sensing technologies and UAV platforms, where the main existing gaps and challenges were evidenced to be addressed during the practical implementation of the case study. This step ensures a solid understanding of the capabilities and limitations that influence their application in building inspection and reconstruction.

For this purpose, a real-world case study is designed, taking place in the “B” building at FEUP and employing the DJI Mavic 2 Enterprise Dual, and an iOS device. The results obtained are then imported into Blender to create a BIM model, supported by the Bonsai add-on, thus implementing an open-source workflow. The approach provides a scalable solution for multi-sensor building modeling and diagnostics by emphasizing accessibility, interoperability, and reproducibility to meet the suggested goals.

1.5. STRUCTURE

This study presents five main chapters that are meant to provide a comprehensive overview of the topic, as described below:

1. Introduction – Presents the study's primary goals, background, and methodology.
2. State of the Art – Describes the general definitions of the studied technologies and explains how the systematic review was done as a base for the literature review, which is explored subsequently, to bring everything together in the Challenges and Gaps section, where the current limitations, uncertainties, and areas needing further research within the technologies or methodologies being studied are identified.
3. Proposed Method – Showcases the approach suggested by this study, addressing the specific UAV model, data acquisition devices, processing software, methodology, applicable legislation, and the setting employed in the research.
4. Case Study – Elaborates on the practical application of the proposed methodology, detailing the process data collection, sensor calibration, setbacks, necessary adjustments, and workflow carried out in the defined setting, followed by a discussion of the results.
5. Conclusions – Summarizes the study's key conclusions, considers their ramifications, and makes suggestions for additional research and real-world uses.

2
STATE OF THE ART

2.1. SUMMARY

This chapter aims to explore the current state of the technologies used for 3D building reconstruction, with a special overall focus on the use of UAVs and their integration with various sensors, particularly those used in photogrammetry, LiDAR scans, and thermal imaging. Studying their differences and how they can complement each other to enhance 3D reconstruction. To achieve a complete review of these topics, this chapter was designed with the following structure. Beginning with the GENERAL DEFINITIONS, this chapter covers the evolution, milestones, and current applications in the construction industry of the studied technologies. The LITERATURE REVIEW chapter shows the data recollection process, from the bibliographic databases used to the selection criteria included in the systematic review. Finally, the Existing Literature chapter explores the gathered information from the literature review to determine the strengths and limitations that these technologies have shown in previous studies and to identify the current trends of these concepts.

2.2. GENERAL DEFINITIONS

2.2.1. UNMANNED AERIAL VEHICLES (UAVS)

Unmanned Aerial Vehicles (UAV) or Unmanned Aircraft Systems (UAS), commonly called drones, historically have been a significant point of interest for technological advancements. Their origins can be traced back over a century, with early designs primarily developed for military purposes. One of the first recorded uses of an unmanned aerial device in combat dates to 1849, during the Austrian siege of Venice. Artillery lieutenant Franz von Uchatius proposed to bomb the city from the air. Each unit was equipped with around a hundred hot-air balloons, eighteen feet in diameter each, and made of paper and cloth. A gunpowder and shrapnel-filled pear-shaped bomb with a half-hour timed burning-fuse mechanism, specially designed for the mission, was attached to each aerostat. These devices were lifted from the seaside, and, drifting with wind power, would arrive in Venice, as seen in *Figure 1*. Despite all these inventions and preparations, efficiency was negligible. According to the Venetians, only one bomb exploded within the city, compared to 60,000 artillery shells fired upon the city with conventional artillery, which seems insignificant (Kozera, 2018; Parracho, 2021). Even though these balloons represent the first known use of unmanned aerial bombing, they’re often not classified as UAVs for modern standards. This is because there’s no way to guide or control them after the launch, they’re left to the wind’s mercy and can’t be piloted in real-time. In comparison, modern UAVs are defined by their ability to be piloted autonomously and remotely, usually with onboard sensors, and navigation and communication systems.

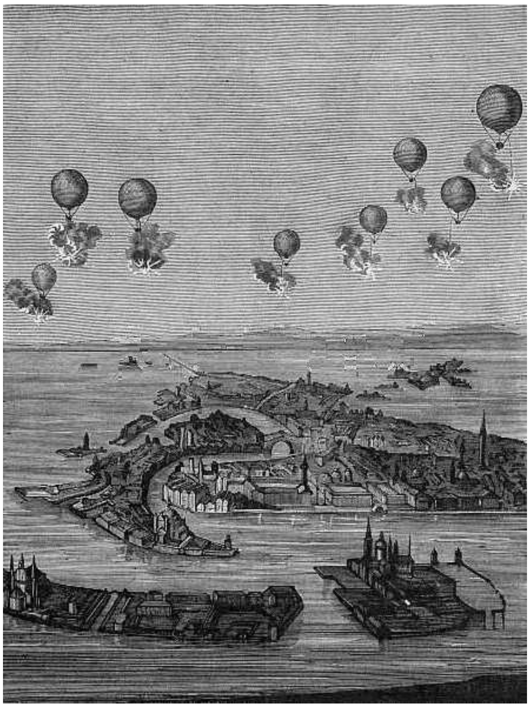

Figure 1- Artistic representation of the 1849 aerial bombardment of Venice. Max de Nansouty's Aerostation - Aviation (1911) artwork.

In 1903, with the first flight taken by the Wright brothers, developments in aviation accelerated and soon the first Unmanned Aerial Vehicle was created. During the First World War, it was very difficult to replace the lost airplanes and pilots, which happened quite frequently due to the mass introduction of warplanes. To solve this problem, military leaders started to think about using Unmanned Aircraft, in certain missions. In November 1917, ordered by the US Military and created by Charles Kettering and Elmer Sperry the Kettering Bug was developed. It consisted of a small-sized biplane, that after take-off, was guided by a gyroscope-based navigation system in the direction of the target, where when the pre-set time passed, the engine stopped, the wings fell, and the torpedo-shaped body filled with 80 kg explosive hit the target and exploded. Although the construction was successful, it didn't participate in the war, because by the time the U.S. Military put it into service, the war had ended (Palik and Nagy, 2019).

After WWI, the advancements in aviation caused the development of faster, more robust and better maneuverability aircraft. These improvements needed a change in the training methods used for pilots. To efficiently simulate these encounters, Pilotless Target Aircraft (PTAs) were introduced. In 1935, one of these programs elicited the creation of the "Queen Bee" in the UK, it was a pioneer UAV that represented an important innovation for aerial training. This system was installed in a De Havilland DH.82 Tiger Moth, with a maximum height of 5200 meters and a top speed of 180km/h. Additionally, the "Queen Bee" is the first aircraft to ever be referred to as "Drone" (Palik and Nagy, 2019). Following WWII, UAV development accelerated with a major focus on reconnaissance methods. At the end of the 20th century, particularly in the 1990s, a great breakthrough was witnessed with the M-1 Predator (*Figure 2)*. Initially created for surveillance, the Predator was eventually armed with "Hellfire" missiles, giving UAVs active combat roles. This change established them not only as observers but as decisive modern warfare tools. The MQ-1 Predator is perhaps the most well-known of all military drones used today. It has a wingspan of 55 feet, a length of 27 feet, and can be remotely piloted from thousands of miles away via satellite communications. The modern Predator drone dates to the GNAT-750 (and "Amber" before it) flown in Bosnia in 1994 by the CIA under codename "LOFTY VIEW". Six years later in 2000, the CIA first started flying Predators in Eastern and Southern Afghanistan for warfare purposes (Shaw, 2013).

Figure 2- MQ-1 Predator [extracted from Shaw (2013)]

In the beginning, UAVs were mainly fixed-wing aircraft, due to their efficiency and longer flights, but this kind of model requires runways for take-off and landing, and present operational limitations when faced with confined spaces and complex environments. Therefore, the necessity of more versatile models led to the adaptation of rotary-wing UAVs. From this group, the quadcopters are the most prominent, they are small agile vehicles controlled by the rotational speed of four rotors. The position of these rotors, relative to the body coordinate system causes two different types of quadrotor configurations: the “x” configuration and the “+” configuration. An x-configuration quadrotor is more stable in comparison to + configuration, which is a more acrobatic structure. The four rotors are aligned such that the rotors on opposite ends rotate in the same direction and the other two in the opposite direction. These multirotor UAV’s offer vertical takeoff and landing (VTOL) capabilities, better maneuverability, and the ability to hover. They're also less susceptible to air turbulence compared with fixed-wing aircraft of similar dimensions, making them suitable for a wide range of applications. These advancements have expanded the applicability of UAVs to areas like urban planning, infrastructure inspection and emergency response. The transition from fixed wings to quadcopters was facilitated by advancements in microelectronics, sensor technology, and control algorithms. The quadcopter can be traced back to 1907, when the Breguet Brothers built the first quadrotor. The flights of the Gyroplane (*Figure 3*) are considered to be the first manned flight of a helicopter, but not an untethered flight. Lack of stability and proper control mechanism caused the machine to never fly completely freely (Norouzi Ghazbi *et al.*, 2016).

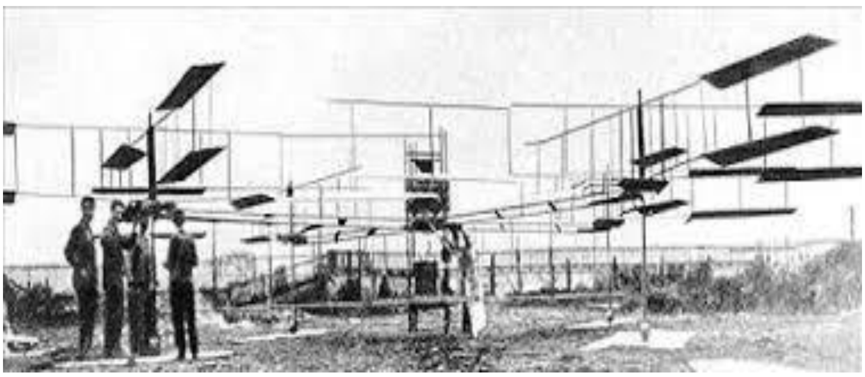

Figure 3- Bréguet Richet Gyroplane No. 1 [extracted from Norouzi Ghazbi et al. (2016)]

The transition from military use to civilian use of the UAV's started in the 1990s, driven by technological advances in sensor miniaturization. This innovation made them more accessible and affordable, allowing their adoption in sectors like environmental monitoring, agriculture and scientific research. The UAV's brought solutions to tasks like surveying and data collection in remote or hard-to-reach areas. Their potential growth was more evident for agriculture uses, where they were used for crops monitoring and precision farming. However, as the UAV's technology grows, the need for regularization, security and privacy grows as well (Skrzypietz, 2012). The first recognition of the potential of commercial drones was in 2006, when the FAA issued the first license for commercial drones, which allowed the use of drones in U.S. civilian airspace to search for survivors of disasters. The licenses raised low interest from companies, but after their price gradually decreased, and its technology became more advanced, many enterprises saw its commercial prospects and began to use it in logistics, security patrol, mining and geological exploration (Liu, 2022).

Inside the construction industry, different studies have proven the importance and usability of UAV's, early instances such as Irizarry et al. (2012) used them as a tool for exploring potential benefits to safety managers within the construction jobsite safety inspection. This study evaluated the potential of small UAV's, equipped with cameras, inside construction sites. It showed that UAVs can aid managers by giving them easy access to images and live videos of various zones around the site. This skill allows for constant monitoring and communication with the workers and improves safety inspections by removing the necessity of physical presence in potentially hazardous zones.

Portugal has made significant efforts to regulate the operation of drones, aligning its national framework with the standards of the European Union Aviation Safety Agency (EASA). As of 2025, drone operations in Portugal are governed by the European Union Aviation Safety Agency (EASA) regulations, specifically Commission Implementing Regulation (EU) 2019/947 and Delegated Regulation (EU) 2019/945. The Portuguese Civil Aviation Authority (ANAC) oversees the enforcement of these regulations within the country. UAV operations shall be performed in the 'Open', 'Specific', or 'Certified' categories.

- Open: Low-risk activities and include drones under 25 kg that operate below 120 meters and within the visual line of sight, the remote pilot must ensure that the unmanned aircraft is kept at a safe distance from people and that it is not flown over assemblies of people, and it cannot carry dangerous goods or drop any material. This category is divided into three subcategories A1, A2, and A3, based on operational limitations, requirements for the remote pilot, and technical requirements for UAS.
  - A1: Flying over uninvolved people is allowed but should be minimized, but flying over assemblies of people is strictly forbidden. The used drones must bear a mark stating either the CE class 0 (weighing less than 250 grams) or 1 (weighing less than 250 grams). For Class 0 drones no formal training is required, while for Class 1 drones it is necessary to complete an online training and pass an examination covering topics such as air safety, airspace restrictions, and privacy considerations.
  - A2: A horizontal distance of at least 30 meters from uninvolved people must be maintained, this distance can be reduced to 5 meters if the drone is equipped with a low-speed mode function. The used drones must weigh less than 4kg and bear a CE class 2 mark. The remote pilot must complete an online training and pass an examination.
  - A3: Is only permitted to fly in areas where no uninvolved people are present. Always ensuring a minimum horizontal distance of 150 meters from residential, commercial, industrial, or recreational areas. This subcategory is aimed for the use of drones that belong to CE class 3, referring to drones weighing less than 25 kilograms, or CE class 4, drones without automatic control mode (also weighing less than 25 kilograms). It is necessary to complete an online training and pass an examination covering operational procedures, safety measures, and emergency protocols.

- Specific: Medium-risk operations requiring risk assessments and operational authorization. The operator shall perform a risk assessment and guarantee adequate mitigating measures
- Certified: High-risk applications, including operations over assemblies of people, or that involves the transport of people, or the carriage of dangerous goods, that may result in high risk for third parties in case of accident.

Overall, drones must be operated within the visual line of sight (VLOS) of the remote pilot, at all times, as shown in *Figure 4*. They aren't allowed to be flown 120 meters above ground level, and in geographic zones, including near airports, over assemblies of people, and in other sensitive locations, without a special authorization. ANAC recommends operators to obtain civil liability insurance to cover potential damage resulting from drone operations. Furthermore, operators must comply with national and EU data protection laws, especially when capturing images or videos that may compromise personal data (European Parliament & Council of the European Union, 2018; EASA, 2021).

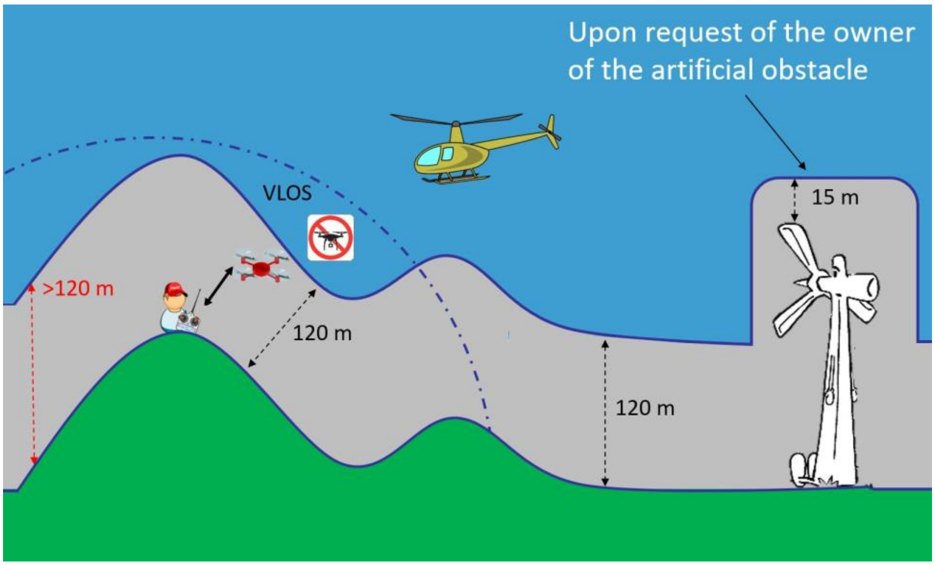

Figure 4- General rules for UAV flights [extracted from EASA (2021)]

From military prototypes to important tools in fields such as construction, agriculture, and various others. UAV integration in civilian life has unlocked great value in terms of security, efficiency, and data accuracy. Their adoption keeps growing as different industries explore their potential. Continuous developments in regulation and technology promote their integration into construction workflows

2.2.2. PHOTOGRAMMETRY

Photogrammetry is a technique that uses a series of overlapping 2D images, taken from different perspectives, identifying common features between them to create precise 3D models. This process is often employed in construction, surveying, and heritage documentation, due to its ability to produce detailed and accurate point clouds and its effortless compatibility with UAVs. Nowadays, the advancements in structure-from-motion (SfM) and image-matching algorithms have increased the precision and efficiency of these processes (Nex and Remondino, 2014; Parracho, 2021).

It had its beginning with the invention of photography by Daguerre and Niepce in 1839. The first generation, from the middle to the end of last century, was very much a pioneering and experimental phase with remarkable achievements in terrestrial and balloon photogrammetry. Albrecht Meydenbauer thought about how indirect measurements could replace the direct measurements of façades in photographic images, after he had an accident, in 1858, and almost fell down from the side-aisle of the cathedral in the city of Wetzlar, while he was working as a building surveyor for the Prussian government. Thus, the basic idea of photogrammetry was born. Meydenbauer performed practical tests during 1867. In the town Freyburg-on-Unstrut, he recorded metric images of the town church, and for topographic purposes he also photographed a sector of the surrounding terrain. In these tests the method proved to be a success, and Meydenbauer could now provide evidence that photogrammetry is suited for architectural surveys and for topographic data acquisition as well. *Figure 5* depicts one of Meydenbauer´s cameras. In the context of these experiments the term "Photogrammetry" was coined. Meydenbauer began his investigations into the use of photographs in measurement without any knowledge about the activities of Aimé Laussedat, a military engineer in France. As early as 1851, Laussedat had begun experiments to use images for topographic mapping purposes. in 1859 the prototype of a topographic camera was built to his specifications. He called his system "Métrophotographie" (Schenk, 2005; Albertz, 2007).

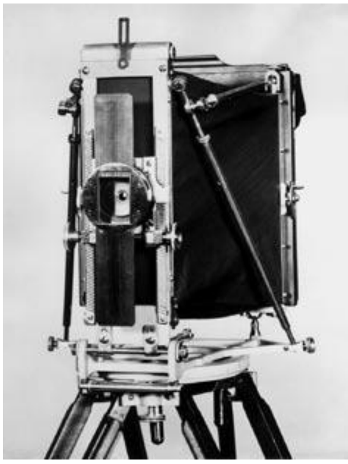

Figure 5- A later model of Meydenbauer's cameras, built around 1890 [extracted from Albertz (2007)]

An important turning point in the scientific study of vision was reached in 1838 with the invention of the stereoscope by Charles Wheatstone. By showing two slightly different images to each eye, Wheatstone's stereoscope produced a powerful illusion of depth, proving that the brain can interpret binocular disparities as spatial information. Wheatstone found that binocular disparity is the main mechanism by which the brain perceives depth. In contrast to other monocular cues or learned associations, his 1838 experiments showed that depth perception could directly result from the differences between the images seen by each eye (Wade, 1987).

Photogrammetry moved into the mainstream when, during World War I, it was introduced as a tool for reconnaissance. It remained an immature technology, and the interpretation of images was initially improvised without formal procedures. However, cameras were soon modified for use in aircraft due to the necessity of gathering intelligence behind enemy lines. *Figure 6*, depicts how manual aerial photos were taken. Aerial photography had become indispensable on the Western Front by 1915, enabling the creation of updated maps that were essential for trench warfare planning and artillery targeting. Aerial photos served as the foundation for completely new maps in areas such as the Middle East, where mapping resources were either inadequate or out-of-date. Although the process was still challenging in the field, the war sparked significant technological advancements like better camera stabilization and interpretation techniques. Even though the methods created were primitive by later standards, they were a significant advancement at the time. Specialized units were formed to decipher photographs and produce updated maps, despite the dearth of training available in the early phases of the war. By 1918, photogrammetry had progressed from scientific curiosity to an essential military tool. After the war, most former belligerent countries carried out significant improvements in camera design for air survey work, although the subsequently standard 230cm² format only appeared just before World War II. Maturity would only be achieved as a consequence of World War II when the truly global nature of the conflict necessitated a considerable investment in resources to create the mapping needed to support military operations. Structured training programs had been designed to teach soldiers how to analyze aerial photographs systematically. Stereoscopic imagery became indispensable, enabling interpreters to detect hidden objects better and perceive depth. With an emphasis on both technical accuracy and visual skills, specialized schools were established to professionalize the training of aerial photo interpreters. Aerial photographs began to influence the public sphere, where they were exhibited and admired for their technological and artistic qualities. The ability to interpret aerial images came to be seen as a unique visual competence, combining the scientific method and aesthetic judgment. Aerial photography has become essential for strategic decision-making and planning in military operations. The development of aerial photography interpretation reflected larger changes in technology, visual culture, and warfare. Both military institutions and the general public's perception of aerial photography had fully institutionalized the practice by the end of World War II (Collier, 2018; Quagliati, 2020).

Figure 6- German observer with a handheld camera taking pictures from an airplane in spring 1917 (Bundesarchiv, Bild 183-R27851) [extracted from (Quagliati, 2020)]

Traditional analog techniques, that depended on mechanical stereo plotters and human interpretation, were replaced by analytic photogrammetry in the 1970s. Due, but not limited, to the widespread practice of equipping existing stereo plotters with simple digitizers, the growing tendency to use minicomputers linked with stereo plotters, and the optimization of the production of digital terrain models by progressive sampling in stereo models. This change was made possible by computers, which allowed for the mathematical modeling of geometric relationships in images. Digital systems started being used to correct for inaccuracies, account for mathematically defined systematic effects, and provide final relative and absolute image orientation. Drawbacks like digitalization and storage of photographs and processing of massive quantities of image data were overcome, and tasks such as stereoscopic measurements, aerial triangulation, and manual procedures that consumed a lot of time were automatized and simplified. Aerial triangulation, which uses computers to automatically determine the spatial relationships between overlapping aerial photos, was one important development that significantly increased the accuracy and efficiency of creating georeferenced models. In a similar vein, algorithm-driven data extraction from stereo imagery replaced contour line generation, which involves drawing lines of equal elevation on topographic maps. These breakthroughs not only augmented the precision of mapping processes, the also reduced the time and work required, marking a critical step toward the complete digitalization of photogrammetric systems (Thompson and Mikhail, 1976).

Building on this shift, the automation of geospatial data collection and analysis was further advanced in the 1990s with the arrival of the Global Positioning System (GPS). It enhanced the ease and versatility of spatial data acquisition and diversified its integration with remote sensing and geographic information systems (GIS). Additionally, GPS technology enabled real-time georeferencing, leading to the acceleration of georeferenced precise model production. Since GPS offers accurate positional data that could be integrated automatically in GIS platforms, it enabled the rapid processing of big datasets while simultaneously improving mapping precision. The modern applications of GPS and GIS were possible thanks to the big change that took place in the 1990s, when these systems started to be relied on, allowing them to improve and facilitate the automatic analysis of geographic information (Gao, 2002).

Early in the 2000s, low-cost digital cameras transformed photogrammetry, particularly in uses that require close-range surface measurement. Originally viewed as a reasonably priced substitute for conventional photogrammetric tools, the resolution of these new digital cameras was such that they rivaled traditional 35 mm film-based cameras. They also eliminated the need for film development by enabling instant image review and integration with processing software, which facilitated faster workflows. Due to these features, digital cameras can be used for a wide range of tasks, such as engineering projects, archaeological documentation, and architectural surveys. Furthermore, the portability of these cameras made it easier to integrate photogrammetry with other technologies, such as laser scanners and GPS, enhancing the overall efficacy of geospatial data collection. Improvements in processing technology and the availability and adaptability of digital cameras not only made photogrammetry more accessible, but they also greatly increased the speed, efficiency, and quality of data collection and analysis. During this period, the field underwent a significant evolution that paved the way for subsequent developments in digital imaging and data analysis (Chandler *et al.*, 2005).

Nowadays, photogrammetry, whether it is held or mounted in a tripod or a UAV, is a technique widely used in the construction industry. Since it allows for gathering geospatial information and monitoring the worksite conditions in a precise, economical, and efficient way. Additionally, this technique makes it possible to document the work progress and to compare the as-built model with the design plans by converting multiple overlapping images into dense point clouds. It has been especially useful for monitoring structural elements, calculating earthwork volumes, and performing visual inspections in hard-to-reach areas. When combined with UAVs, photogrammetry allows for rapid and frequent site surveys, significantly cutting down on the time and labor required for conventional surveying techniques. Additionally, by enabling the comparison of digital and physical site conditions, its integration with Geographic Information Systems (GIS) and Building Information Modeling (BIM) has enhanced coordination between design and construction teams. These features have shown promise in identifying deviations, cutting down on rework, and improving stakeholder communication (Fobiri, Musonda and Muleya, 2022).

2.2.3. LiDAR

Understanding the fundamentals of LiDAR technology's main component, the laser is crucial to comprehend how it functions. A laser, short for "Light Amplification by Stimulated Emission of Radiation," is a device that produces a highly collimated, monochromatic, and coherent beam of light through optical amplification. These characteristics, in particular coherence and directionality, set lasers apart from other types of light sources and make them ideal for precision applications in a variety of industries, such as remote sensing, medicine, and telecommunications. Leveraging these capabilities, LiDAR (Light Detection and Ranging) was developed as a technique that determines distances by emitting laser pulses and measuring the time it takes for the light to reflect from a surface. LiDAR systems can produce three-dimensional, high-resolution images of the surroundings by precisely timing these returns. Conceptually similar to radar, LiDAR uses light waves rather than radio waves to operate, providing much higher spatial resolution. This makes it particularly useful for forestry, urban infrastructure monitoring, bathymetric surveys, and topographic mapping (Wehr and Lohr, 1999).

In 1960, Theodore Maiman at Hughes Research Laboratories demonstrated the first functional laser, a ruby laser, which emitted coherent light suitable for precise measurements. This breakthrough spurred interest in applying lasers to range-finding applications. Within seven months, researchers at Bell Labs developed the helium-neon (He–Ne) gas laser, the first to generate a continuous beam of coherent light, emitting an orange or red beam at 0.633 mm. By 1961, lasers were being sold commercially by such companies as Spectra-Physics and Perkin-Elmer, and early lasers were deployed to assess natural resources, in tasks such as measuring sea ice surface roughness, making near-shore bathymetric measurements, penetrating forests to make detailed topographic measurements, fluoresce oceanic phytoplankton for surface current studies and fluoresce terrestrial vegetation. As early as 1964, researchers noted vegetation returns acquired using the airborne helium-neon (He-Ne), 0.63 mm, continuous wave (CW) laser. A decade and many airborne studies later, scientists with TRANARG, a mapping and surveying company in Caracas, Venezuela, conducted aerial surveys covering more than 11,000 km, with flight lines spaced 1.5 km apart, to generate a topographic map intended to support the selection of a new reservoir site, marking one of the first real-world uses of airborne LiDAR for topographic mapping. They noted 35-40 m median canopy heights with towering trees up to 55 m in their profiles. Trees came to be regarded as a signal rather than noise in the mid-1970s. Comparably, in 1976 in the Soviet Union, Russian researchers cut down a birch and a spruce and aimed a He-Ne CW laser with a spot size of approximately 25 mm at the horizontal trees, to produce a profilograph (a graphical representation of surface elevation or contour), then compared it with tape measurements, and concluded that, with increased power, such a laser could be mounted on an aircraft to remotely measure forest canopies. In 1979, they mounted their He-Ne laser on an AN-2 biplane and acquired their first airborne profiles (Nelson, 2013).

Advances in laser engineering, sensor miniaturization, and computing power allowed LiDAR technology to evolve from these early experimental applications to complex digital, multi-return platforms. The four primary components of most contemporary LiDAR systems are a pulsed laser scanner, a GPS receiver for positioning, an inertial measurement unit (IMU) for tracking orientation and movement, and data processing software for reconstructing three-dimensional information. Together, these elements record not just one distance per pulse but frequently several returns, providing a detailed picture of the topography, vegetation layers, and building façades. The integration of these systems aboard aircraft, drones, and even handheld devices has made LiDAR a cornerstone technology for a broad range of geospatial and engineering applications, offering unmatched accuracy and resolution in spatial data acquisition (Wehr and Lohr, 1999).

During the 2000s, terrestrial laser scanners (TLS) experimented major developments, going from niche applications to being utilized widely in fields such as architecture, heritage documentation, and civil engineering. Improvements in the laser scanner hardware, processing data software, and computational capabilities, made the acquisitions of 3D information more accessible and efficient. In architecture, TLS allowed for the accurate obtention of as-built documentation, aiding renovation and restoration by providing detailed geometric information of existing elements. And for heritage preservation, it became an essential tool for the development of thorough models of historical sites. Furthermore, inside the civil engineering field, this technology has been majorly used in the monitorization of structures, detection of structural deformations, progress monitoring, and quality control of big-scale projects. Ultimately, TLS integration with BIM has widened its applications even more, by enabling data analysis and management, of new or existing structures, in a comprehensive and realistic manner (Garnero, Godone and Bacciocchi, 2010; Rashidi *et al.*, 2020).

In the modern context, advancements in reality capture techniques have transformed the use of 3D datasets into a crucial resource for surveying and documentation in the Architectural, Engineering, and Construction (AEC) field. The construction industry's spatial data acquisition workflows have significantly improved with the shift from static TLS setups to UAV-mounted platforms with multi-sensor payloads. Large, complex construction environments can now be scanned quickly and repeatedly thanks to UAV-based LiDAR systems, which can capture dense point clouds with an average vertical and horizontal accuracy of 2-5 cm. The combination of LiDAR and GNSS/INS (satellite positioning combined with inertial sensors) units, to improve location accuracy, allows for precise georeferencing and increased point density, producing models suitable for detailed surface reconstruction of built environments. UAV-based LiDAR technology has emerged as a promising tool, with superior coverage and accuracy compared to other methods, like photogrammetry. Even though both technologies can generate quality results, the accuracy, price, and applications might vary, especially considering that LiDAR scanners are expensive, and more energy-dependent equipment compared to camera drones (Guan, Zhu and Wang, 2022; Yucel, Liu and Alathamneh, 2024).

LiDAR technology was initially created for remote sensing in large-scale surveying applications and has significantly decreased in size and cost in recent decades. This evolution has enabled its gradual integration into off-the-shelf devices, with a major milestone reached in 2020, when Apple released the iPad Pro and iPhone 12 Pro with built-in LiDAR sensor, mainly devoted to Augmented Reality (AR) applications. The use of these mobile devices for metric survey purposes is of high interest for the research community, for both outdoor and indoor environments, and especially when speed, portability and cost-benefit optimization are essential requirements, not always easy to meet using high-end surveying instruments. This was a turning point in the democratization of LiDAR, turning it from specialized, costly equipment to a portable, approachable tool that could be used by a wider range of people. Allowing to conduct metric characteristics evaluation of point clouds, acquired by the iPad Pro, using free applications such as SiteScape, as shown in *Figure 7*. The iPad Pro has proven to produce point clouds with centimetric precision and accuracy, suitable for a 1:200 map scale. Although LiDAR systems originally focused primarily on outdoor and industrial applications, its inclusion into mobile devices opened new possibilities for indoor mapping, augmented reality, rapid architectural documentation, and Scan-to-BIM applications (Spreafico *et al.*, 2021).

Figure 7- Comparison Between Test Area Photo and Point Cloud from a Single iPad Pro Scan (Low Resolution) [extracted from Spreafico et al. (2021)]

2.2.4. THERMAL IMAGING

Thermography, also known as thermal infrared (IR) imaging, is a non-destructive imaging tool that captures the IR electromagnetic radiation emitted by objects to visualize and measure surface temperature variations. Any object with a temperature other than absolute zero (-273,15ºC or 0 K) emits infrared radiation, which increases with temperature. IR thermal cameras make images of the thermal patterns and are calibrated to measure the emissivity of surfaces in an area at various temperature ranges. They use a lens to focus the emitted IR radiation onto a detector and the electromagnetic signal is converted into visual display (digital picture) in which the different colors (or shades of grey) correspond to various temperature levels of the surface on which is focused. This technique can be a powerful tool for fast and accurate building diagnostics quantifying potential energy savings and detecting anomalies such as moisture intrusion, insulation defects, or structural weaknesses in buildings, as these issues often produce distinct thermal signatures (Balaras and Argiriou, 2002).

Infrared radiation (IR) itself was unknown until the early 19th century, when Herschel’s experiment was first reported, which involved passing sunlight through a prism and measuring the temperature of each color with thermometers, it led to the discovery of infrared radiation just beyond the red part of the visible spectrum. For the thirty years following Herschel’s discovery, very little progress was made beyond establishing that infrared radiation obeyed the simplest laws of optics. Slow progress in the study of infrared was caused by the lack of sensitive and accurate detectors, resulting in few real-world uses for infrared sensing in that period. The next real advancement came with Thomas Seebeck’s discovery of the thermoelectric effect in 1821, where a temperature difference across two different metals produced a small electric current. Nobili and Melloni used this idea to create thermocouples (a pair of metal wires that create voltage when heated) and thermopiles (a group of thermocouples used to better detect heat), putting several thermocouples in series to increase sensitivity. These thermopiles were revolutionary at the time because they could sense a person's body temperature from 30 feet away. Samuel Langley then created the bolometer in 1880, which allowed for accurate solar and atmospheric radiation measurements by employing platinum foils in a Wheatstone bridge to measure minute temperature changes.

Significant advancements in infrared detection occurred in the late 19th and early 20th centuries. Langley's bolometer was far more sensitive than thermopiles, detecting temperature variations as tiny as 0.0001°C. The primary applications of these early instruments were in atmospheric science and astronomy. By the early 1900s, infrared detectors were also being used to study blackbody radiation, leading to developments in thermal theory such as Stefan-Boltzmann's law. Bolometers were first used in 1914 to detect people at 200 meters and airplanes at 1,000 meters, foreshadowing their use in military applications. In the 1920s and 1930s, photoelectric and photoconductive effects were studied using materials like selenium and thallous sulfide. In 1930, German scientists began developing lead sulfide (PbS) quantum detectors with sensitivity in the 1.5–3 µm range. These detectors enabled military use in devices like infrared direction finders. They were the first steps toward real thermal imaging, even though imaging still relied on scanning and had extremely low resolution. The technology remained mostly in laboratories or military projects, limited by poor stability, high cost, and very long response times.

Infrared technology saw a boom in innovation during World War II. With effective detection ranges of up to 30 km for ships, the German military employed PbS detectors in airborne infrared systems such as the Kiel IV. The 1P25 image converter tube for night vision scopes such as the "Snooperscope" and "Sniperscope" was created in the US by RCA. Despite being rudimentary, these systems allowed soldiers to see in complete darkness by employing active infrared illumination. Samuel Langley's bolometer, meanwhile, developed into increasingly advanced devices. To enhance heat-seeking capabilities, cooled PbS detectors were incorporated into the Sidewinder missile in the 1950s. At this point, line-scan imaging started to replace basic radiometric measurements. First-generation thermal cameras appeared using thermopiles and bolometers, with image exposure times ranging from 4 to 20 minutes. These systems were used for early attempts at thermography but were far from practical. Still, the foundational elements of modern thermal imaging, sensor arrays, cooling systems, and scanning optics, began to take shape during this period.

Thermography began to be used in civilian settings in the post-war period. The U.S., U.K., France, and others enhanced infrared sensors with materials such as mercury cadmium telluride (HgCdTe) and indium antimonide (InSb), propelled by Cold War investments. These made it possible to operate in the long-wave (8–14 µm) and medium-wave (3–5 µm) infrared ranges. The first LWIR forward-looking infrared (FLIR) systems were made possible in 1961 by extrinsic Ge:Hg sensors. The AGA 660, the first commercial thermography camera, was introduced in Sweden in 1965. It produced black-and-white images that are helpful for medical diagnostics, especially the detection of breast cancer, using single-element detectors and a mechanical scanner. IR systems were used to track the heat signatures of people, vehicles, and terrain during the Vietnam War. At the same time, thermography was used by civil engineers to find electrical problems and thermal leaks. However, these systems were bulky, expensive, and required liquid nitrogen cooling. Despite these limitations, thermography became accepted in fields like medicine, electrical engineering, and construction by the 1980s.

The development of uncooled infrared detectors, in particular microbolometers, in the 1990s was revolutionary. Microbolometers composed of amorphous silicon (a-Si) or vanadium oxide (VOx) could operate at room temperature, but most detectors previously required cryogenic cooling. Originally funded by the military, these devices made their way into the commercial market by the mid-1990s. The development of focal plane arrays (FPAs) allowed for the high-resolution real-time recording of entire thermal scenes. By the 2000s, thermal cameras were within the reach of consumers, building inspectors, and electricians thanks to companies like FLIR, which sold them for less than $1,000. With the popularity of smartphones, thermal imaging accessories became widely available. Applications in law enforcement, firefighting, industrial monitoring, automotive safety (night vision), and even veterinary medicine expanded quickly. With VOx controlling more than 95% of the market in 2010, uncooled FPAs now control most of the market. Mass production and developments in CMOS and MEMS technology enabled the democratization of thermography, transforming a once-military-only technology into a tool for everyday use (Rogalski, 2012).

Currently, thermography has proven to be a valid assessment method for envelopes, especially for energy audits, defect detection, building inspection, and scenarios where thermal stability is critical. This methodology shows its vast application potential, particularly when it's integrated with UAVs, facilitating its use in big-scale and hard-to-reach environments, reducing the risks related to performing an inspection, like in the case of building façades, in which traditional terrestrial methods have difficulties accessing. These technologies, when combined, allow the detection of thermic anomalies that can be caused by isolation flaws, the presence of humidity, and structural defects that can affect the building’s energetic behavior. Furthermore, when photogrammetry is added, UAV surveys provide a more complete understanding and greater ease to the study of these elements. Nonetheless, the efficiency of this methodology depends on distinct factors, such as precise flight planning, the correct calibration of the different sensors, and the advanced image processing techniques to assure the reliability of the results (Gil-Docampo *et al.*, 2023).

2.2.5. OPEN-SOURCE BIM

Open source refers to software that is released under a license which meets the criteria of the Open-Source Definition, a set of ten principles established by the Open-Source Initiative, (2024) which was derived from the Debian Free Software Guidelines (DFSG), to ensure users have the freedom to use, modify, and redistribute software. These guidelines include nondiscrimination, permission for derivative works, required source code access, and license integrity across distributions. Transparency, flexibility, and a community-driven development process are the main advantages of open source; it is not just "free of charge." Open-source software is now widely used by businesses, governments, and developers, and it is a vital component of the digital economy, according to Hoffmann, Nagle and Zhou (2024), open-source software represents a fundamental part of the current digital economy, with widespread adoption by companies, governments, and developers. The study shows that open source not only reduces development costs and fosters innovation but also provides strategic value to organizations that both consume and support it. From a licensing model, open source has developed into a global tool for technological sovereignty, economic growth, and cooperation.

Whereas Building Information Modeling (BIM) refers to the digital representation of a building's physical and functional characteristics that serves as a shared knowledge resource to support decision-making throughout a project's lifecycle. Unlike traditional drawings or 3D models, BIM integrates multidimensional data, including geometry, spatial relationships, geographic information, quantities, and properties, to produce a coherent and interoperable model. This improved digital model allows architects, engineers, contractors, and owners to work together by providing a single source of truth that improves communication, reduces errors, and boosts efficiency. The BIM process transforms construction and facility management by enabling early detection of conflicts, optimizing scheduling, cost estimation, and sustainability analysis. BIM is not just software but a methodological framework that integrates technology, people, and processes to improve project outcomes across the entire built environment (Eastman *et al.*, 2018).

The push towards open-source BIM finds its roots in the evolving concept of Open Infrastructure BIM (Open I BIM), which emphasizes the use of open standards and collaborative platforms in digital construction. In the systematic review carried out by Salzano *et al.* (2023) of 198 peer-reviewed publications published between 2013 and 2023, provided a comprehensive review and critical analysis of the state of Open BIM use in the infrastructure industry today, with an emphasis on the advancement of the tools and techniques employed. It illustrated how Open I BIM ensures vendor-neutral, transparent data interchange across infrastructure projects by utilizing openly defined formats, like IFC. This widespread adoption of open standards reflects a key pivot away from siloed, proprietary BIM tools toward an ecosystem where stakeholders can seamlessly share, visualize, and modify data with a shared view in cloud environments.

The BlenderBIM Addon, created by the IfcOpenShell community to incorporate native IFC modeling into Blender, is one of the most well-known examples of Open I BIM in action. According to the official Blender Extensions directory, this add-on supports comprehensive BIM functions including IFC import/export, parametric geometry editing, property management, clash detection, quantity take-off, scheduling (4D), and infrastructure-oriented workflows, all within Blender's open-source environment. In August of 2024, the add-on was rebranded as "Bonsai", with its official publication date recorded as August 13, 2024, in Blender's addon registry. The 0.8.2 update, released shortly thereafter, brought in full IFC4X3 infrastructure support, enhanced georeferencing, and improved BIM workflows, efforts that boosted its user base to nearly 59,000 downloads by mid-2025. Its rapid acceptance in academic and professional circles is further demonstrated by the fact that Bonsai is regarded as a free, open-source "NativeIFC AECO toolkit," used in courses, and commended for its open-standards architecture (IfcOpenShell, 2024; OSArch Community, 2025).

2.3. Literature Review

The state of the art was determined through a systematic literature review and a qualitative content analysis conducted using SCOPUS and Web of Science as data bases, with the following search terms: [(UAV* And Fa?ade*) And (LiDAR Or Photogrammetr* Or RGB Or Point?cloud* Or Unman* Or Infra?red) And (Open?Source Or build* Or UAS* Or Image* Or Reconstruction Or Aerial) And (model* Or Visual* Or Compar*)]. For a better comprehension on how these terms were used, *Table 1* demonstrates the logic considered, for which the search would show results that contain every term from Group A and at least one of the terms of the rest of the groups.

The initial set of results from the Scopus database search was examined using VOSviewer, a tool designed to create and visualize bibliometric networks. This early analysis made it possible to identify the most frequent keywords and understand how they relate to each other, offering an overview of key research trends and the main themes within the selected literature. It also helped confirm that the search terms were well-chosen by revealing clear keyword groupings. Furthermore, the analysis identified some new areas of interest, particularly in the modeling and façade inspection applications of UAV-based sensing technologies.

Table 1- Keyword Groups

Keywords			
And			
And	Or	Or	Or
Grupo A	Grupo B	Grupo C	Grupo D
UAV*	LiDAR	Open?Source	model*
Fa?ade*	Photogrammetr*	build*	Visual*
	RGB	UAS*	Compar*
	Point?cloud*	Image*	
	Unman*	Reconstruction	
	Infra?red	Aerial	

The VOSviewer-generated cluster visualization (*Figure 8*) presents a co-occurrence analysis of existing keywords. The network shows five main thematic clusters. The red cluster, centered around photogrammetry, survey, and documentation, highlights traditional surveying techniques and their application in cultural heritage and terrestrial laser scanning. The yellow cluster, which is dominated by mapping, texture, and imagery, connects the acquisition of visual data with structural and environmental elements such as ground, road, and tree. The green cluster centers on feature, segmentation, and inspection, demonstrating a close relationship to machine learning applications like convolutional neural networks and deep learning, which are frequently employed for performance evaluation and damage detection. The blue cluster brings together terms like sensor, BIM, case study, and project, pointing to a strong relationship between how data is collected and how it's applied within Building Information Modeling. This part of the network also reflects how UAV technologies are assessed and adapted based on the specific needs of different projects. Just below, the light blue subcluster includes words such as drone, geometry, and flight, which seem to represent the more practical, hands-on aspects of using UAVs and the challenges that come with them. Altogether, the image presents a field shaped by the intersection of technology, automation, and careful documentation across multiple disciplines.

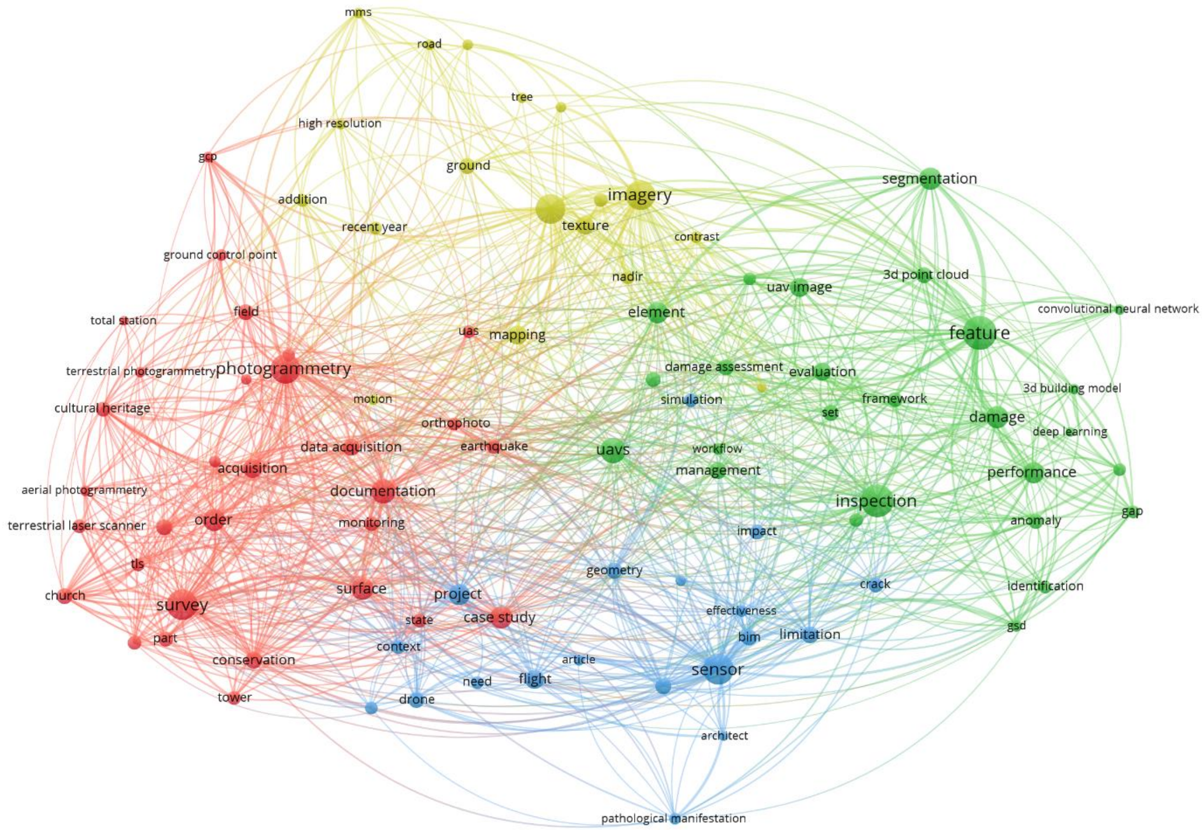

Figure 8- Keyword Network Visualization

The results from the overall search were filtered to detect any duplicates and to dispose of those that weren't aligned with the objectives of the dissertation. For this, the studies were labeled, according to their work frame, with the following inclusion tags:

- Comparison
- Integration
- Laser Scanning
- LiDAR

- Open Source
- Photogrammetry
- Thermal
- Other

In *Figure 9* a chart is presented showing the results from this filtering and how many articles were included to develop the state-of-the-art:

Scopus	144
Web of Science	64
Overall Count	208
Duplicates	52
Non-duplicated dataset	156
Excluded	10
Maybe	9
Included	137

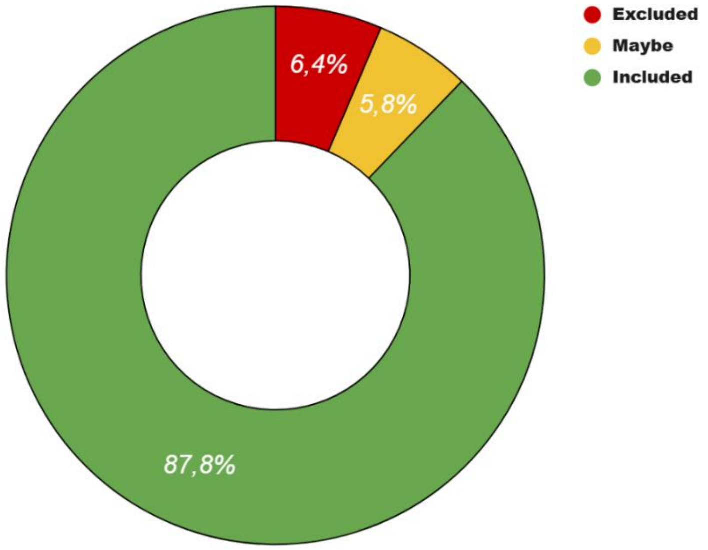

Figure 9- Article Screening

For the articles to be considered on the included or maybe pile, they had to be aligned with at least one of the inclusion tags. The graph in *Figure 10* shows the number of articles that were associated with each label (the articles could also be associated with multiple labels):

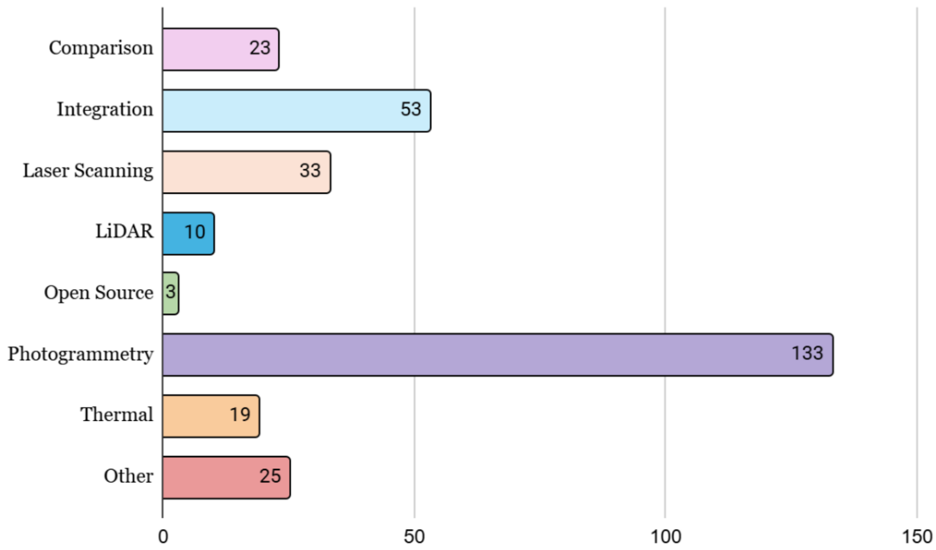

Figure 10- Article Categorization by Label

The label “Other” refers to technologies that were compared or integrated with the technologies studied in this paper (photogrammetry, LiDAR, thermal imaging). The studies referred to in this chart are among the included and maybe pile, but only the ones that were classified as included were considered for the realization of the state of the art. Although there were 137 studies considered as “Included”, an additional filtering step was applied to assess how closely each study aligned with the objectives of this dissertation, based on their abstracts and main topics. Leaving 31 studies to be analyzed in the following section.

2.3.1. EXISTING LITERATURE

2.3.1.1. DAMAGE DETECTION USING UAV-BASED POINT CLOUDS

Thanks to the advancements in photography, deep learning and 3D point cloud gathering technologies, the use of UAVs for building documentation has significantly increased in the last years. Due to their high-definition images and Multiview capabilities, the UAV represents a non-invasive and efficient way to extract detailed models of building facades. Various studies have demonstrated the value of digital 3D façade reconstruction and the capabilities of the associated technologies. For instance, manual damage assessment is often expensive, time-consuming, and may be hindered by site accessibility problems, Vetrivel et al. (2015) state that the identification of damage in buildings based on the gaps present in 3D point clouds from very high-resolution oblique airborne images can provide the essential geometric and radiometric features of both the roof and façades of the building. However, they can contain gaps that result either from physical damage or from a range of image errors or data acquisition conditions. Accurately classifying these gap types is critical for 3D geometry-based damage assessment. The study developed a methodology to address this issue; it delineates buildings from a point cloud generated from UAV imagery and classifies the present gaps in them. This was accomplished by locating and merging the roof components of separate buildings in the previously segmented 3D point cloud. This approach detected 96% of the buildings from a point cloud generated using airborne oblique images. The gap detection and classification methods were tested using two other data sets obtained with UAV images with a ground resolution of around 1–2 cm. The gaps due to damage were identified based on the surrounding damage pattern, applying Gabor wavelets and a histogram of gradient orientation features. Two learning algorithms, SVM and Random Forests, were tested for mapping the damaged regions. The learning model based on Gabor features with Random Forests performed best, identifying 95% of the damaged regions, when used in a supervised learning approach.

Still within the scope of damage assessment, (Vetrivel *et al.*, 2018) hypothesized that the use of convolutional neural networks (CNN) features, either independently or in combination with 3D point cloud features, would yield improved performance in damage detection. They used CNN and 3D features, both independently and in combination, using images from manned and unmanned aerial platforms over several geographic locations that vary significantly in terms of image and scene characteristics. Several automated methods based on supervised learning have already been demonstrated for damage detection using oblique airborne images. However, they often do not generalize well when data from new unseen sites need to be processed, hampering their practical use. To address this, they introduce a multiple-kernel-learning framework, an effective way for integrating features from different modalities. In this case, it was used to integrate 3D point cloud-based features and CNN features for classification and is also used as a feature selection approach by inferring the contribution of each feature subset in the classification accuracy. Ultimately, the CNN features produced an average classification accuracy of about 91%, and the integration of 3D point-cloud features led to an additional improvement of about 3% (94%). Moreover, this integration significantly enhanced the model's transferability accuracy by up to 7% compared to using CNN features alone.

2.3.1.2. OBLIQUE AND NADIR PHOTOGRAMMETRY FOR 3D MODELING

The use of oblique images to build 3D models has been experimented since 2008-2009, however, the integration of computer vision algorithms in common software tools critically increased the method's potentiality. Aicardi et al. (2016) evaluated the possibility of acquiring and using oblique images obtained by UAV and traditional COTS (Commercial Off-the-Shelf) digital cameras for the 3D reconstruction of historical buildings. The system was tested in the S. Maria Chapel, a part of the Novalesa Abbey (Italy). Instead of a nadir camera and 4 oblique (45°) sensors pointing to the cardinal directions, a common Hexacopter (Mikrokopter) mini-UAV was used for data acquisition. It has a payload of 2 Kg and a flight time of about 10-12 minutes. A common digital camera (Sony ILCE-5100) was also employed. The acquired data was processed using the Structure from Motion (SfM) approach implemented in different software tools based on algorithms of photogrammetry and computer vision (CV): Agisoft Photoscan Professional (PS), Pix4D, 3Df Zephyr (3DZ), SURE, MicMac (MM), VisualSFM (VSFM), and ContextCapture (CC) package. MicMac and VisualSfM are open-source software. The results achieved were analyzed and compared with the reference LiDAR data obtained from a terrestrial laser scanner (TLS) survey, using the FARO Focus 3D. This study proves how 3D reconstruction of buildings can be performed using low-cost alternatives without necessarily giving up quality.

Photorealistic 3D models are fundamental to the spatial data infrastructure of a digital city and have numerous potential applications in areas such as urban management and environmental studies. 3D models generated from aerial oblique imagery in urban areas may show geometric defects and blurred textures, especially on building façades, due to problems such as occlusion and large camera tilt angles. Meanwhile, mobile mapping systems (MMSs) can capture terrestrial images of close-range objects from a complementary view on the ground at a high level of detail but do not offer full coverage. Moreover, in urban areas, Global Navigation Satellite System (GNSS) positioning may be inaccurate due to the blocking of signals by tall buildings, causing the error to be as large as 5 m or even worse, which is below the required level of accuracy (better than 1 m) for city modeling. These two methodologies could be integrated through automatic feature matching and combined bundle adjustment (BA), yielding optimal image orientation parameters that better co-register the aerial and terrestrial datasets. The combined data can be imported to generate dense point clouds and surface models with better geometric accuracy using existing scene reconstruction software. Finally, the textures of building façades are optimized using image patches from terrestrial views, resulting in higher-quality 3D models. A fundamental step is to ensure that both data sets are georeferenced and, at least, have a unique spatial reference. As their images are captured separately by sensors onboard different platforms, inconsistencies between them are inevitable. The integrated aerial-ground environment can be used for numerous 3D mapping and modeling tasks with improved performances (Wu *et al.*, 2018).

Within the photogrammetry framework, as shown before, several methods exist for capturing this data, with nadir imaging being one of the most widely used, particularly for mapping purposes. Nadir surveys mean that the images are shot with the camera axis along the vertical direction; they provide both a forward overlap between shots and a side one between strips, allowing for the reconstruction of the surveyed territory or object in 3D. This type of survey is not appropriate for 3D modeling of towns or cities, where it is important to have a complete 3D modeling of each building, including the façades and footprints of buildings. The data from Nadir UAV surveys can be completed with point clouds gathered with other types of sensors, producing a 3D model that is both complete and more accurate (Vacca, Dessì and Sacco, 2017). The research studies the potential use of images from both nadir and oblique UAV surveys for the measurement of the dimensions of buildings, such as heights, areas, and volumes, to set the parameters related to the production of urban and suburban planning. First, a nadir flight acquired images over an area of about 3.5 hectares containing 30 buildings, then a second flight, performed with both a nadir camera and an oblique camera, was conducted on a single building. The images from the flights were processed with Photoscan software by Agisoft and with Pix4D, studying their different potentialities and functionality. The FlyNovex UAV system by FlyTop S.p.A., a hexacopter weighing 6 kg with a 5 km range and 20 min autonomy, was used for both case studies. The system contains an IMU (inertial measurement unit), a GPS receiver, and a camera mounted on the gimbal. The UAV has a wireless connection with a computer working as the ground control station. The camera is a Sony Alfa 6000 with a resolution of 6000 × 4000 pixel, a focal length of 16 mm, a sensor size of 23.5 mm × 15.6 mm, and a pixel size of 3.92 µm. The images were processed using two programs that employ the Structure from Motion (SfM) technique: Photoscan and Pix4D. SfM is a low-cost technique for creating complex 3D models from overlapping images. It uses bundle adjustment and automatically matches points across images to determine the 3D structure and camera positions. This technique works best with images that overlap a lot and are taken from different angles. The results of the second case were compared with those obtained from a TLS survey using a Faro Focus 3D. This instrument is a compact scanner that is characterized by an operative range that varies between 0.6 m and 120 m, with a linear distance error of ±2 mm for scanner-object distances comprised between 10 m and 25 m. The processing of the scans was done using the JRC Reconstructor Software v. 3.1.0 by Gexcel Ltd. (Spin-Off of the University of Brescia, Bergamo, Italy). The comparison was carried out by comparing the measurements of distances, areas, and volumes taken on the point clouds obtained from UAV and TLS surveys, and comparing the point clouds themselves using the open-source software CloudCompare. It was done by calculating the minimal distance between every point of the models using the nearest neighbor algorithm. Furthermore, the software allows the calculation of statistical values, such as the minimal distance, maximal distance, average distance, and standard deviation. The study shows that the integration of the nadir and the oblique flight increases the number of recorded points considerably, describing the façade in much greater detail.

2.3.1.3. Integration of Photogrammetry and Laser Scanning

Photogrammetry has been shown to integrate easily with other point cloud data acquisition methods since it is considered cost-effective, and efficient and allows a better interpretation of surface linear characteristics for representing real-world structures in a high-quality 3D textured model. The major advancements in computer vision and algorithms automated the procedures available to obtain the corresponding point for most pixels in the image. The result is dense, textured 3D point clouds. Combining laser scanning and photogrammetric techniques to overcome existing bottlenecks has proved to be the most effective way to record large and complex heritage sites in applications for documentation, structure assessment, texture mapping, and feature extraction (Alshawabkeh, Baik and Miky, 2021). The study combines TLS with 3D photogrammetric point clouds to create HBIM (Heritage BIM) objects that accurately represent the detailed shapes of the scanned structures. This workflow provides an effective methodology for data fusion using the Iterative Closest Point (ICP) algorithm to produce complete and accurate geometry. In this instance, common features at roof edges and corners were used to manually select matching points to estimate the initial alignment between the two-point clouds. Translation and rotation parameters (Tx, Ty, Tz, ω Φ ƙ), shown in *Figure 11*, were used to characterize the position and orientation differences between the TLS and image models. The alignment was then adjusted using the ICP algorithm. The study goes beyond just geometrical representation; it presents a comprehensive Building Information Model of the architectural elements that was produced by importing the point cloud into Revit. Depending on their degree of detail and shape complexity, components were categorized as either regular or irregular surfaces. While irregular elements, like doors and windows, required more attention because of their complex features, regular elements, like floors, roofs, columns, and walls, were modeled using Revit's basic tools. In cases of complex geometry, the point cloud data provided precise dimensions for modeling and regular objects and vertical grid sections were manually traced. Following modeling, an HBIM library was linked to a database that allowed for parameter-based changes, and material, texture, and historical context were added. avoiding the need to start from scratch, thus simplifying the modeling process for buildings with comparable shapes.

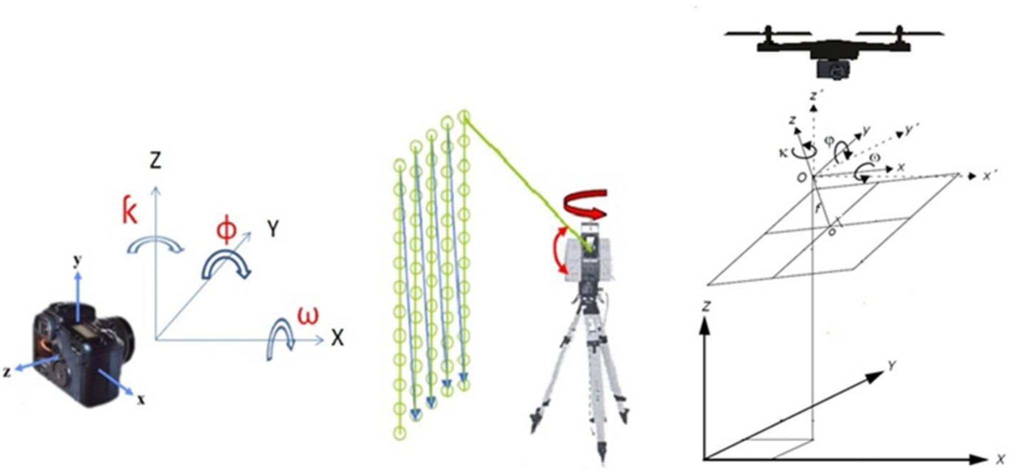

Figure 11- Translation and Rotation Parameters [extracted from Alshawabkeh et al. (2021)]

Alternatively, UAV photogrammetry can be integrated with laser scanning in a different manner, Chen et al. (2022) pr proposed a framework, where instead of combining the results of surveys utilizing different sensors, it first realizes a photogrammetry UAV survey to construct a low-resolution 3D model, to use as a reference for TLS candidate scan positions simulation. Currently, the scan positions are mainly determined by the experience of the operators, and it can easily lead to data redundancy and data holes, while seriously affecting the efficiency, cost, and data quality. It is necessary to intelligently plan the TLS observation network so that the operators can directly and quickly acquire high-quality building facade TLS point clouds according to the planned scan positions in a field campaign. Light detection and ranging (LiDAR) is usually used for capturing the three-dimensional data of facades, such as mobile laser scanning (MLS), terrestrial laser scanning (TLS), and backpack laser scanning (BLS). In particular, because of high integrity, high density, high accuracy, and flexible station setting, TLS has become the most commonly used means to capture building facade point clouds. The studied methodology aims to resolve the drawbacks of current planning techniques and produces high-quality point clouds, by decreasing the computational burden and increasing the dependability using a weighted greedy algorithm and registration assessment method. Ultimately, when compared with conventional 2D techniques, the experimental results show better performance in complex environments, with notably gains on the coverage of buildings during actual scanning experiments.

Rebelo et al. (2015) carries out a comparison between airborne LiDAR and stereo aerial images for extracting building parameters (facade height and volume), using open-source software. In the study, surveys were conducted at Praia de Faro, on the South Coast of Portugal. Using a TopEye MK II, attached to a helicopter, at a flight height of 500m above ground, for the LiDAR survey. Plus, a Swinglet CAM (fixed-wing UAV) produced by SenseFLY Company, was employed to acquire the UAV imagery data. Using a higher endlap (along flight) of 90% and a sidelap (between flight lines) of 60%, at last, the study area was covered by 46 aerial images. The results obtained were very similar to using both LiDAR and UAV. However, the study concludes that if the urban area has dense vegetation and tall trees near the buildings, UAV data can be more appropriate, because it does not introduce residual information in the process. Nonetheless, this is only true if trees do not completely surround the building, otherwise, there would be gaps in the buildings. Furthermore, the study demonstrates that low-cost UAV imagery, together with a robust methodology, using open-source tools can be very useful in the production of 3D building models for urban planning. The accuracy of the results shows that it can be enough for monitoring the built area, and that UAV technologies are a viable alternative to LiDAR.

An innovative take on how to combine photogrammetry and LiDAR can be seen in the study realized by (Andaru *et al.*, 2019). The study combined terrestrial Lidar and UAV photogrammetry, using Iterative Closest Point (ICP) algorithms into one reference system. to create detailed and realistic 3D models of architectural heritage employing Unity 3D Game Engine. The combination of both data can produce the entire building from the bottom to the rooftop in detail, completely, and realistically. The study states that Unity 3D Game Engine is the highest quality game engine available in the market. Furthermore, 3D game engines can be repurposed for better visualization, format interoperability, and other spatial-related functions or applications. To produce 3D models, researchers used laser scanners and UAV imagery to gather data from Kotagede Great Mosque and Vredenburg Fort Museum (Indonesia). Before integrating point clouds into complex models using Autodesk Maya and Unity3D, they processed and enhanced them using a range of tools and techniques, including Motion and Multi-View Stereo (SfM-MVS), Agisoft Metashape, and Random Forest Machine Learning (RFML). The final 3D models were textured and exported for interactive visualization to achieve resolution and accuracy comparable to traditional TLS techniques. The result was an interactive 3D model of an architectural heritage building in LOD3 with spatial function for measuring the size and dimension, as well as the area of the object. Ultimately, the researchers created an online version of an interactive 3D viewer utilizing WebGL API and Mapbox Unity SDK. The study proves that the integration of UAV photogrammetry and Terrestrial Lidar is an effective way to achieve quick and precise results in alternative platforms.

2.3.1.4. THERMAL IMAGING FOR ENERGY AND FAÇADE ANALYSIS

Thermography is a method used to detect surface temperature values of building envelopes to measure energy loss. Hou et al. (2021) presented a framework for integrating RGB and thermal imagery from UAVs, to enable large-scale 3D thermal mapping for energy audits. In the proposed approach, UAVs mounted infrared thermal (IRT) cameras were deployed to collect data. The images are then used to reconstruct 3D models with photogrammetry technology, which allows city and building managers to fully audit an entire district, construct 3D as-is building energy models, and conduct energy simulations and diagnostics. A FLIR DUO Pro R camera was used in the data collection system, this camera has both a thermal lens and an optical RGB lens in a single integrated package. One of the benefits of using this camera is that both thermal and RGB images can be obtained with one flight task, and the gap between them is shorter than if using two separate cameras, which can reduce the uncertainties for image registration. By locating feature points shared by several images that store important spatial and visual information, also known as tie points, photogrammetry algorithms can reconstruct 3D models. A significant limitation is that thermal images aren't sufficiently detailed, meanwhile, RGB images offer high-resolution data that is perfect for identifying tie points. To get around this, the study uses high-resolution RGB images to create a mapping model and then adds thermal information to the tie points in the RGB mapping model. The main process included four steps: data collection under varying conditions (altitudes, angles, flight paths, and building styles), image preprocessing and registration, thermal-RGB tie point fusion during photogrammetry, and performance evaluation using metrics like mean square error. This research demonstrated that using high flight altitudes could reduce the ability of tie points to link to more thermal images. The number of tie points, which had the number of k (number of associated thermal images) greater than 5 in the 45-degree experiment was greater than the number of tie points in the 30-degree experiment. The 30-degree experiment also diminished the possibilities for tie points to find more thermal image sources. Indicating that a 30-degree thermal camera angle is better for roof inspection, while a 45-degree thermal camera angle is suggested for façade inspection when using the tie point data fusion approach. Additionally, the research demonstrated that the data fusion approach performed better when surveying traditional urban European buildings than when surveying modern buildings on campus, and that the Y flight performed better than the mesh grid flight path for the tie point data fusion approach. Although thermal image resolution and edge distortion are still issues, mapping accuracy is greatly improved by aligning thermal and RGB images at tie points.

Mapping UAV-based thermal images of building façades onto BIM can greatly support building energy audits. However, accurately registering these images is challenging due to the thermal image's unique characteristics of low texture and high distortion. Zhang et al. (2023) proposed a multi-source image fusion framework to address these issues. First, the study develops a low-cost target, using 3D printing, for calibrating UAV thermal cameras. To accurately register thermal images with BIM, the rectified thermal images are subsequently fused with RGB images using homography transformation. By identifying similarities between the RGB and thermal images, the study calculated the homography matrices. As shown in *Figure 12*, these features were then matched across image pairs, and the homography matrix H was estimated to convert coordinates from the thermal image plane to the RGB image plane, thereby warping the thermal image to match the RGB one. Pixel-level fusion was made possible by superimposing the converted thermal images on top of the RGB images after homography was applied. This step was critical before applying histogram-based thermal enhancement and later using the fused images for texturing the BIM model. Additionally, the study also proposes a histogram-based approach to correct the thermally inconsistent phenomenon and enhance the contrast to produce high-contrast thermal-textured BIM. Ultimately, the study conducts a case study on a masonry building, demonstrating the feasibility and effectiveness of the proposed framework. The developed target can provide high-contrast thermal images for thermal camera calibration. Moreover, the rectified thermal images can be registered and fused with the corresponding RGB images with a mean error of around 5.713 pixels. Finally, the histogram-based approach can correct thermally inconsistent phenomenon between adjacent thermal images and further enhance the image contrast of thermal orthophoto. Thermal damage can be identified from the enhanced thermal orthophoto thanks to its high contrast.

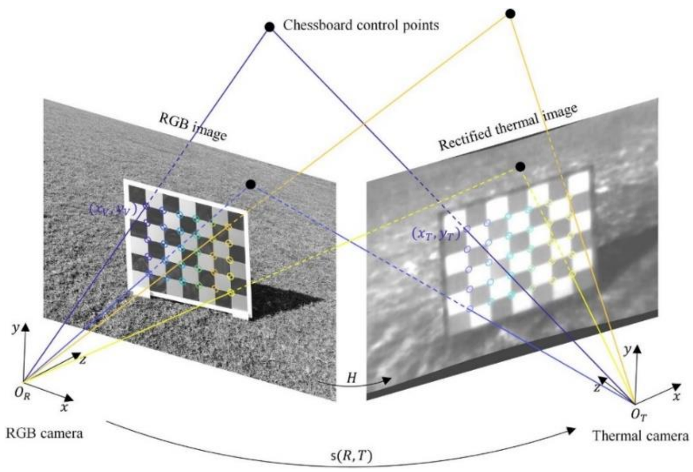

Figure 12- Homography transformation from RGB image to rectified thermal image [extracted from Zhang et al. (2023)]

Alternatively, Ma et al. (2024) proposed a different framework regarding the use of thermal imagery in façade inspection. It explains how identifying irregularities in adhesive tiling systems on building façades is essential for preserving structural integrity because debonding is a serious risk because it is common and invisible. Commonly used for facades, ceramic tiles can develop flaws due to non-standard construction and exposure to the elements, which can cause detachment and possible pedestrian hazards. These irregularities expose the interior structure of the building to the elements, which speeds up deterioration by causing moisture intrusion and changing the distribution of thermal stress. The study employs infrared images to analyze façade tile behavior based on the impact of variations according to three factors (angle, distance, and solar illumination). For this, an experimental study was conducted using a masonry wall clothed with tiles for inspection that was built in a laboratory. White elongated tiles were used for this case since they are one of the most widely used types from the late 1990s to the early 21st century in China. The setup was intended to mimic a natural setting for ceramic tiles, and debonding defects were purposefully produced by applying mortar only to half of each tile. The study used a Littro uncooled thermal camera to take pictures and created datasets based on angle, distance, and solar illumination factors to simulate real-world conditions. It is necessary to specify that the camera was mounted on a 600 mm high tripod and was connected to a laptop through a data cable, to simulate a drone's flight by controlling and adjusting the position of the infrared camera. The study concludes that the camera lens should maintain a principal axis angle of no more than 55° horizontally from the normal vector of the facade for successful UAV-mounted infrared imaging. If the distance is greater than 4 meters, the angle should be adjusted to no more than 45°. The optimal shooting range is between 1.50 and 4.75 meters; longer distances are acceptable but not less than 1.50 meters. The optimal time to acquire infrared images is between 9 a.m. and 3 p.m.; after this, efficacy decreases. Moreover, this study shows an alternative application for thermography in façade inspection.

The approach taken in this dissertation draws from a study by Parracho (2021), who provided support in the development of this work. The study states that thermography allows the examination of building behaviors and faults by detecting temperature variations on surfaces, which reflect the emissivity differences and material properties. As energy consumption in buildings has increased due to population growth and improved living standards, there is a growing interest in analyzing building energy performance using BIM and Building Energy Models (BEM), which streamline data integration. To enable the quantitative energetic analysis of building envelopes, the study focuses on developing a methodology that can digitally integrate the data obtained through photogrammetry and thermography of a building to a BIM environment, exclusively using UAV-mounted sensors for the data collection. It also explores the European and Portuguese regulations for UAVs implemented in 2021. Additionally, it facilitates comprehensive 3D geometric and thermal analysis of existing buildings (as-is) for future energetic assessments. For his end, the study utilized a DJI Mavic 2 Enterprise Dual from FEUP's Civil Construction Lab and the open-source software Blender to integrate these technologies, it also relied on existing marking onsite, to replace traditional GCPs, using them as reference marks for the alignment of the collected datasets. Finally, to ensure more exact outcomes and safer operations, critical calibrations were performed, including vision systems, infrared sensors, and IMU components.

2.3.2. Challenges And Gaps

The literature currently in publication indicates that while UAV-based technologies such as photogrammetry, LiDAR, and thermal imaging have all demonstrated significant promise in the context of building inspection and 3D façade reconstruction, few studies integrate these three sensing methods into a coherent workflow. Most research efforts focus on one or two of these technologies in isolation, addressing specific applications like geometric modeling, damage detection, or thermal diagnostics. Very few studies attempt to combine even two of them, and almost no one fully explores the integration of all three in a unified process for façade modeling, particularly when aiming to do so using open-access software environments. By suggesting an integrated methodology that concurrently utilizes UAV-based photogrammetry and thermography, as well as an iOS device equipped with LiDAR, to process and combine the gathered data using open-source tools like Blender and the Bonsai add-on, this dissertation identifies and attempts to fill this research gap. However, the development of such a workflow faces several technological and methodological challenges.

First, the existing research is fragmented and lacks cross-disciplinary integration. Given that photogrammetry can produce visually rich and high-resolution models, it is still widely used even though environmental factors like lighting, surface texture, and occlusions affect its accuracy. In urban or semi-enclosed settings, such as the FEUP's "B" building, this is especially problematic because various elements may be shaded, reflective, or have repetitive textures, which hinder feature matching and produce incomplete models. Although oblique image capture enhances detail on vertical surfaces, it also causes problems with flight planning and processing time, especially when using computationally demanding Structure from Motion (SfM) and Multi-View Stereo (MVS) algorithms that are prone to gaps when surface contrast is low.

On the other hand, LiDAR works well in any lighting situation and offers high-accuracy geometric data. However, its high cost, weight, and energy consumption limit the viability of using it on smaller UAVs or for extended missions. In addition to being visually sparse, LiDAR's dense point clouds require extensive post-processing and filtering, particularly when combined with texture-rich photogrammetric models. When trying to register LiDAR data to photogrammetric meshes or thermal overlays, it is important to pay close attention to the point density, acquisition angle, and GNSS/IMU calibration as these factors also impact model consistency and spatial alignment.

Moreover, complexity gets increased by adding thermal imaging, whereas it provides useful diagnostic information, such as identifying heat loss, moisture intrusion, or insulation failures, its spatial resolution is poor, its geometric accuracy is limited, and it is more susceptible to environmental influences. Thermal image quality can be compromised depending on the angle and distance between the UAV and the studied element, surface emissivity, solar exposure, and time of day. According to the literature, thermal data is rarely directly aligned with 3D models; when it is, proprietary software or simplified 2D overlays are typically used. For projects like this one, where thermal data is anticipated to make a substantial contribution to the spatial and diagnostic analysis of buildings, this is a major drawback.

A key challenge lies in the fusion of these three data types into a single, coherent 3D model. The resolutions, data formats, and spatial references of the outputs produced by each technology vary. LiDAR produces sparse but extremely accurate point clouds with embedded geolocation; photogrammetry produces dense point clouds or color-rich meshes from RGB imagery; and thermal cameras provide pixel-based raster data that needs to be geometrically corrected and mapped onto intricate surfaces. It is technically difficult to align these datasets, especially when open-access software is used and does not have specific tools for automatic scale adjustment or multimodal registration. Most integration efforts reported in the literature either depend on manual alignment, external proprietary software, or customized code that is not openly documented, limiting reproducibility and practical adoption.

Additionally, while commercial platforms now offer semi-integrated solutions for combining RGB, LiDAR, and thermal data, these solutions are still costly and often difficult to use or customize. However, while open-source tools like Blender, CloudCompare, and Meshroom offer flexibility, they lack standardized, user-friendly procedures for integrating multi-sensor UAV datasets. Therefore, a major obstacle to widespread adoption is the lack of documented, interoperable, and scalable workflows utilizing only open-source tools.

Lastly, multi-sensor integration becomes increasingly complex due to operational limitations associated with UAVs. It is challenging to gather all three forms of data in a single mission with lightweight drones like the DJI Mavic 2 Enterprise series due to payload and flight time constraints. The use of multi-pass approaches involving different UAVs require careful planning, standardized flight settings, and accurate co-registration techniques. In addition, logistical and legal constraints, especially in dense urban environments, limit the flexibility of acquiring optimal datasets. These factors include flight height restrictions, GPS interference near structures, and EU laws that demand visual line-of-sight.

In summary, while the benefits of UAV-based photogrammetry, LiDAR, and thermal imaging are well known, little is known about how these technologies can be combined for an open-source Scan-to-BIM purposes. The integration of image-based data into BIM workflows as textures (Image-to-BIM) is also underexplored, particularly when relying solely on open-source tools. The operational limitations of open-access workflows, small UAV platforms, the lack of integrated, and the technical difficulties of data fusion are the primary challenges this dissertation aims to address.

3
PROPOSED METHOD

3.1. OBJECTIVE

To display the application potential of UAV-mounted photogrammetry, LiDAR, and thermography by developing a work frame where these three technologies are employed in the same scenario, with similar conditions, for Scan-to-BIM purposes. To examine and compare the results obtained and eventually integrate them into a single workflow seeking that their strengths compensate for each other's weaknesses. This method is proposed to address the gap observed in the previous chapter, where the integration of these three methodologies for façade reconstruction hasn't been addressed yet.

3.2. PROPOSED METHODOLOGY

In this section, the proposed methodology is presented for the conduction of the open-source Scan-to-BIM approach and the different surveys taking place in the study, establishing a continuous workflow starting with an initial assessment phase, where the applicable flight legislation will be reviewed, the initial site survey will take place to recognize the main characteristics of the field, and the aerial and manual surveys' trajectories will be planned. Subsequently, the activities associated with data acquisition and processing will be conducted to finally fuse the gathered information associating semantic data with the elements, to create an Open-BIM (open-source BIM) model, to finally carry out a qualitative assessment to integrate the RGB and thermal images in an Image-to-BIM procedure.

Figure 13, adapted from (Parracho, 2021), shows the proposed workflow for the case study, which will be discussed in greater depth in the following sections.

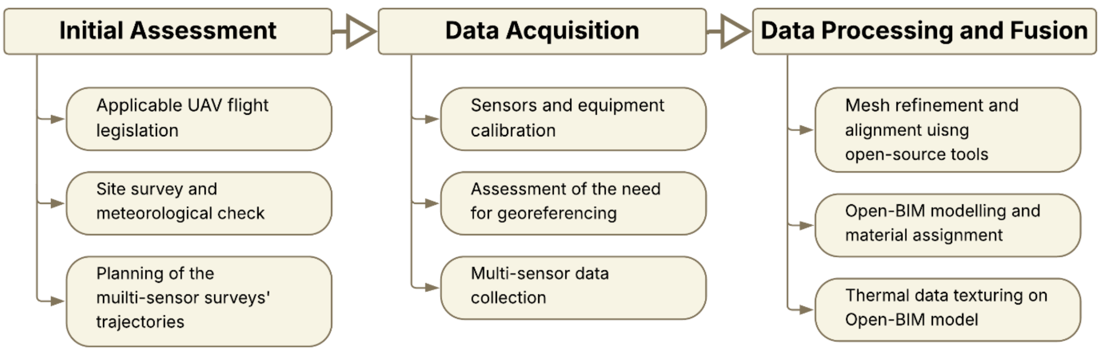

Figure 13- Proposed Workflow for the Case Study

To address the research objectives, a structured open-source Scan-to-BIM methodology was developed, starting with aerial and handheld surveys to gather the spatial data. With the aerial surveys, deploying the DJI Mavic 2 Enterprise Dual, RGB and thermal images will be collected from the façade of the building, the RGB images will then be imported into an open-source photogrammetry software (Meshroom), where from these images a point cloud with the building's geometry is generated, this open-source software can directly export the model as mesh in an .obj file, that will get imported into another open-source software (Blender), where the mesh will be optimized and refined. Meanwhile, the handheld surveys, employing an iPad Pro 11, will take place inside the building, where using the open-access app Scaniverse, the built-in LiDAR will be leveraged to acquire precise geometric and colorimetric data, this open-access app autonomously creates the geometric meshes from the surveys, which are aligned and stitched back together inside Blender. From this point the rest of the methodology will take place solely inside Blender, to further establish the open-source Scan-to-BIM methodology. Once both meshes have been properly processed, they will be matched and aligned using the native Blender's tools, then the open-source add-on Bonsai will be activated to launch the BIM stage of the methodology, where the conjoined mesh is used as a base upon which the BIM elements are traced by overlaying it. With the Open-BIM (open-source BIM) model completed, the proposed methodology takes the Scan-to-BIM a step further by conducting Image-to-BIM procedures with the initial RGB and thermal images acquired from the aerial surveys.

3.2.1. INITIAL ASSESSMENT

This section focuses on determining the precise features of the built environment to be scanned, forming an essential basis for the 3D data collection procedure. In this phase, the general legal framework regarding UAV flights in the selected field is evaluated, and the key aspects such as the overall geometry, surface materials, lighting and weather conditions, and potential obstructions are analyzed to guide the selection and configuration of the UAV and handheld surveys. Special attention is paid to the interior environment, where LiDAR can potentially perform better than UAV-based techniques, especially in terms of capturing complex geometric features. The analysis also takes into account material reflectivity and the angle at which the laser strikes a surface, as both have a direct impact on the density and accuracy of LiDAR data, and possible obstacles that can interfere with the handheld survey trajectory.

3.2.1.1. APPLICABLE UAV FLIGHT LEGISLATION

To assess the applicable legislation for the case study, first, the Geographical Zone (GZ) of the studied building should be identified, that is specified by the Commission Implementing Regulation (EU) 2019/947, which is implemented in Portugal by the Autoridade Nacional da Aviação Civil (ANAC). To identify the geographical zone in which the "B" building at FEUP belongs, the website *https://uas.anac.pt/registry/explore* was accessed, and *Figure 14* was extracted and adapted to better illustrate the separation of the GZs.

Figure 14- FEUP's Building "B" Geographical Zone [adapted from uas.anac.pt]

Area 1 (originally yellow) was tinted with a redder tone to increase the contrast between the zones and show the proximity of the building to this zone where the flight regulations are more restricted. The studied building was highlighted in purple to illustrate that it is in Area 2. Moreover, the accessed website provided the information in *Table 2*:

Table 2- UAS Geographical Zone Information for Area 2 (FEUP Building "B")

Nome/Name	Aeroporto do Porto - Área 2
Identificador/Identifier	1064UA
País/Country	PRT
Tipo/Type	COMMON
Restrição/Restriction	CONDITIONAL
Razão/Reason	AIR_TRAFFIC
ARC	ARC-d
EN-Open Cat up to 60mSFC or obstacle in 75m Radius. Mandatory equipment to provide height above SFC.	

In summary, the used UAV can only be flown up to 60 m above ground level or obstacle height within a 75 m radius, and be capable of reporting height above surface level. In addition to the restrictions related to the GZ 2 due to the building's proximity to Porto's Airport, since the UAV is equipped with a visual recording system, for the aerial surveys taking place in this study, it is necessary to obtain prior authorization from the Autoridade Aeronáutica Nacional (AAN) to ensure compliance with privacy regulations, Furthermore, according to the Regulations (EU) 2019/947 and (EU) 2019/945, and since the maximum take-off mass (MTOM) of the UAV is 1100g (C2 class), and the flights will be conducted near a building and avoiding flying over people, the operations realized in this study fall under the "Open" category and under the A2 subcategories, hence a pertinent license is required. To clarify the regulatory requirements for operating drones with different classifications and weights, *Table 3* summarizes the pilot training, flight zone restrictions, and drone specifications relevant to the A1, A2, and A3 subcategories under the EU Open Category regulations.

Table 3- Comparison of Open Subcategories Requirements for UAV Operations

Subcategory	Flight Over People	Weight/Class (MTOM)	Pilot Training	Min Distance from People
A1	Allowed - not over assemblies	C0, C1 (<900g)	Basic test	Avoid overflight if possible
A2	Not allowed - proximity is permitted	C2 (<4kg)	Extended test	≥30m (or ≥5m with slow mode)
A3	Not allowed	C2, C3, C4 (<25kg)	Basic test	≥150m from people/areas

Although the A2 certification is required for the planned operations, the author still completed the online training to be able to operate UAVs in the subcategories A1/A3, shown in *Figure 15*, to achieve a solid foundational understanding of the restrictions of drone operations in a variety of environments. This broad training enhances overall operational safety and awareness, complementing the specific skills required for A2.

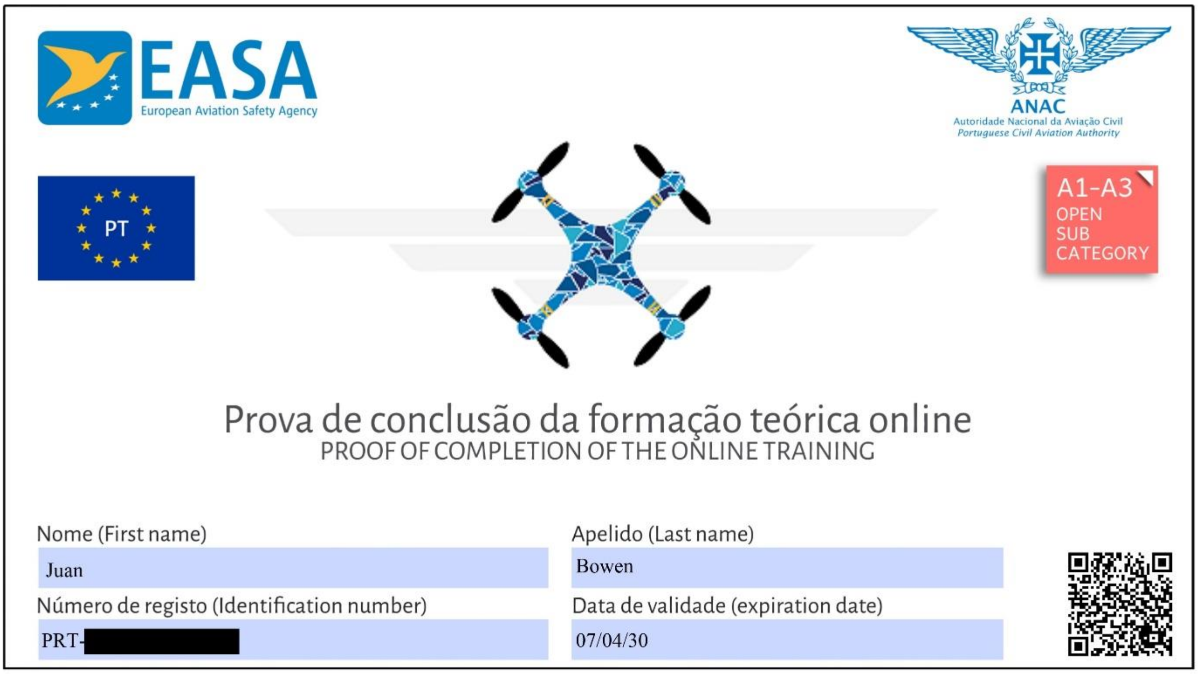
EASA
European Aviation Safety Agency
ANAC
Autoridade Nacional da Aviação Civil
Portuguese Civil Aviation Authority
PT
A1-A3
OPEN
SUB
CATEGORY
Prova de conclusão da formação teórica online
PROOF OF COMPLETION OF THE ONLINE TRAINING
Nome (First name): Juan
Apelido (Last name): Bowen
Número de registo (Identification number): PRT-[redacted]
Data de validade (expiration date): 07/04/30

Figure 15- Proof of completion of the online training [author's collection]

The Regulations (EU) 2019/947 and (EU) 2019/945 state that each remote pilot should cover the following elements:

1. Air safety: non-reckless behavior, safety precautions for UAS operations, and basic requirements regarding dangerous goods. Starting or stopping the operations considering environmental factors, UAS conditions and limitations, remote pilot limitations, and human factors.
2. Operation in visual line of sight (VLOS): keeping a safe distance from people, animals, property, vehicles, and other airspace users. Assuring a code of conduct in case the Unmanned Aircraft (UA) encounters other aerial traffic. Respect the height limitation, and when using a UA observer, ensure the responsibilities and communication between the UA observer and the remote pilot
3. Human performance limitations: the influence of psychoactive substances and alcohol, or when the remote pilot is unfit to perform their tasks due to injury, fatigue, medication, sickness, or other causes.

3.2.1.2. Site Survey And Meteorological Check

UAV operations in the “Open” category should follow the following operational procedures as indicated by the Regulations (EU) 2019/947 and (EU) 2019/945. During the pre-flight phase, an assessment of the area of operation and the surrounding area must be carried out, including the terrain and potential obstacles and obstructions for keeping VLOS of the UA, potential overflight of uninvolved persons, and the potential overflight of critical infrastructure. All removable components of the UA must be properly secured. A safe area where the remote pilot can perform a practice flight must be identified, and the environmental and weather conditions (factors that can affect the performance of the UAS such as electromagnetic interference, wind, temperature, etc.) should be evaluated using methods of obtaining weather forecasts, and, if needed, calibrate the instruments on board the UA. Lastly, it is important to confirm the UAS's conditions, including its structural soundness, battery levels, and the operation of all its parts and communications systems. Throughout the flight, the operator must follow standard operating procedures and be prepared for unanticipated events such as system failures or lost data link connections. In the post-flight phase, the UAS must undergo any necessary maintenance, and the flight details must be accurately logged (EASA, 2021).

For an overall site survey, the main factor that always must be assured is safety, before starting any UAV operations. The field can be examined using tools that provide clear satellite images (such as Google Maps or Drone Deploy). Even though this task can be realized using specialized tools, manual or visual reconnaissance should not be overlooked and should still be performed, as they remain effective and provide updated and real-time information and better spatial awareness. Trees, power lines, buildings, and other structures could be visible in this step. Additionally, mobile elements such as involved and uninvolved individuals, vehicles, and other UAVs must be identified, limited, minimized, and always kept a safe distance from. Once these steps are completed, an optimal takeoff and landing area must be identified, prioritizing flat, stable, and obstacle-free surfaces. An authorization from the AAN is also required when flights may affect individuals’ privacy, ensuring that all legal and ethical standards are met.

Alongside the physical assessment of the field, a detailed meteorological check is required to confirm the feasibility of the UAV flight. Weather parameters such as wind speed, visibility, temperature, humidity, and the likelihood of precipitation must be assessed using reliable tools like UAV Forecast, Windy, or Meteoblue. Maintaining visual line-of-sight and capturing high-quality imagery requires clear visibility, and wind speed should not exceed the drone's operating range specified by the manufacturer. During photogrammetry missions, it is also advised to check the solar conditions to avoid glare and to check the dew point to prevent lenses from fogging. Moreover, for thermal imagery capturing it’s recommended to acquire the infrared images between 9 a.m. and 3 p.m. These assessments should be performed 24 and 1 hour before the flight.

3.2.1.3. Planning Of The Multi-Sensor Surveys' Trajectories

Given that the study involves outdoor UAV operations, as well as indoor handheld data acquisition surveys, their trajectories should be planned carefully. These trajectories are conditioned by the existing obstacles in the respective field. For the iOS devices equipped with a built-in LiDAR sensor, the internal survey trajectory is automatically recorded using the device’s integrated inertial sensors, camera, and LiDAR system. This enables accurate tracking of handheld movements and real-time spatial mapping without the need for external positioning equipment. In the case of UAV surveys, the remote pilot can plan the flights using tools, such as Drone Deploy, capable of determining a flight path for the UAV to follow autonomously. This kind of tool allows the predefinition of the overlapping percentage and the camera angle (Parracho, 2021).

Mueller et al. (2023) state that there are several options for UAV flight trajectories, and each of them shows a different performance depending on the scanning objective, target geometry, and environmental constraints. This study evaluates multiple UAV flight strategies, which are presented below.

- Nadir Grid Pattern: The path is composed of parallel lines, where the spacing is defined based on the overlapping percentage, and the camera is perpendicular to the ground. This technique is mostly used on top-down orthomosaics, and terrain models.
- Oblique Grid Pattern: Uses the same grid pattern principle but tilts the camera to better record vertical elements, it's frequently used in buildings and urban settings.
- Circle (Orbit or Perimeter): Instead of a grid, the UAV follows a circular trajectory centered on the studied element, often with a constant tilt angle. Typically implemented on towers, monuments, or isolated buildings.
- Spiral / Helical Path: Multiple angles are recorded as the UAV circles the structure along its vertical axis. This method is ideal for tall buildings, such as lighthouses or chimneys.

3.2.2. Data Acquisition

To set the foundation of the Scan-to-BIM process, the data acquisition workflow must be carefully assessed beforehand and strictly followed throughout execution. This study employed an unmanned aerial vehicle integrated with photogrammetry and thermal imaging sensors; it also employed an iOS device equipped with a LiDAR sensor to capture detailed information for interior 3D reconstruction. Each technology was used under consistent environmental conditions to enable comparative analysis and the applicability of an integrated workflow. To achieve optimal results in the realization of the different surveys, the multiple equipment and sensors had to be calibrated accordingly to ensure accurate data alignment, consistent measurements, and compatibility across all datasets.

3.2.2.1. SENSORS AND EQUIPMENT CALIBRATION

As previously stated, this study employs multiple devices for data collection, and each of them must be calibrated according to its specific sensor characteristics. For the acquisition of photogrammetric and thermal information, this study used the DJI Mavic 2 Enterprise Dual equipped with both sensors. A 12 MP RGB camera with a pixel size of 1,55 µm and an approximate field of view (FOV) of 85º. "Additionally, it features a FLIR Lepton uncooled VOx microbolometer infrared sensor with a resolution of 160 by 120 pixels, operating within the 8 to 14 µm spectral range, a pixel size of 12 µm, and a horizontal field of view (HFOV) of 57º.

The calibration of the visual (RGB) camera is essential to ensure accurate image capture and optimal performance. First, the UAV is connected to the remote controller using the DJI Pilot app. To ensure the camera alignment with the horizon, the option “Gimbal Auto Calibration” must be selected in the camera settings menu, and for geometric accuracy in mapping tasks, lens calibration using photogrammetry software should be performed involving the capturing of a series of overlapping images of a known calibration target, control marker or flat surface from multiple angles, which the software then can use to correct for lens distortions and optimize internal parameters. For indoor surveys, the lighting conditions should be adjusted to avoid any over-reflective surfaces that can interfere with the camera's performance, and the compass calibration is not necessary as stated in the DJI Mavic 2 Enterprise Series User Manual (DJI, 2021).

When the DJI Mavic 2 Enterprise Dual first boots up, it automatically calibrates its FLIR thermal sensor. However, manual calibration, referred to as Flat Field Correction (FFC), can also be triggered through the DJI Pilot app by selecting the thermal settings and tapping the refresh (calibrate) icon. FFC should be performed before each flight and frequently during lengthy flights, especially when the ambient temperature fluctuates significantly. For more accurate surface temperature measurements, users should adjust emissivity values and enter relevant environmental factors (like humidity and ambient temperature) depending on the materials being examined. For specialized industrial or inspection use cases, such as evaluating energy loss in building façades or detecting overheating equipment, precise calibration is especially important. In such scenarios, the thermal sensor's accuracy can be fine-tuned by comparing its readings to those of a known-temperature reference surface with established thermal characteristics. While DJI provides basic calibration functionality, advanced workflows often rely on external thermal standards or blackbody references to improve measurement precision in technical applications (DJI, 2021).

Finally, for the LiDAR survey, the handheld iOS devices equipped with this technology do not demand technical user-performed adjustments or manual calibration like professional-grade LiDAR equipment, hence calibration typically involves ensuring the sensor is functioning optimally and that the scanning environment is suitable. Nonetheless, users should perform certain checks before each survey, such as ensuring that the iOS device is updated to the latest firmware and that the scanning app employed is properly configured. Maintaining favorable conditions (optimal light levels or a clean line of sight) for the use of these handheld devices can enhance the data accuracy of this process. Furthermore, another relevant factor in these surveys is the scale fidelity. This can be achieved by using specific 3D reconstruction apps that adjust the scale automatically or let users place a reference object of known size to improve scale accuracy and point cloud alignment. Moreover, it is worth noting that the results obtained using this method may not match the precision achieved using professional-grade equipment. According to context the specific requirements of their surveying tasks should be considered when choosing the appropriate tools (Aksu, Günaydın and Duran, 2024).

3.2.2.2. ASSESSMENT OF THE NEED FOR GEOREFERENCING

Georeferencing is the process of aligning spatial data (such as point clouds or digital meshes) to a real-world coordinate system. Assessing the need for georeferencing is essential since it directly impacts the scale accuracy, spatial alignment, and interoperability of 3D models. To create a scaled model for design validation, construction planning, or comparison with BIM, accurate georeferencing is critical. However, since a significant objective of the study is integrating technologies on the same object, relative accuracy may be sufficient. It's important to keep into account the fact that outdoor surveys, especially façades or construction sites, benefit greatly from real-world positioning to connect scans from different flights or devices. Simultaneously, indoor surveys often don't need full georeferencing unless integrated with GIS or floor plans. Furthermore, having a shared or local coordinate system, or at least reference points, such as Ground Control Points (GCPs), is necessary for merging these datasets for alignment and comparison (Azari *et al.*, 2025).

3.2.2.3. MULTI-SENSOR DATA COLLECTION

As previously mentioned, for the multi-sensor workflow, photogrammetric data will be collected in outdoor settings using the DJI Mavic 2 Enterprise Dual for this methodology. This UAV is equipped with a high-resolution RGB camera capable of capturing overlapping images suitable for 3D reconstruction through photogrammetry. In order to ensure sufficient image overlaps while accounting for obstacles and lighting constraints, the UAV will be manually piloted along low-speed, low-altitude routes designed for the confined indoor spaces. Flights will adhere to the pre-planned trajectories to facilitate complete coverage. This unified UAV-based approach simplifies data acquisition and ensures consistency across different spatial conditions.

For the capture of the thermal data in both exterior and interior environments, the same UAV will also be used. Its integrated thermal camera allows for detailed mapping of temperature variations on building surfaces, helping to identify issues such as insulation defects, moisture infiltration, and heat loss. UAV operations may be limited or impractical for the indoor survey; to address this, a portable thermal imaging device will be employed as an alternative. The objective is to gather data from both environments and by combining these methods, accessibility, and precision will be assured.

Finally, a LiDAR-equipped iOS device will be used to generate an additional point cloud of the interior setting. This portable and lightweight tool offers a practical alternative for documenting indoor geometry, particularly in locations where UAV operation is restricted. While the accuracy is lower than that of professional-grade LiDAR systems, the iOS LiDAR provides adequate spatial data for preliminary modeling and will serve as a reference for comparing outputs from photogrammetry and thermography workflows.

3.2.3. DATA PROCESSING AND FUSION

In the processing phase, once all spatial and thermal data have been collected, this information will be converted into usable outputs for analysis and comparison. The various datasets obtained are processed using open-source software enabling the generation of dense point clouds and thermal overlays, by refining and aligning the acquired point clouds, and analyzing the RGB and thermal data to use it as a texture in the 3D model, following an Image-to-BIM procedure. Ensuring data alignment, improving model accuracy, and preparing the results for integration into the visualization and evaluation processes depend on this phase.

3.2.3.1. Mesh Refinement And Alignment Using Open-Source Tools

Following the collection of spatial data (photogrammetry and LiDAR), an unrefined or raw point cloud is generated, which often contains noise, outliers, and redundant points that decrease the model quality. Several techniques can be then applied to refine these point clouds, such as statistical outlier removal and radius-based filtering, removing all unnecessary data and keeping only the relevant spatial points. Since this study is working with multiple datasets, aligning them can represent a difficult yet important task to achieve an integrated workflow, algorithms such as ICP are often used in the aligning process.

For managing the point cloud data, Blender, a popular open-source 3D program, offers a variety of tools and plugins. The raw point clouds can be processed, refined, and aligned inside the software, using its native mesh editing features and implementing the Bonsai add-on. This can be done by selecting corresponding control points in overlapping areas or using automated registration functions. Furthermore, the software can enhance the efficiency of the model by reducing point cloud density, in cases where the model can be considered heavily loaded, assuring smooth and continuous surfaces.

3.2.3.2. Open-BIM Modelling And Material Assignment

Once the data gathered from the multiple surveys has been integrated into a single 3D model; to complete the Scan-to-BIM methodology, the aligned results will serve as a guide for modeling the identified elements with the respective IFC semantic information inside the Open-BIM software. The objective of this process is to develop an Open-BIM model by giving the modeled elements meaning by labeling and classifying architectural elements such as walls, windows, doors, slabs and other components. Using the Bonsai add-on tools and external data, objects can be classified manually based on their geometry, material and purpose, following the BIM methodology.

This enriched model supports more advanced applications such as condition assessment or maintenance planning, making the integrated dataset not only more informative but also actionable within various professional and technical workflows. Finally, the model gains interpretative value from this semantic layer, which turns it from a purely spatial or visual representation into a structured information source for analysis and decision-making.

Once the model is completed, and taking advantage of Blender's versability, the captured thermal images will be added to the model as a texture, following an Image-to-BIM framework, allowing for detailed thermal visualization directly on the 3D surface.

A practical example of Image-to-BIM can be found in (Zhang, Wang, *et al.*, 2023). To facilitate damage inspection and visualization, their research created a BIM-based image management framework that allows UAV images of building façades to be registered and projected into a BIM model. To precisely map visual inspection data (such as cracks and spalling) to building components, they aligned UAV-acquired images with an existing BIM model of a building façade. Additionally, the study generated template images with a field of view (FoV) that matched the UAV photos and used GPS and IMU data from UAV image EXIF files to position virtual cameras in Revit. Finally, they used perspective transformation to project UAV images onto the BIM's elevation view, achieving mean Image-to-BIM registration accuracy of under 21 mm in real-world tests.

3.2.3.3. THERMAL DATA TEXTURING ON OPEN-BIM MODEL

In the case of the acquired thermal data, and after completing the Open-BIM model, a similar procedure with additional steps is performed. The dataset must undergo different procedures such as lens distortion correction, temperature range adjustment for better contrast, and noise removal to isolate the relevant patterns. In function of the quality level and the data gathering conditions, additional steps such as radiometric calibration or image stitching may be applied to unify multiple thermal frames into a continuous dataset.

Following the alignment and correction process, the thermal data is prepared for texture mapping onto the 3D models derived from the photogrammetry and LiDAR scans. Using Blender, the infrared imagery is projected onto the surface of the Open-BIM elements by managing specific nodes in the built-in visual programming view in Blender and aligning the relative scale and position values, mapping the 2D texture (UV) coordinates into the 3D model, achieving a thermal Image-to-BIM workflow. This process aims to create a thermally textured model that visually integrates the achieved geometric details with the surface temperature variation data acquired with the IR cameras. Thus, producing a unified 3D representation that allows the precise identification of thermal anomalies including insulation failures, moisture intrusion, and thermal bridges.

This approach is informed by previous research, such as Zhang, Zou, et al. (2023), this research focuses on mapping UAV-collected thermal images onto an existing as-is BIM model to create a thermal-textured BIM, which is used for building energy audits. Furthermore, they used a custom 3D-printed calibration target made of PLA and matt aluminum for accurate thermal camera calibration. Similarly to the proposed framework, this study uses UAVs to capture thermal and RGB images simultaneously. RGB images are registered with the BIM using a Generalized Hough Transform (GHT) from a previous study, by matching facade components, then, matched RGB features are projected into the thermal images, transferring their BIM alignment. The final enhanced thermal orthophoto is colorized and textured onto the BIM surfaces using a Dynamo prototype, completing the Image-to-BIM pipeline.

3.3. TOOLS AND TECHNOLOGIES

3.3.1. BLENDER

The main objective of this study is to develop an open-source Scan-to-BIM workflow, for which Blender was chosen as the primary platform. Blender is a free and open-source 3D creation suite. It supports the entirety of the 3D pipeline: modeling, rigging, animation, simulation, rendering, compositing, motion tracking and video editing. It provides consistent experience across Linux, macOS, and Windows operating systems via OpenGL. Its wide variety of tools makes it suitable for almost any sort of media production. Professionals, hobbyists, and studios around the world use it for creating animations, game assets, motion graphics, TV shows, concept art and feature films. Developed collaboratively by the Blender Foundation and its global community under the GNU General Public License (GPL), Blender is a cross-platform application featuring a uniform OpenGL-based graphical user interface across all major operating systems, and is further customizable through Python scripting, making it one of the most versatile open-source tools currently available. Furthermore, through community contributions, Blender is constantly being improved, encouraging the creation of responsive features and broad adoption across various digital media domains (Blender Foundation, 2025). To get access to the Blender software, the author downloaded the latest released version at the time of writing (4.4.3) from the official Blender website.

To use Blender as BIM software, the Bonsai add-on must be implemented (*Figure 16*). This add-on by IfcOpenShell allows to natively support Industry Foundation Classes (IFC) inside Blender's 3D environment. Enabling the manipulation and edition of IFC models. Additionally, this add-on is capable to carry out other BIM processes, such as clash detection and the creation of 2D documentation. By incorporating Bonsai, Blender becomes a comprehensive platform for BIM tasks, offering a cost-effective alternative to traditional proprietary BIM software.

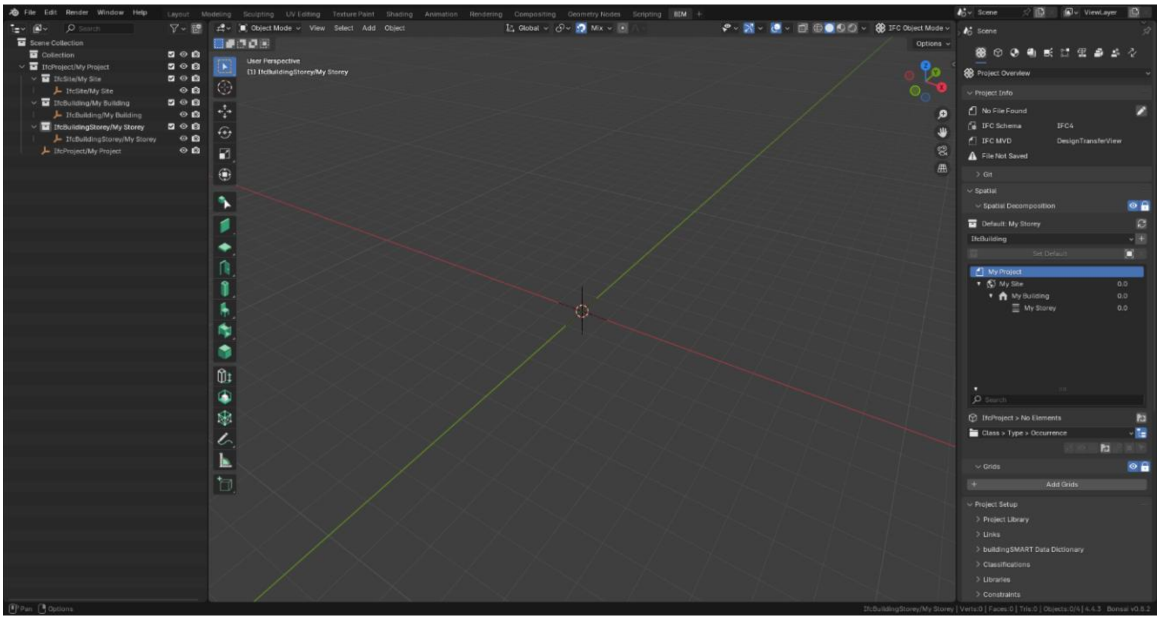

Figure 16- Blender Bonsai Layout [author's collection]

Bonsai can be downloaded from the Blender Extensions website, in this study the 0.8.2 was used to perform the BIM workflow since it's the latest release available at the time of writing. Once the addon is downloaded, to install it it's necessary to go into Blender, go to the "Edit" menu, and navigate to the "Preferences" panel, select the "Add-ons" tab, click "Install," and then choosing the downloaded .zip file. After installation, the add-on must be activated by checking the corresponding box in the add-ons list.

Blender has shown its worth in both traditional media production and more complex workflows like heritage modeling and scan-to-BIM. Several studies have demonstrated Blender's effectiveness in architectural and cultural heritage documentation. Blender 3.6.5 LTS (Long-Term Support) was utilized as a key tool by Angheluță et al. (2023) to optimize and prepare the 3D digitized model of a 17th-century church for web visualization. Mainly Blender was employed to import both high-poly and low-poly photogrammetric meshes, align them manually, and split the low-poly mesh into sections of interest based on architectural elements and imaging target. Aerial RGB and thermal textures from the original low-poly mesh were also baked onto the new UV (2D coordinate system) maps using Blender's Cycles rendering engine (*Figure 17*).

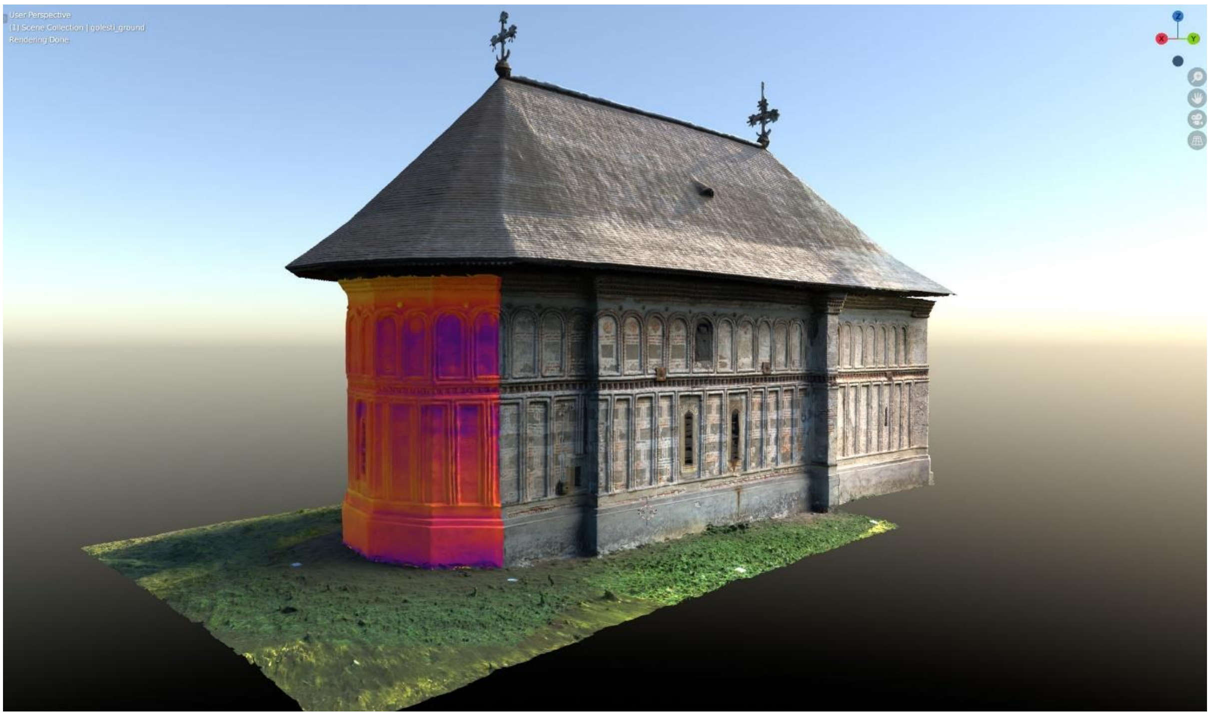

Figure 17- Aerial thermal texture baked into the 3D model [extracted from Angheluță et al. (2023)]

Another noteworthy example can be found in Lombardi & Rizzi (2024), where Blender was widely used in conjunction with BlenderBIM and the Extended Matrix (EM) Tool as part of a multidisciplinary workflow for 3D semantic modeling of archaeological sites. To model Stratigraphic Units (SU) using simplified "proxy geometries" that archaeologists developed using TLS and photogrammetric data. Additionally, with the BlenderBIM addon, these proxy geometries were transformed into IFC-compliant BIM objects (like IfcWall), enabling data exchange with software like Revit. This kept the semantic link intact and added BIM parameters to the geometry. Another salient instance is presented by Oostwegel et al. (2022), the BlenderBIM add-on was also the main tool used in this study to create the HBIM model of Mrak's homestead, a heritage building from the 17th century. The model’s elements were structured directly in Blender using IFC schema classes, which avoids data loss common in commercial software, and adding properties such as vulnerability, significance, and dates programmatically via IfcOpenShell and Python, improving overall efficiency.

Blender has earned increasing recognition in the entertainment world, which adds to its credibility outside of academic circles. Its tools for rendering and animation have been put to the test in real production settings, for example, in the award-winning Netflix series Love, Death & Robots (2019), and again in the film Flow (2024) from Blender Studio (Figure 18), which also received accolades, including a handful of Annecy Cristals, a Golden Globe for Best Animation, a César, and an Academy Award. These projects help show that Blender isn’t just useful for creative work; it’s also a capable and dependable option in areas like architecture, BIM, and even preserving cultural heritage (Crawford, 2019; Siddi, 2025).

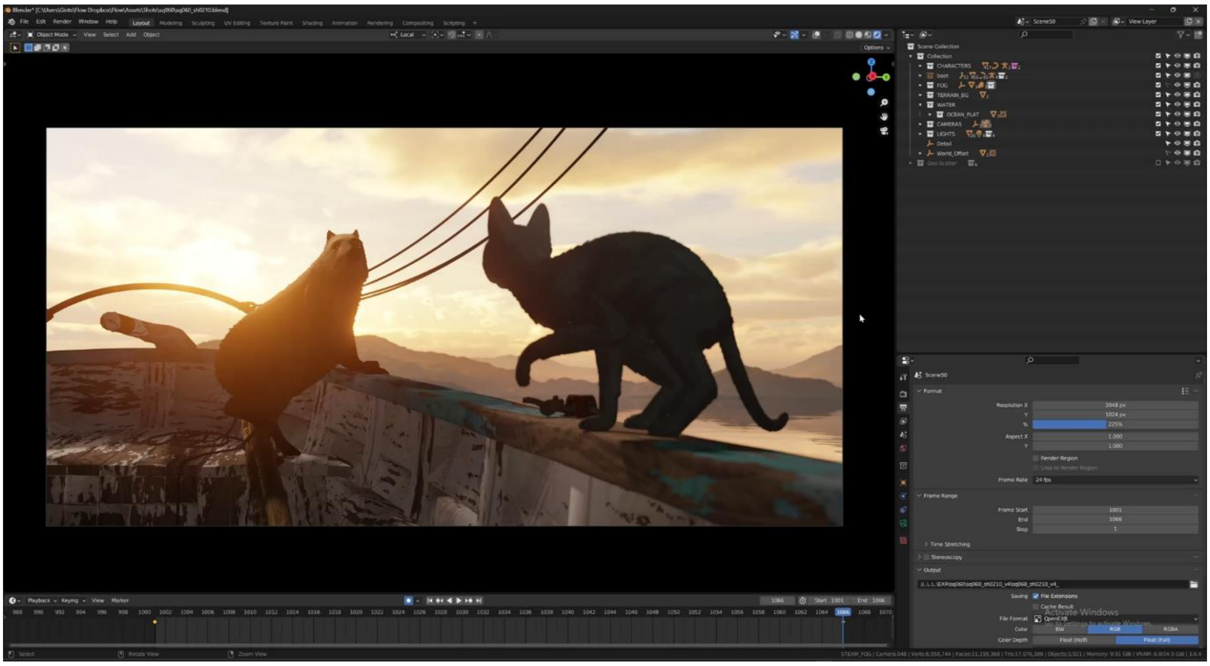

Figure 18- Animation preview inside Blender [extracted from Siddi (2025)]

3.3.2. DJI MAVIC 2 ENTERPRISE DUAL

As stated before, for the aerial surveys the DJI Mavic 2 Enterprise Dual will be employed for the aerial surveys, since it is a versatile drone designed specifically for professional use in industries such as construction, public safety, and inspection. This UAV is a part of The DJI Mavic 2 Enterprise series; this series features omnidirectional Vision Systems and Infrared Sensing Systems. Furthermore, DJI signature technologies such as Obstacle Sensing and the Advanced Pilot Assistance System help the user capture complex shots effortlessly. Additional features like the built-in AirSense make the pilot aware of the surrounding airspace, and password protection helps to maintain secure access to the aircraft and data protection. The Mavic 2 Enterprise series also present attachable modular accessories like the M2E Spotlight, M2E Beacon and M2E speaker that are purpose-built for various industrial applications.

The Mavic 2 Enterprise Dual features a fully stabilized 3-axis gimbal camera with a FLIR longwave infrared thermal camera and a visual camera, providing both infrared and visible light imaging simultaneously. Its dual-sensor capability makes it extremely useful for applications where detecting heat differences is critical, like energy audits, building inspections, and search and rescue missions. The infrared thermal camera records 640×480 video, and the visual camera captures 4K videos and 12MP photos, as shown in *Figure 19*. Meaning that it combines a high-resolution RGB camera with a thermal imaging sensor, which is optimal for the purpose of this study, since it enables users to capture both visual and thermal data simultaneously. The drone's small and foldable design, its obstacle avoidance system, and its advanced flight autonomy make it an easily portable device.

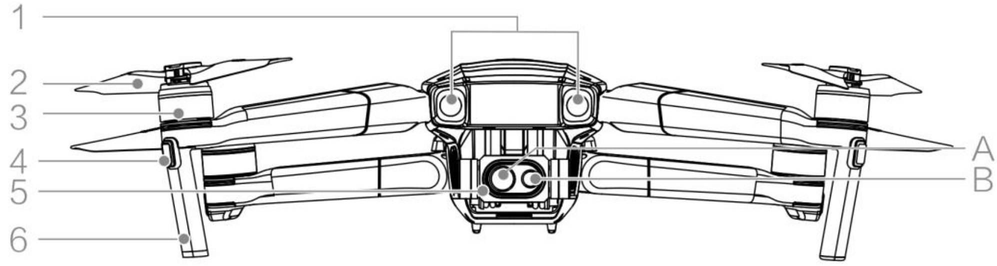

Figure 19- DJI Mavic 2 Enterprise Dual's Parts [extracted from DJI (2021)]

(1. Forward Vision System / 2. Propellers / 3. Motors / 4. Front LEDs / 5. Gimbal and Camera - A. Visual Camera - B. Thermal Camera / 6. Antennas)

The UAV includes its own proprietary remote control *(Figure 20)*, and built into it is the DJI's long-range transmission technology OcuSync ^{TM} 2.0, offering a maximum transmission range of 6.2 mi (10 km) and displaying video from the aircraft to DJI Pilot on a mobile device at up to 1080p. The remote controller works at both 2.4 GHz and 5.8 GHz, and it can select the best transmission channel automatically without any latency. The aircraft and camera can easily be controlled using the onboard buttons. An onboard LCD screen gives real-time aircraft data information, and the detachable control sticks make the remote controller easier to store. The maximum run time is 2 hours and 15 minutes. The Mavic 2 Enterprise series boast a maximum flight speed of 44.7 mph (72 kph) and a maximum flight time of 31 minutes (DJI, 2021).

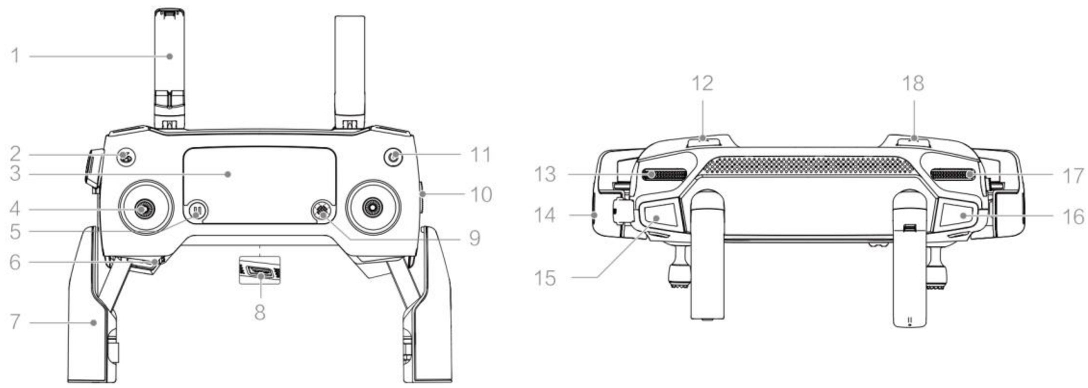

Figure 20- DJI Mavic 2 Enterprise Dual's Remote Controller [extracted from DJI (2021)]

(1. Antennas / 2. Return to Home (RTH) Button / 3. LCD Screen / 4. Removable Control Sticks / 5. Flight Pause Button / 6. Control Sticks Storage Slot / 7. Mobile Device Clamps / 8. Reserve / 9. 5D Button / 10. Flight Mode Switch / 11. Power Button / 12. C1 Button (Customizable) / 13. Gimbal Dial / 14. Video-Downlink/Power Port (micro-USB) / 15. Record Button / 16. Focus/Shutter Button)

3.3.3. IPAD PRO 11

Building on the DJI Mavic Enterprise Dual's aerial surveys, this study will use the iPad Pro 11-inch (4th generation), model A2759 with 256 GB of capacity (*Figure 21*), for handheld surveys due to its sophisticated LiDAR capabilities. This device, which was unveiled by Apple Inc. in 2022, is a strong and adaptable tablet made for both professionals and artists. Featuring the cutting-edge Apple M2 chip, delivering exceptional performance for multitasking, graphic-intensive applications, and complex data processing. This device enables precise depth sensing and high-resolution spatial mapping due to its built in LiDAR scanner, which plays a key role for capturing accurate as-built interior models. Its lightweight and portable design makes it ideal for on-site interior use within FEUP's facilities, especially inside the studied auditoriums, allowing seamless data collection and immediate processing without the need for bulky equipment (Apple Inc., 2022).

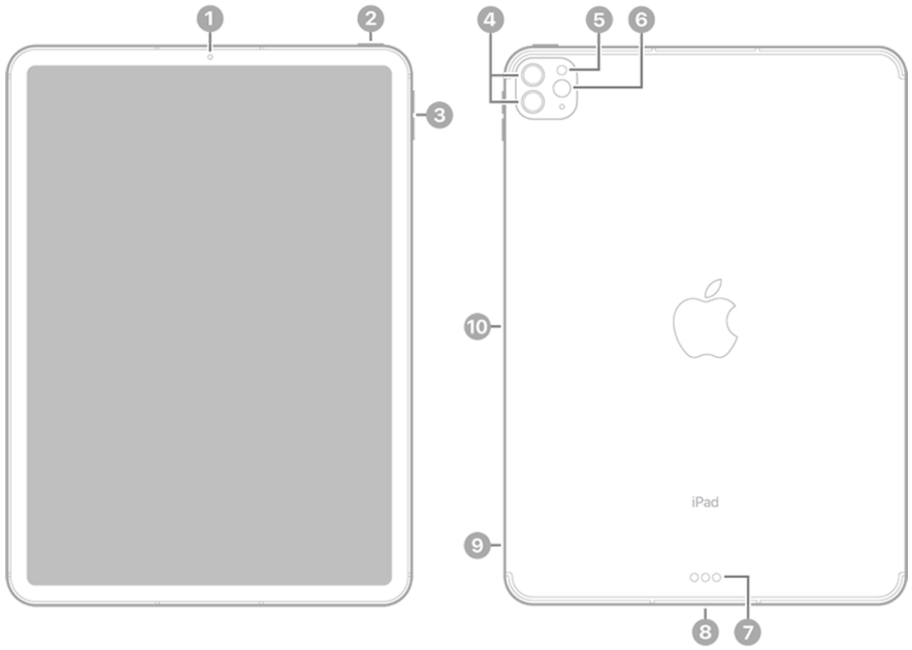

Figure 21- iPad Pro's Parts [extracted from Apple Inc. (2022)]

(1. Front camera / 2. Top button / 3. Volume buttons / 4. Rear cameras / 5. Flash / 6. LiDAR Scanner / 7. Smart Connector / 8. Thunderbolt / USB 4 connector / 9. SIM tray (Wi-Fi + Cellular) / 10. Magnetic connector for Apple Pencil)

3.4. SURVEY LOCATION

As previously mentioned, the subject of study is the B001, B002, and B003 rooms at the Faculty of Engineering of the University of Porto (FEUP). These are auditoriums located within the B building, a central facility on campus, informally known as the "Queijos" (cheeses) due to their distinctive rounded, wedge-like shape resembling cheese wedges, stand out architecturally within the faculty. These auditoriums, along with the B building, are examples of modernist architecture. The rooms have been updated since they were built, but the focus has been on technological improvements like newer audiovisual equipment, better lighting, and updated seating to make them more comfortable and accessible while preserving the original structural layout.

Located at the core of the B building, these auditoriums usually are used by multiple departments and academic programs at FEUP. With a combined area of 442,3 m2 (147 +148 + 147,3 respectively) and an overall capacity of 552 seats (184 each), these three auditoriums provide a spacious and adaptable environment ideal for large-scale academic activities including lectures, seminars and workshops (FEUP, no date). Moreover, these rooms feature an entry hall with multiple doors and an accessibility ramp, as shown in *Figure 22*.

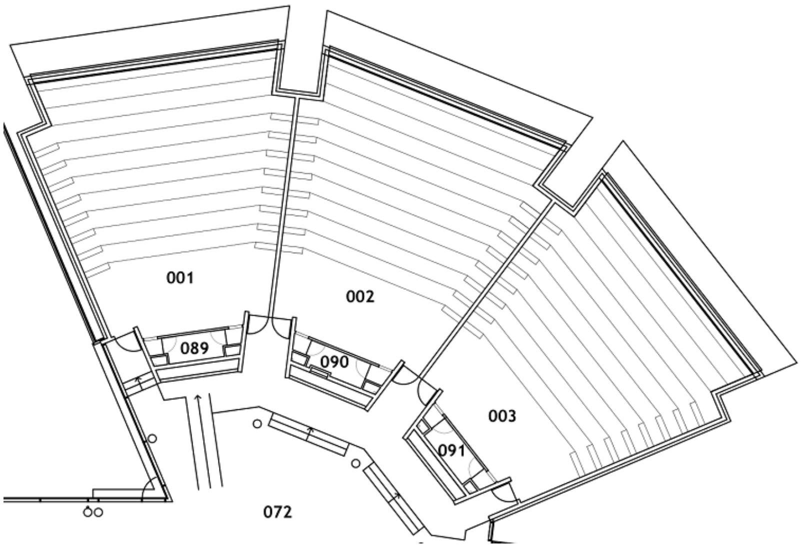

Figure 22- Auditoriums Ground floor layout [extracted from FEUP (n.d.)]

These rooms are highly relevant to this dissertation because of their size, accessibility, layout, and easily identifiable façade (*Figure 23*). They offer a perfect setting for the deployment and testing of cutting-edge multi-sensor technologies like photogrammetry, LiDAR scanning, and thermography, facilitating the collection and analysis of detailed spatial data in an academic setting.

Figure 23- Auditoriums' Façade [author's collection]

3.5. Evaluation Strategy

To assess the geometrical accuracy of the final model, a simple comparison will take place between key dimensions extracted from the model and ground truth measurements. To first register the deviation in scale to subsequently adjust the model's scale to match the reference measurements. This evaluation plays an essential role in confirming that the model accurately represents the actual proportions and measurements found in reality. Proper scaling is fundamental to guarantee that the model remains dependable for subsequent analysis, detailed documentation, and seamless incorporation into the BIM workflow. If any inconsistencies or deviations are identified during this assessment, they will inform the adjustments needed to enhance both the precision and practical application of the model.

4
CASE STUDY

4.1. OBJECTIVE

This chapter aims to address and validate the proposed multi-sensor and open-source Scan-to-BIM workflow, previously presented, by carrying out a case study within the premises of FEUP. It enables a thorough assessment of the suggested methodology's actual application in a built environment. The intended outcome of the workflow is that it can be assessed not only in terms of technical performance but also in terms of adaptability to existing architectural conditions.

The chapter concludes with a discussion of the results, providing additional context to the topics and findings previously covered. This includes reflections on data accuracy, processing limitations, and overall efficiency of the workflow. The insights gathered help to reinforce the relevance of open-source tools in academic and professional environments while also identifying possible areas for improvement or further development.

Figure 24, adapted from (Parracho, Martins and Barreira, 2022), illustrates the methodology that was applied throughout the case study. It visually outlines the sequential steps and tools used, serving as a reference framework for the practical implementation of the workflow. The process begins with the UAV capturing aerial RGB and thermic images which are processed to generate a point-cloud using the open-source photogrammetry software Meshroom, this point-cloud is imported into Blender as a .obj file (3D mesh). Separately, interior spatial data is captured through handheld surveys using the iOS device and the Scaniverse app, these scans are imported into Blender as an .obj file where they are stitched together to produce a complete 3D interior model. Once the exterior and interior meshes have imported and refined inside Blender, they're aligned to achieve a full digital reconstruction of the auditoriums. Subsequently, the Bonsai add-on, which enables Blender to function as BIM software, is activated to start modelling all the BIM elements over the acquired reference mesh. After the full Open-BIM model is completed, the RGB and thermic images obtained from the aerial survey are used to texturize the model, using the visual programmer inside Blender, following an Image-to-BIM workflow.

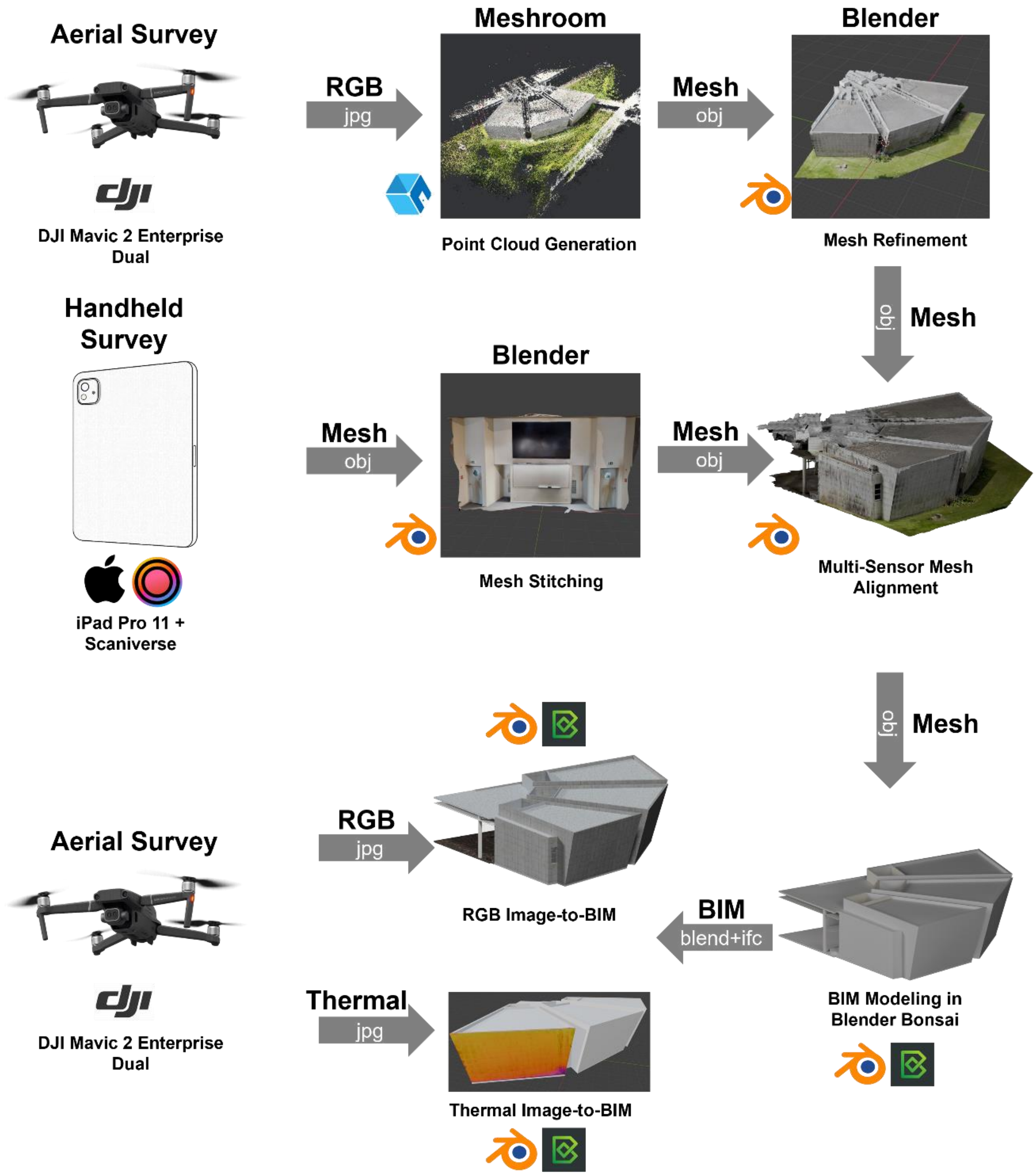

Figure 24- Proposed Methodology

4.2. Data Collection

Since one of the main objectives of this study is to integrate multiple sensors for digital surveying, the employment of each sensor needs to be planned to have an efficient workflow. The planning and execution of these surveys are explained in the following sections, detailing the tools, methodology and coordination required to optimize data acquisition and processing.

4.2.1. PHOTOGRAMMETRY

As detailed before, for the photogrammetry surveys, the DJI Mavic 2 Enterprise Dual, made available to the author by the Department of Civil and Georesources Engineering (DECG), was used to perform the aerial surveys (*Figure 25*), and Engineer Diogo Parracho supported this flights by using the DJI Pilot app and complementing it with the Drone Harmony Legacy app to define the flights trajectories, and by manually piloting the UAV when necessary.

Figure 25- DJI Mavic 2 Enterprise Dual supplied by the DECG [author's collection]

Two surveys were conducted in June, when wind and temperature conditions were considered good enough to operate the equipment. However, during the test and recognition flight, local fauna, specifically seagulls, interfered with the UAV, as shown in *Figure 26*, which caused a temporal pause to guarantee the safety and integrity of all the elements in play. Once it was considered secure to proceed with the flights, a triple grid flight path was developed to cover the entire roof of the auditoriums and partially the façade, considering nearby obstacles (trees). Additionally, the flight was set to a 15m height to maintain a safe distance from the building, and the gimbal was set to a 55°.

Figure 26- Local fauna interference [author's collection]

The second survey was focused on gathering data specifically from the façade and the areas the first flight had trouble reaching. To assure maneuverability and safety, this aerial survey was carried out manually, at a low height and keeping a safe distance from obstacles. *Figure 27* shows the execution of the manual flight led by engineer Diogo (the individual shown in the image is the author, who assisted during the flight).

Figure 27- Manual UAV flight [Supplied by Diogo Parracho]

4.2.2. LIDAR

For the interior surveys, an iPad pro with the open-access app Scaniverse was utilized to carry out the LiDAR scans. This mobile 3D scanning app uses light to measure depth and gather precise spatial data from the LiDAR sensor built into compatible iOS devices. Since the application handles all processing on the device, effective real-time feedback during data acquisition is made possible. The resulting models integrate depth information with color textures captured from the camera and can be exported in formats such as OBJ, FBX, PLY, and USDZ.

Scaniverse has several tools to help with scanning. It counts with "Splat" rendering, a crucial feature that enables users to share their scans to a global 3D map and contributes to a collaborative spatial database by representing points as tiny discs for improved visualization. However, this feature was not used in the dissertation. Instead, the classic mode "Mesh" was used since it presents more export options and still shows in the map where each of the scans were performed, including precise geographic coordinates (*Figure 28*), without sharing the data to the public.

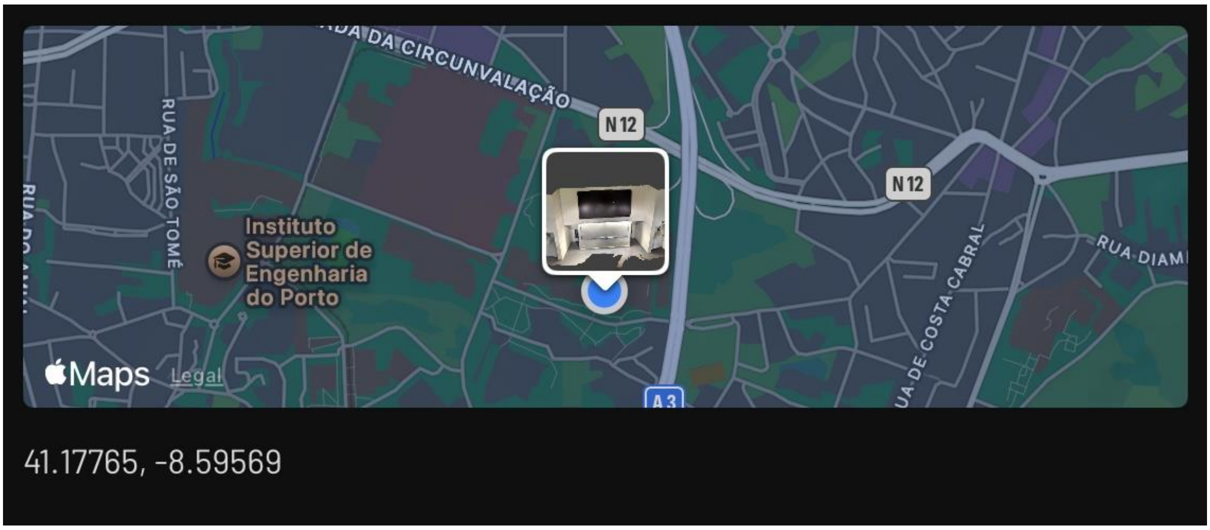

Figure 28- Scan location overview inside Scaniverse [author's collection]

While realizing these surveys, the built-in display simultaneously assists the operator by keeping track of the duration of each read, and the unscanned elements by covering them with a white and red striped hatch (*Figure 29*). It additionally shows messages with instructions on how to perform the scans and the pace the user must maintain.

Figure 29- Scaniverse´s on-screen scan progress and guidance view [author's collection]

To execute these surveys, and as suggested by the developer, scanning trajectories were planned, dividing the auditoriums and the hall into sections. Each of these sections represent a 1–3-minute scan that eventually were optimized, through the same clean-up process as the photogrammetry point cloud aligned, and aligned in Blender to achieve optimal results, since longer scans may cause a decrease in quality (Scaniverse, 2024). This was confirmed by the author; by experimenting with partial and full scans, certain flaws were identified in both instances. When long surveys are performed using this app, redundancy of scanned objects is expected, the software can wrongly interpret these redundancies as different objects and it creates double elements that are shifted from its original location, polluting the results. As stated before, this can be minimized by dividing the survey into multiple scans, nonetheless, to further reduce redundant points, the trajectory of each scan must be analyzed before begging to avoid going back to already scanned elements.

To scan the studied auditoriums, and considering their substantial geometric similarity, an overall scan plan was developed. This plan divided the room into 3 main components: perimeter, seats and ceiling, each of these components had its own subdivisions to limit the scans time to 3 minutes. The perimeter walls were divided into 4 scans, one for each wall (front, left, right and back). For the seating area, the manual survey was conducted by walking through every third or fourth aisle and holding the device approximately 30° off the floor, since no data from the walls or ceiling needed to be captured at these readings, and panning the equipment as far as possible while rotating it to get as much detail possible from the chairs. Four scans were needed to complete the seating area. Finally, for the ceiling, just one scan was needed because of its relatively simple geometry and lack of obstacles. To facilitate the eventual alignment of the scans, it’s important that in each scan, identifiable features such as wall corners are included. In other words, each scan shall capture specific elements, even though they are not the focus of the scan, they must be included to allow alignment with the previous scan and to ensure that the subsequent scan can also be matched to it.

Figure 30 shows the first scan done utilizing this method already (imported in Blender), it was limited to a duration no longer than 3 minutes, making sure that enough spatial data was acquired to eventually align it with its respectively conjoined elements, in this case it was the edges for the lateral walls and the superior and inferior borders to match it with the ceiling and floor. Additionally, redundant readings were avoided to prevent the creation of duplicated geometry.

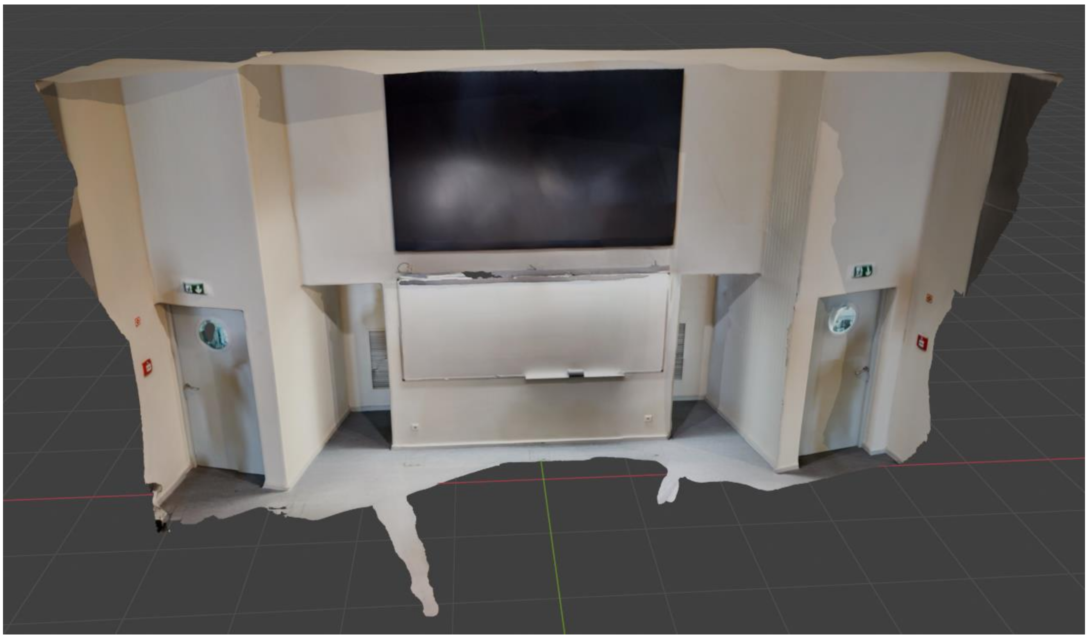

Figure 30- LiDAR mesh of the front Wall of room B001 [author's collection]

For the hall, a simplified workflow, similarly to the one used in the auditoriums, was followed. For this instance, only 2 surveys were required, one that collected data about the main objects needed for the reconstruction, and a second one to fully connect the first scan with the façade.

4.2.3. THERMOGRAPHY

For the thermography surveys, the thermal camera included in the DJI Mavic 2 Enterprise Dual was also employed for this end. Aerial surveys were performed to gather thermal information from the façade, and for the interior surveys, the UAV was used as a handheld device by taking the propellers off the equipment. This task required two operators, one carefully holding the equipment and pointing it at the surfaces studied, meanwhile the other operator uses the remote controller, connected to a mobile device, to register the feedback from the UAV sensors and assists by giving verbal instructions about where and how the device must be pointed at.

To get optimal results, another thermal camera was used to calibrate the UAV and to ensure the data values are coherent and reliable. To achieve this, a FLIR thermal camera was employed, and multiple physical points were chosen to get readings with both devices at the same time and then compare the obtained values. The firefighting equipment cabinet in the hall and the left entry door was chosen for this purpose, with both devices pointing at the same spot, on the lettering over the equipment cabinet and the top left corner. *Figure 31* shows the thermal readings obtained from each device, allowing for a direct comparison of temperature values and confirming the alignment and accuracy of the UAV-mounted thermal sensor.

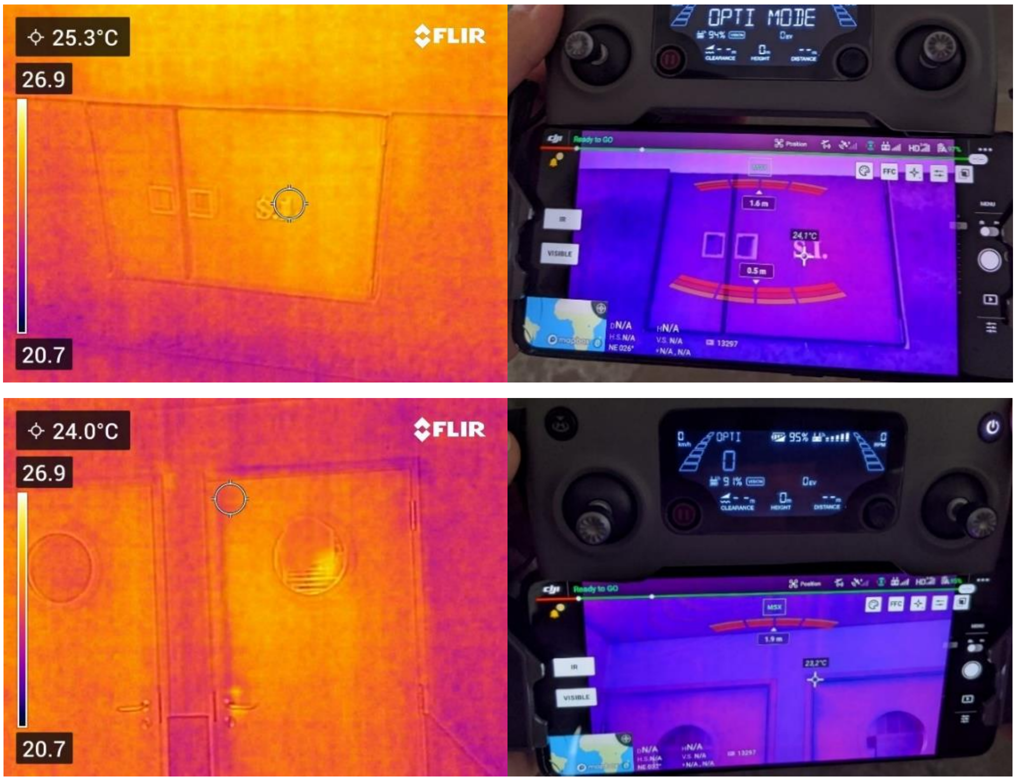

Figure 31- Thermal Calibration Reference: FLIR Camera vs. UAV Readings [author's collection]

It can be observed that the FLIR camera reading (left) indicates 25.3 °C on the cabinet and 24.0 °C on the door, while the UAV reading simultaneously recorded 24.1°C on the cabinet and 23.2°C at the door. This results in a difference of 1.2°C and 0.8 °C respectively, which falls within an acceptable tolerance for the purposes of this study.

4.3. Data Process And Refinement

4.3.1. Meshroom

During the UAV surveys, 446 RGB images were taken, and for the purposes of this study, the software Meshroom was employed to create the 3D model from the gathered images. Meshroom is a free open-source 3D reconstruction software that creates 3D models from photogrammetry, by using a node-based visual programming framework (shown in *Figure 32*). It is built on top of the AliceVision framework and provides a user-friendly, node-based interface that lets users control and customize each step of the 3D reconstruction pipeline.

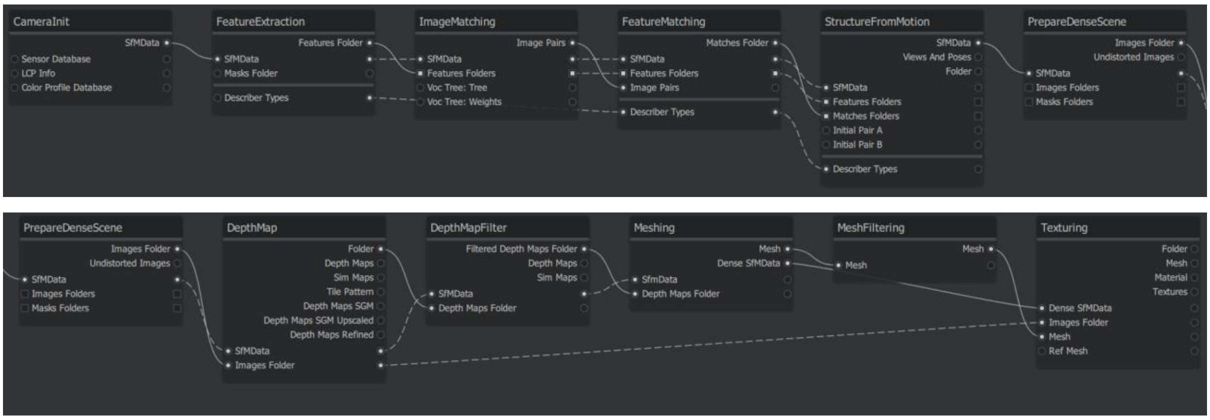

Figure 32- Meshroom's visual programming framework [author's collection]

However, since images from the interior of the building also were taken (using the UAV as a handheld device) the software had issues with the last nodes of its processing workflow. To resolve this, 88 (interior) images were filtered away leaving a preliminary data set of 356 images that were imported to the software, where another 8 were discarded automatically. *Figure 33* illustrates the façade point cloud obtained with Meshroom photogrammetry software.

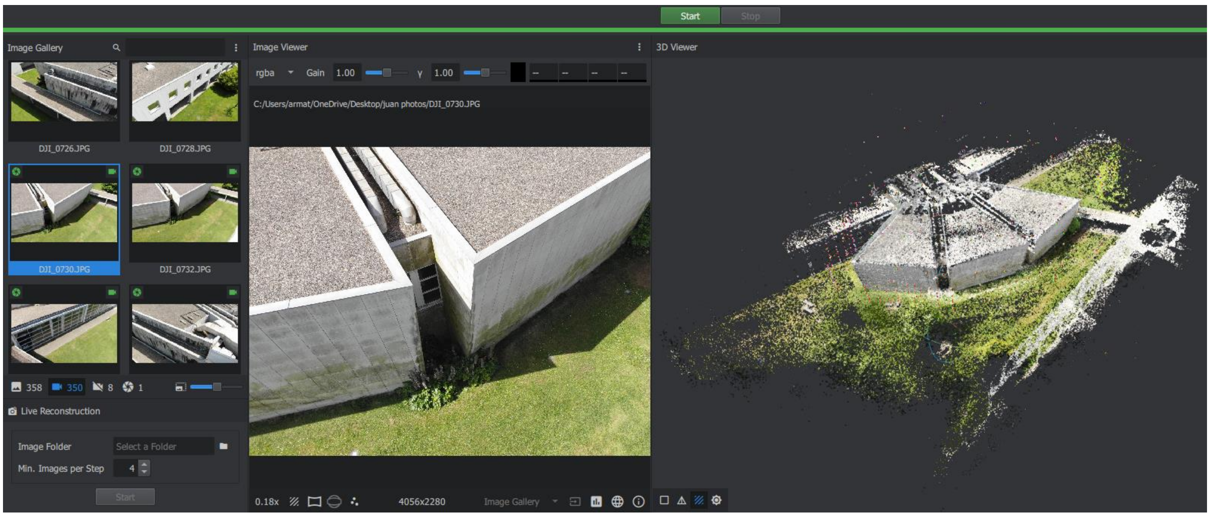

Figure 33- Façade point cloud generated using Meshroom photogrammetry software [author's collection]

The point cloud obtained from this software was imported, cleaned and optimized in Blender, where using the in-built modifiers and commands to delete loose parts, to decimate the mesh to lower the polygon count and to crop out irrelevant elements. *Figure 34* shows the mesh (obj) as it was originally imported to Blender from Meshroom.

Figure 34- Original imported mesh from Meshroom to Blender [author's collection]

It can be appreciated how the zones further from the auditoriums (where the surveys were focused), are distorted and present low quality since the software didn't have enough images to complete all the volumes. Nevertheless, these zones were eventually filtered out in the cleaning process. Additionally on the top left corner of the image, the statistics can be seen, showing the exact number of vertices (3,154,117), edges (9,453,767) and faces (6,302,283), which clearly shows the degree of detail and geometric complexity of the model. However, after refinement, these figures will be much lower because superfluous geometry will be eliminated.

To ensure a workable optimal mesh, different tools inside Blender were used. Initially, to get rid of redundant, overlapping and clustered vertices, all of them were selected in Edit Mode, and then in the Mesh tab, Clean Up, Merge by Distance, and a Merge distance to 1 cm was introduced (this distance can be set to a higher value, but detail will be lost). Subsequently, still in Edit Mode, using the selecting tool, the unwanted geometry that is irrelevant to the studied auditoriums, was selected, and ultimately eliminated from the dataset to ensure accuracy and reduce unnecessary complexity. Once the geometry is established, a quick check for loose parts was carried out by going to the Select tab, then Select All by Trait and selecting Loose Geometry, if any geometry was selected, it should've been evaluated if it is kept or eliminated. Finally, in Object Mode, on the Modifiers tab, the Decimate modifier was selected and the Ratio set to 0.5 (lowering the current vertex number by half). *Figure 35* presents the result of this process.

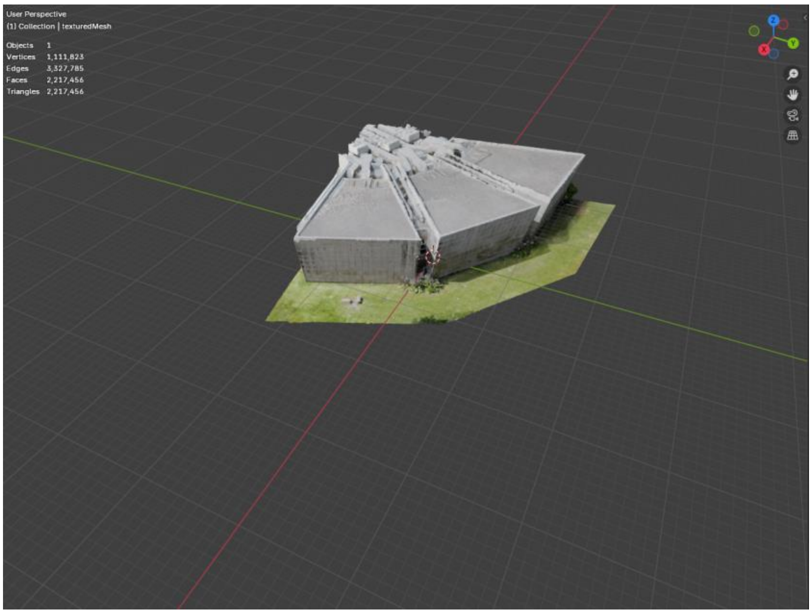

Figure 35- Refined façade mesh in Blender [author's collection]

The refined version of the mesh now features 1,111,823 vertices, 3,327,785 edges and 2,217,456 faces. Comparing the scene statistics of the two meshes, the geometry was reduced by approximately one-third, significantly lowering the mesh's geometric complexity and improving its efficiency for further processing, without losing significant detail.

4.3.2. LIDAR

Internal surveys were carried out inside the auditoriums and the entry hall; to get access to rooms, the corresponding permission was requested from the Technical Services for Maintenance and Environment at FEUP in the month of June. The author carried out these handheld surveys carefully, guaranteeing that the rooms weren't obstructed by other individuals and taking particular care not to trip over or damage any existing elements or infrastructure during the process. *Figure 36* depicts the author executing these reads employing the iPad Pro 11 with the Scaniverse app.

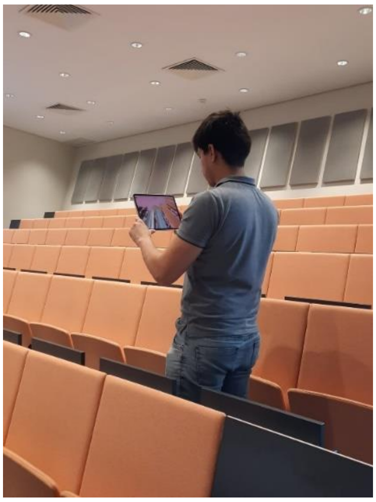

Figure 36- LiDAR surveys inside the auditoriums conducted by the author [Supplied by Diogo Parracho]

Since the Scaniverse app already created the 3D model, additional processing software wasn't needed. Nevertheless, for cleaning and aligning the multiple meshes Blender was also employed for aligning the scans to complete the models of all the rooms (3 auditoriums + hall).

Figure 37 shows an orthographic view of the 4 scans taken for the perimeter walls of room B001, before (left) and after (right) they were aligned. Blender was also used to carry out the same cleanup process detailed in the previous section, with the exception that the Decimate modifier wasn't used, since these meshes weren't as heavy as the photogrammetry one.

Figure 37- Comparison Between Aligned and Unaligned Scans [author's collection]

The stitching of all the scans proved to be a time-consuming task, since it required manual rotating and translating each of them with precision to ensure accuracy throughout the model. Although Blender provided an intuitive interface and tools to achieve this, the need to switch between views, make incremental adjustments, and constantly verify alignment of the overlapping points made the task repetitive and meticulous. Since this process mirrors the assembly of a 3D puzzle, minor misalignments between any of the meshes could mean that the model cannot be completed, forcing several iterations of correction and refinement. This step greatly increased the overall workflow duration and required patience and attention to detail.

4.4. BIM MODELLING

With all the multi-sensor generated meshes properly refined, the process can advance towards the BIM domain of the workflow. In the presented methodology, the Scan-to-BIM work frame is achieved by using the multi-sensor meshes as a base upon which the BIM elements are traced by overlaying it, creating an accurate Open-BIM model. Complementarily, once this model is finished, images from the aerial surveys will be used to texture the elements to achieve an even more close to reality model, achieving in this way an Image-to-BIM approach that enriches the semantic and visual detail of the final output, facilitating better analysis, visualization.

4.4.1.1. Multi-Sensor Results Alignment

Once all the acquired meshes are cleaned and optimized, they are imported into Blender to begin the Scan-to-BIM workflow. First, the location and rotation of the largest mesh are locked along the X, Y, and Z axis to serve as a reference or starting point. In this study, the largest mesh is the one generated through UAV-based photogrammetry, which depicts the façade of the studied auditoriums. In this step, the scale assessment takes place as well, by comparing physical measurements, of the same piece of granite in the façade, taken on-site during the field visit conducted for the multi-sensor surveys, and measurements taken using the *Measure* tool inside Blender. It's ideal to do this assessment during this step since only the mesh that will be used as reference has been imported, meaning that if any alterations to the scale must be made, the rest of the meshes can be adapted accordingly in a sequential manner. *Figure 38* illustrates the vertical and horizontal on-site measurements of the piece of granite, with the final value zoomed in for a better assessment, and *Figure 39* shows the digital vertical and horizontal measurements in Blender taken from the same piece

a)

b)

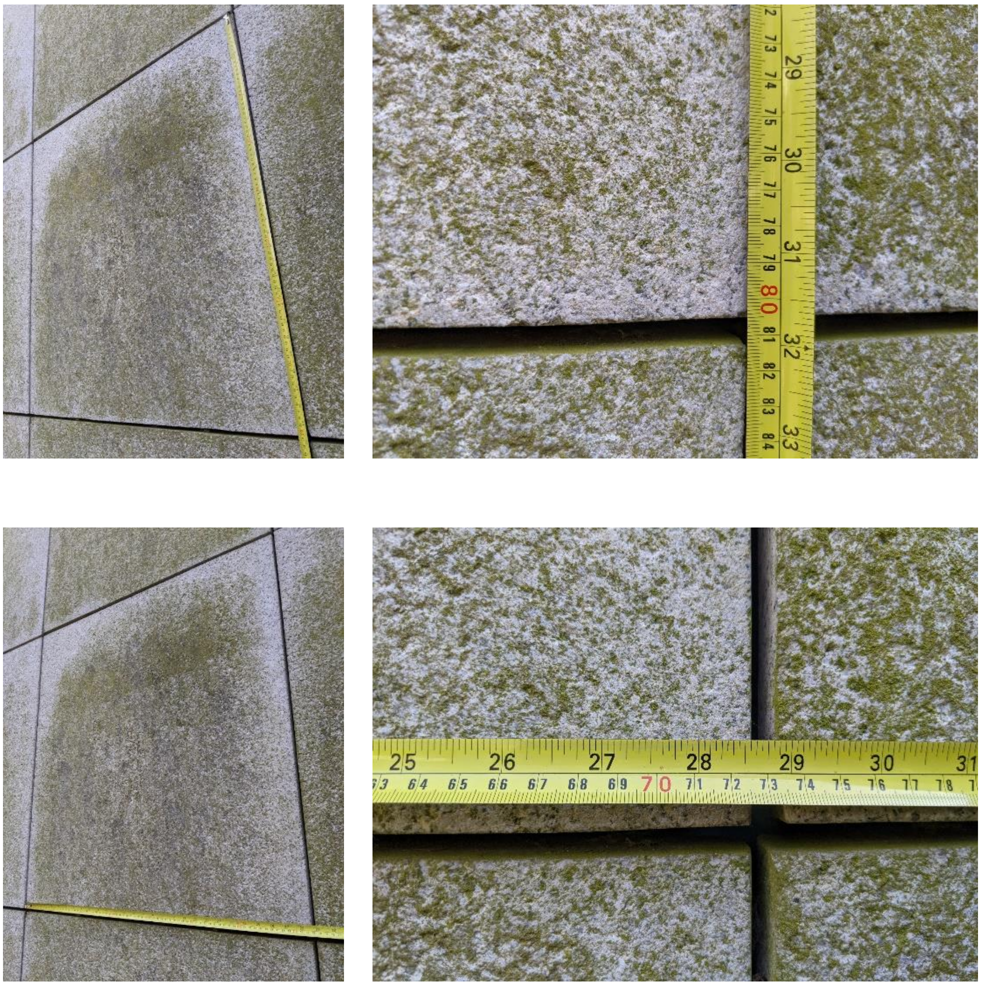

Figure 38- On-Site Measurements: a) vertical; b) horizontal [author's collection]

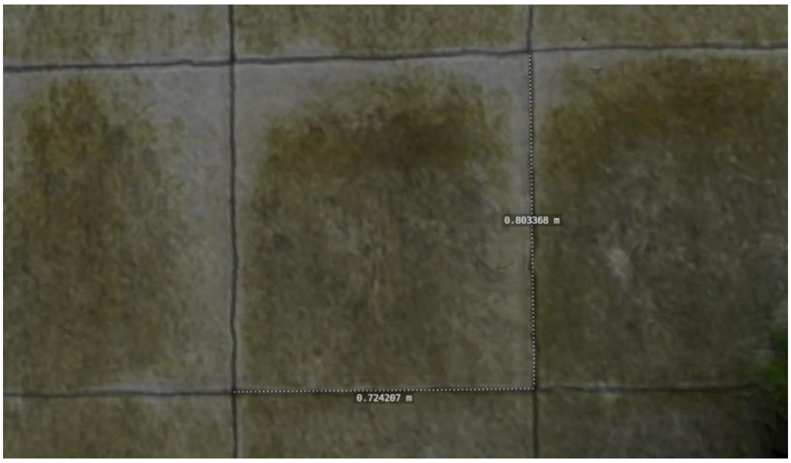

Figure 39- Digital Measurements [author's collection]

The on-site measurements are 0,805m vertically, and 0,725m horizontally, meanwhile the digital measurements show 0,803368m vertically, and 0,724207m horizontally, indicating a minimal deviation of less than 2 mm in both directions, thereby proving millimetric-level accuracy between the physical and digital data. This comparison demonstrates the geometrical fidelity of the photogrammetry survey, processed only using open-source software.

Subsequently, the remaining meshes are aligned to the façade mesh by identifying common reference points or vertices between them, enabling the snapping tool and the X-Ray mode (optionally), and using the transformation commands "G" (grab) and "R" (rotate) along each axis. In the specific case of this study, multiple alignments were performed. After locking the location and rotation values of the façade mesh, the LiDAR acquired mesh from the main hall was rotated and aligned to the façade, by taking advantage of the façade points that were gathered in the hall survey through windows, and by shared walls visible in both scans. To align the meshes depicting the three auditoriums, the same process was followed, aligning shared points and surfaces present, through windows and adjoining walls, in various scans. During this step, it was identified that little to no requirement for scale adjustment was needed to match and align the datasets acquired. At this stage, the Bonsai add-on is not yet required, as these meshes do not contain IFC information.

4.4.1.2. MODELLING

After all the meshes have been aligned, the Bonsai add-on can be activated to begin working with BIM elements. A new IFC project had to be created for this purpose. To do so, within the Bonsai interface, in the *Project Overview* tab, the "IFC4 Demo Template" option was selected, to facilitate element creation, since it has default elements that illustrate how to structure and organize new BIM components, and the *Create Project* button was clicked.

After the IFC project is created, BIM elements can start to be modeled. To assure geometrical compliance with the multi-sensor mesh, it's essential to lock the values of the mesh's transformation and rotation, to avoid any accidental misalignments. At this point the multi-sensor mesh is used as a foundation base, thus permitting the different IFC elements to be added in by overlaying the new element on its geometry. *Figure 40* demonstrates this procedure by tracing a wall directly over the multi-sensor mesh using Blender's built-in X-ray view. This mode allows the user to see through the mesh, enabling precise alignment and accurate reproduction of the as-built conditions.

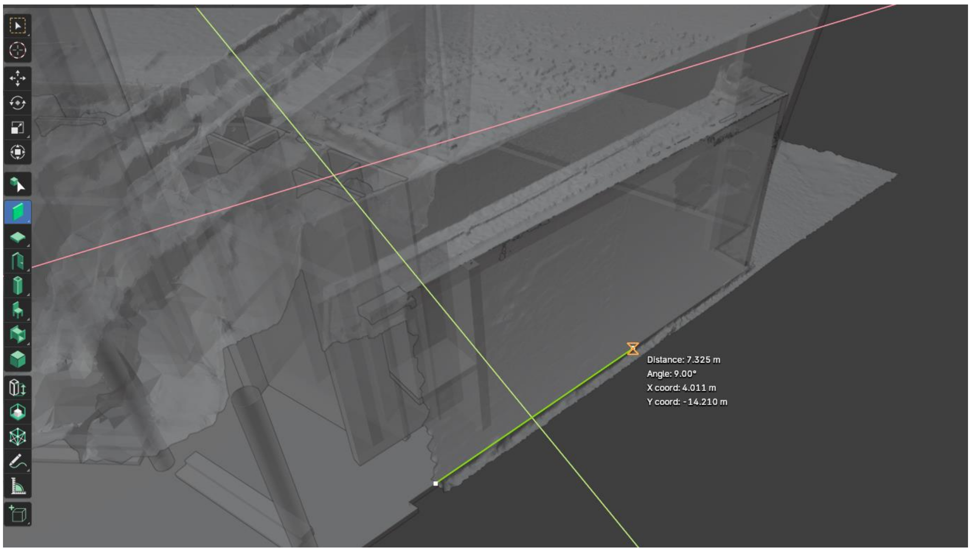

Figure 40- Wall Modeling by Tracing Multi-Sensor Mesh with Blender X-Ray View [author's collection]

The walls and slabs were initially added using and modifying the default IFC element types offered by the Bonsai add-on. By measuring the thickness of the corresponding elements and aligning the new elements with the multi-sensor meshes, it was ensured that each element had the proper size and placement. Then, the sizes and locations of the columns were similarly matched, using the corresponding vertical structural parts seen in the scan data. In the same way, windows and doors were then carefully placed on the respective walls. To add the stairs and the ramp, the mesh's spatial configuration was traced by modifying normal cubes to match the stairs and ramp geometry, verifying the heights of the risers and the depths of the treads so that they matched the references, and then assigning them the corresponding IFC type. *Figure 41* presents a comparison between the scanned model and the BIM model created using it as a reference, illustrating how the overall geometry was aligned based on the meshes.

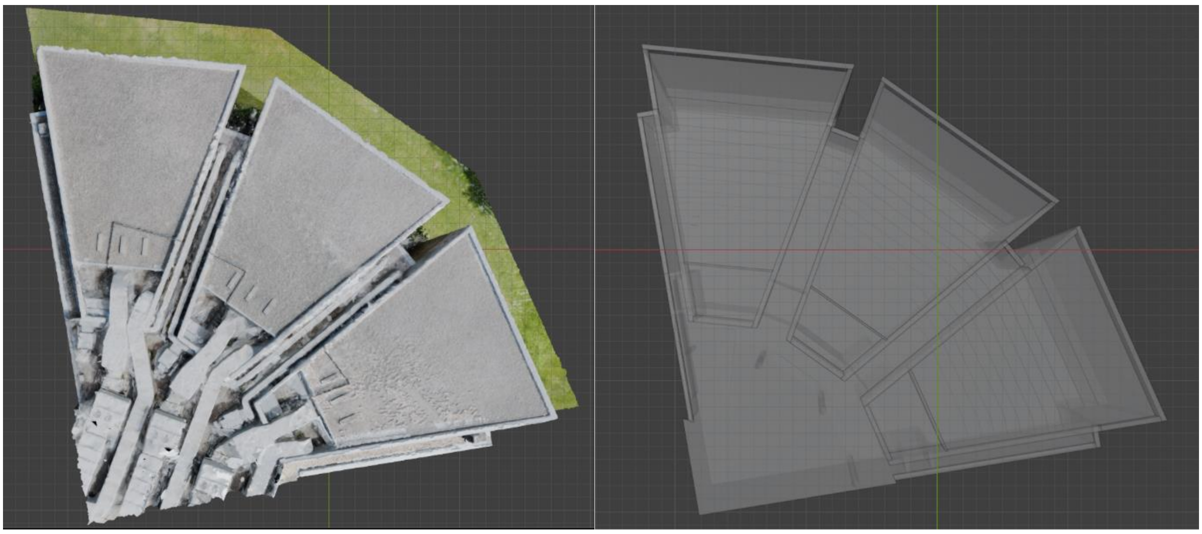

Figure 41- Scanned Geometry and aligned BIM model [author's collection]

Since the scans only gathered superficial data, non-visible elements were impossible to model. Thus, for the purpose of this study, only the existing walls, slabs, columns, doors, windows, and stairs are included in the BIM model. Elements related to building services, such as plumbing, electrical systems, and HVAC, as well as components hidden within the construction layers, like the insulation of walls, were not modeled, as they were neither visible in the scans nor essential to the objectives of this reconstruction. *Figure 42* shows some of the modelled walls, slabs, columns and stairs modeled inside Blender.

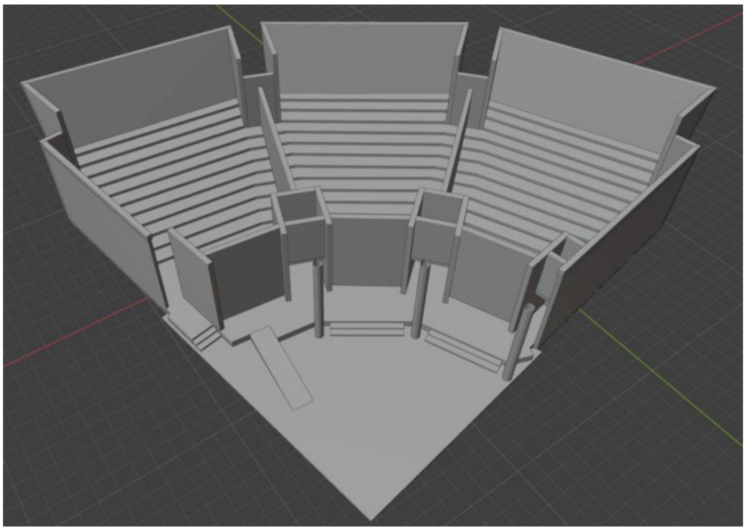

Figure 42- Auditoriums' early-stage BIM model [author's collection]

Once the walls and slabs were modeled, entries and openings can start to be defined and eventually added to the project. For this, Bonsai counts with default elements that can be parametrically modified to attend specific requirements. The existing doors and windows in the project were incorporated using this function, allowing for precise adjustment of their dimensions and properties to align with the overall design. *Figure 43* showcases three window types, with different number of panels, used in the project, created through parametric modifications.

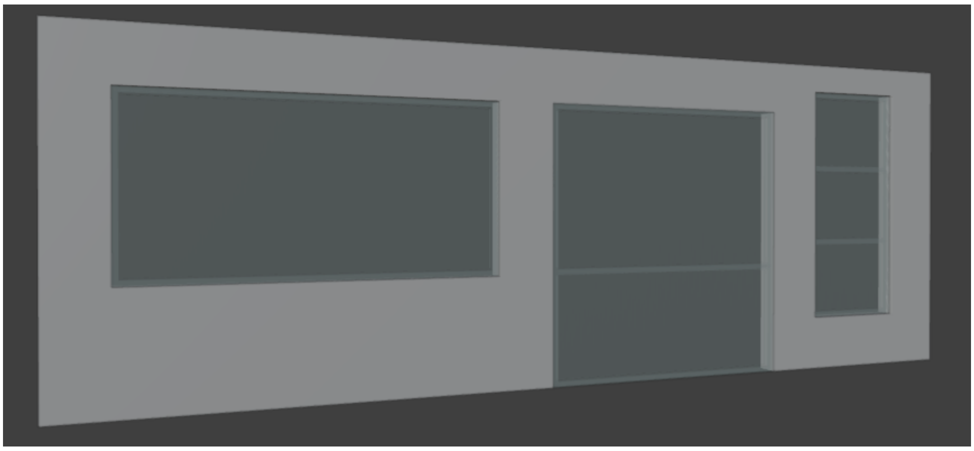

Figure 43- Three Parametrically Defined IFC Window Variants [author's collection]

Nonetheless, there were instances where the parametric modifications weren't enough to accurately represent certain elements. This was evident in the case of the doors present in the main entrance of the auditoriums, that counted with circular windows in their structure. Yet, the mesh from the default door model included in Bonsai, was used as a base for these doors. It was copied, modified and textured to comply with the specified geometry, to subsequently assign a new door type, ensuring it is IFC-compliant (*Figure 44*).

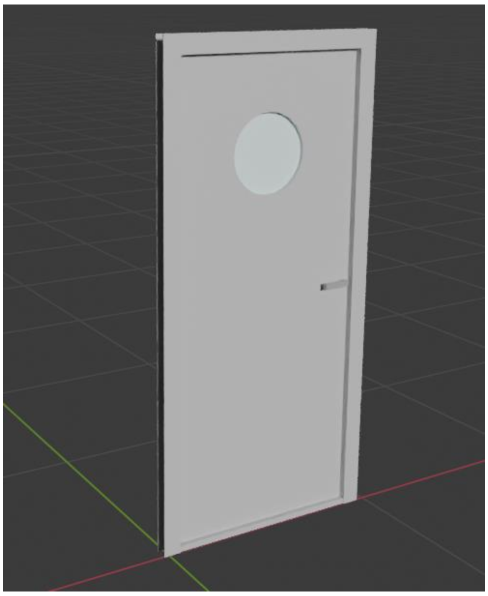

Figure 44- Custom-Made Door Type with IFC Classification [author's collection]

For the fixed furniture elements, similarly to the previous illustrated doors, no suitable default parametric components were available within Bonsai. Consequently, specific objects had to be created entirely from scratch using the standard Blender modeling tools. Although Blender enables extremely detailed 3D modeling, basic geometry was adequate for this study's needs. Once modeled, each furniture object was manually assigned the appropriate IFC type to ensure proper classification and interoperability within the BIM workflow. *Figure 45* shows the chair model with texture variants corresponding to rooms B001, B002, and B003.

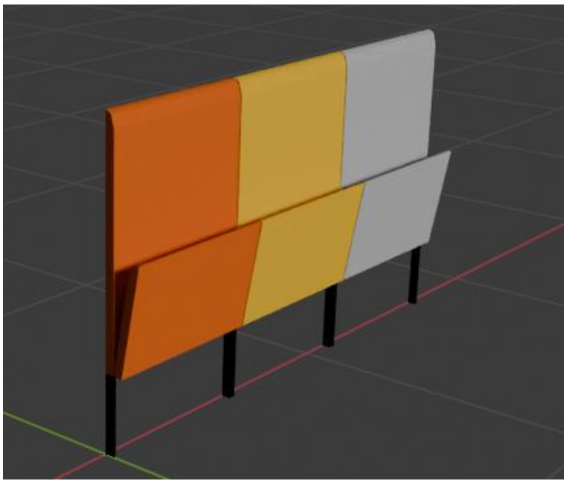

Figure 45- Custom-made Chair Types with Applied Textures [author's collection]

Figure 46 displays the 3D model that includes both the custom-made and parametrically defined elements. To better visualize the interior layout, the ceiling has been hidden, allowing clear views into the three rooms within the model. This representation highlights the combination of parametric and manually created components integrated into the project.

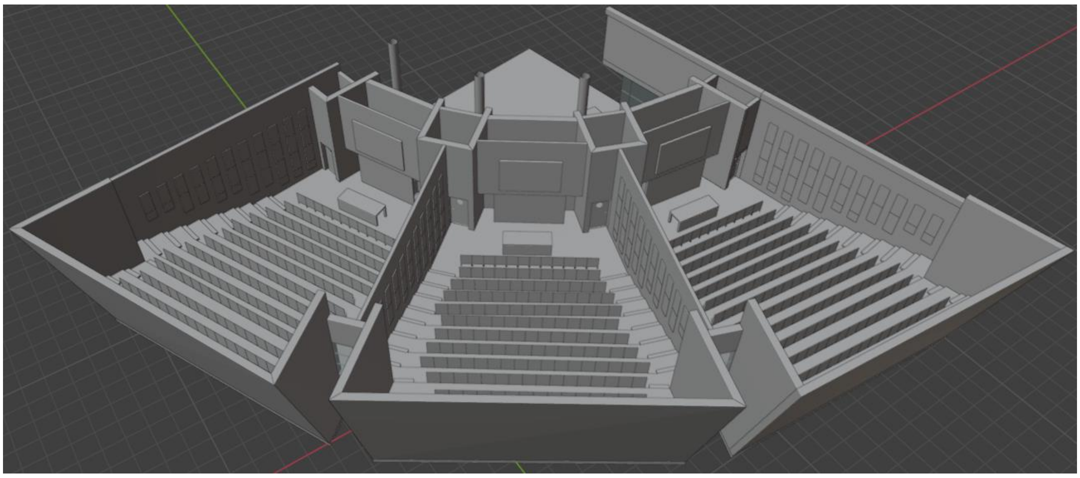

Figure 46- Visualization of the Auditoriums with Parametric and Custom Elements [author's collection]

The use of Blender Bonsai in this project revealed several technical and practical challenges. Since this software wasn't conceived originally, and solely, for BIM modeling, to be compatible with IFC it separates the project into 2 files: the .blend, which contains the native geometry and materials, and a parallel .ifc structure file that stores the element classifications, relationships, and metadata. Because of this, there's a considerable learning curve for first users, even intermediate or occasional Blender users can find unexpected setbacks while implementing Bonsai. For instance, the .ifc file doesn't register geometrical changes made to an object using Edit Mode, after its first assignment. Nonetheless, it does register transformations in the coordinates and rotation values, but it has trouble tracking any changes to the origin point, the reference point that defines the position and orientation of each individual object in Blender. To better illustrate this, *Figure 47* shows an initial exported .ifc file, imported back into Blender in a new project.

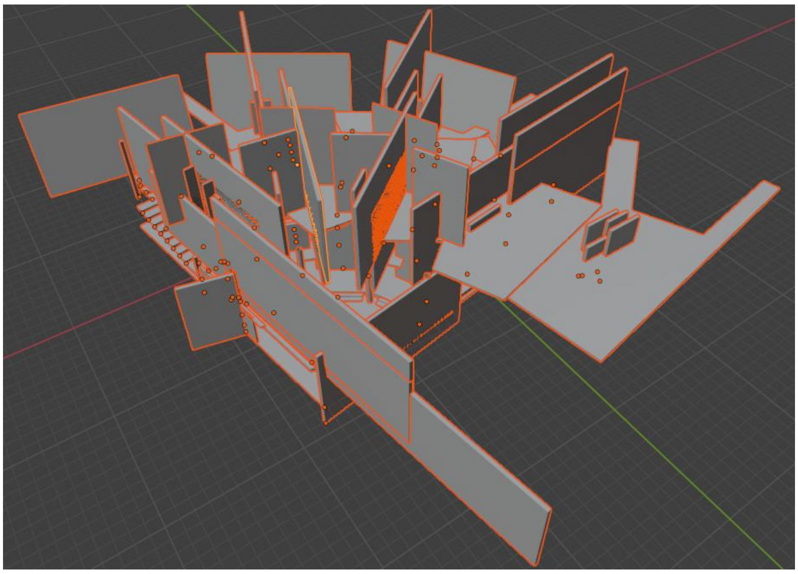

Figure 47- Misaligned IFC Export from Blender Bonsai [author's collection]

In this case, the elements are highlighted with an orange outline, since all of them are selected, to visualize the origin points of each object. It can be appreciated how most assets are misaligned, spatially shifted, and with out-of-bound geometry. This is mainly because once an IFC element is created in Blender Bonsai, the program registers it based on its initial geometry, which then can be altered by using the parametric options that Bonsai provides. However, these options are limited, in the case of slabs, they primarily affect the thickness, inclination and the type of slab, meaning that any alteration of the rest of the geometry, such as the alteration of vertices or the creation of new ones, won't be registered in the .ifc file, consequently if any mistakes are made in the original assignment, the entire element has to be redone. Alternatively, in the case of walls, the parametric options primarily affect thickness height and length, limiting its geometry to a prism. Generally, rotation and translation values are registered correctly, unless the origin point is altered independently of the object's position, causing potential misalignments in the exported model.

Another challenge encountered when exporting the .ifc model is that sometimes a bug causes the representation structure of the program to stop working in certain elements. Producing only the outline of the element when imported to a new project. *Figure 48* shows a wall element affected by this issue, with only its outline (highlighted in orange) visible in the IFC model.

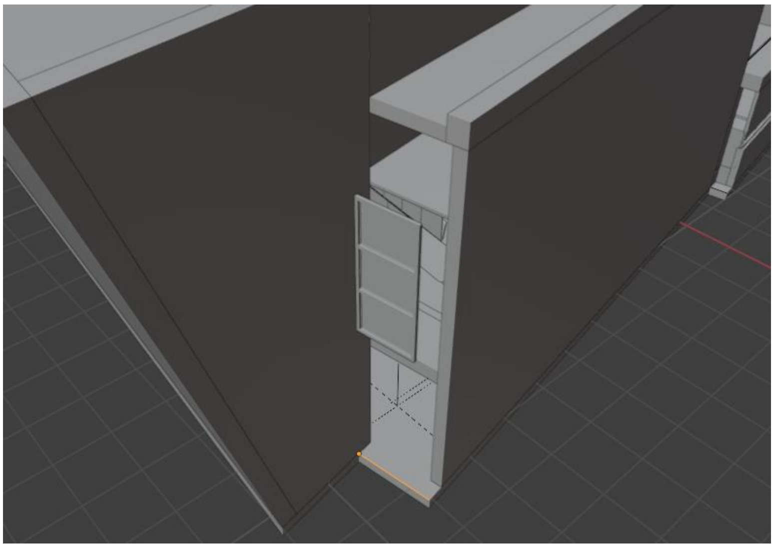

Figure 48- Wall Element Exported with Missing Geometry in IFC File [author's collection]

These challenges can be overcome by better understanding the software behavior and limitations. For instance. The first issue previously presented, can be avoided by leaving the origin point unchanged, on its relative location within the element, and to keep from changing objects geometries using Edit Mode, after the original assignment, instead geometry changes must be limited to the parametric option. In case that the element at hand needs a more complicated geometry, define it by changing its mesh using Edit Mode, and creating a new IFC type of said element. To resolve the issue of the outline-only representation, the object must be selected, and within the BIM view (introduced by the add-on), the Geometry and Materials tab accessed. In the Representations panel, a new representation should be added by selecting the *Full Representation* option. Subsequently, the .ifc file can be saved to apply these changes. *Figure 49* shows the corrected IFC export with the full geometry representation properly included.

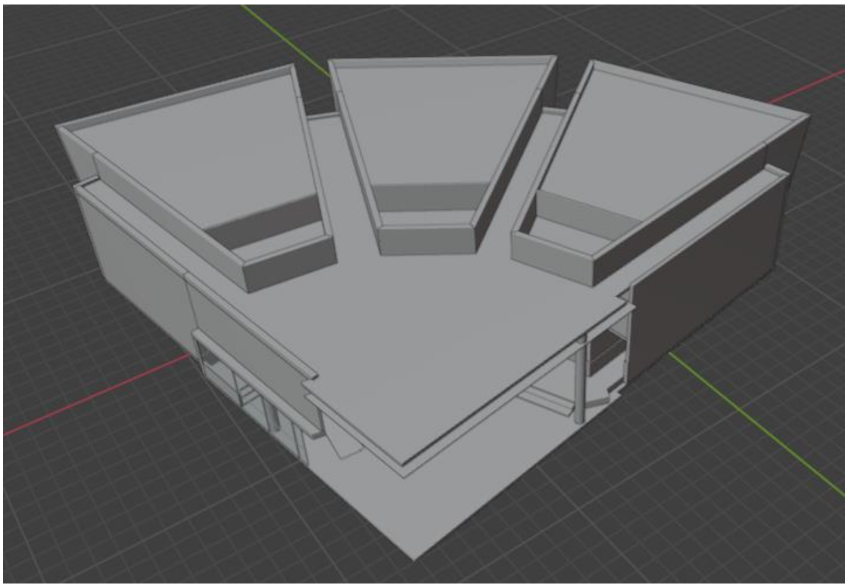

Figure 49- Corrected IFC Export from Blender Bonsai [author's collection]

This IFC file is a crucial asset for the project as it enables the full application of the BIM workflow, including seamless interoperability with other BIM software platforms. BIM Vision, a freeware IFC model viewer developed by Datacomp, it allows to view the virtual models coming from CAD systems like Revit, Archicad, BricsCAD BIM, Advance, DDS-CAD, Tekla, Nemetschek VectorWorks, Bentley, Allplan, Strakon and others without necessity of commercial licenses (Datacomp IT Sp. z o.o., no date). As demonstrated in *Figure 50,* which presents screenshots from BIM Vision, different perspectives of the unaltered IFC model directly imported using the .ifc file Blender Bonsai are shown. This visualization confirms that the model retains its structural and parametric integrity, facilitating collaboration and further development across various BIM environments, in line with Open-BIM standards that promote open standards and interoperability.

a)

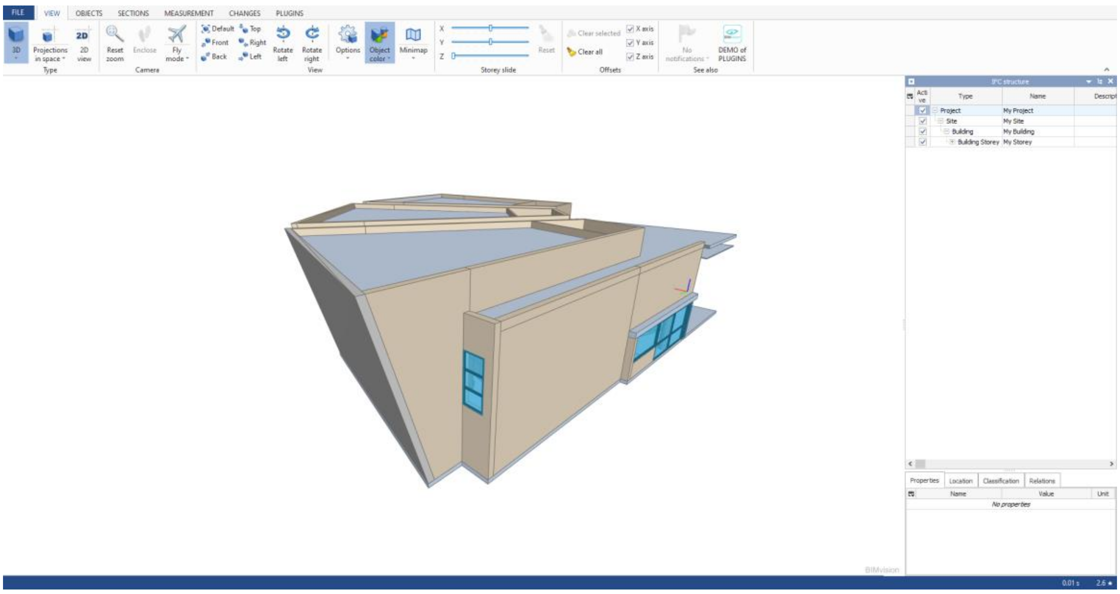

b)

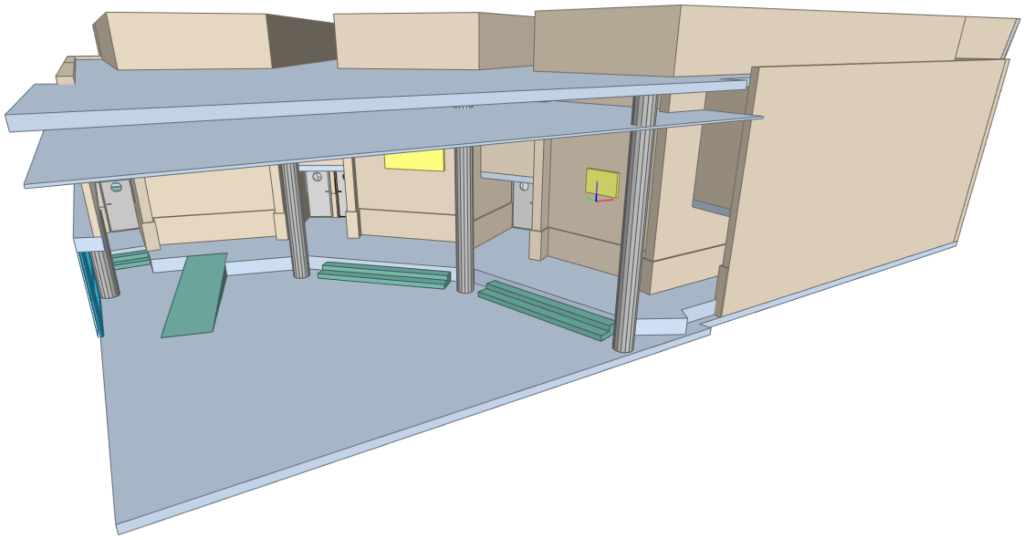

Figure 50- Views of the Unaltered IFC Model Imported into BIM Vision: a) façade; b) hall [author's collection]

4.4.1.3. TEXTURING

Once the BIM model is completed, texturing is necessary to fulfill the Image-to-BIM workflow. To this end, various methods were used, in the first method, specific textures from the RGB surveys were used to UV wrap some of the elements that have unique textures. To complement this method, free online available textures, and adapting materials settings inside Blender, were also used to complete the texturing phase. Additionally, the gathered thermal images were also used to UV wrap some elements inside Blender, to prove that thermal and pathologies and anomalies can also be identified and studied using the proposed workflow. Blender offers a versatile set of tools for texturing objects, including UV mapping, shader node customization, and real-time previewing, which makes it a suitable platform for developing efficient and flexible visualization workflows.

The targeted element that the images gathered by the UAV surveys were used as a texture for the BIM model, is the main façade, because of its uniqueness. The façade presents tiled rectangular pieces of Porto granite (also known as "Granito do Porto"), which, because of its historical and cultural significance in Porto, has been designated as a UNESCO Heritage Stone Silva (2024).

The first step taken was to identify an optimal image that contains unobstructed data of the selected texture, to then crop it and warp it to get a regularized grid. The main objective is to end up with an image that can be used as a repeatable tile across the façade. *Figure 51* shows the selected image after being adapted, a texture composed of a grid of 6x4 tiles meant to be tiled throughout the façade, as a single texture.

Figure 51- Adapted Façade Texture [author's collection]

After defining the texture, the target elements were chosen in Blender, UV unwrapped using Cube Projection, and given a new material by selecting the Material Properties tab. This new material was edited, employing the built-in visual programmer, in the Shading tab using nodes. First an Image Texture node was added, with the adapted texture, and connected to the Base Color socket in the existing Principled BDSF node, this is for mapping the selected image onto the surface of the object. Subsequently, a Mapping node is introduced, changing the scale and the location values to better adjust the image to the selected elements, since this node allows for precise control over the texture's position, rotation, and scale, enabling accurate alignment of the image with the geometry of the object. Finally, a Texture Coordinate node is included to provide coordinates for tiling the texture correctly across the surface of the object's geometry. *Figure 52* shows the final layout of the described nodes inside Blender.

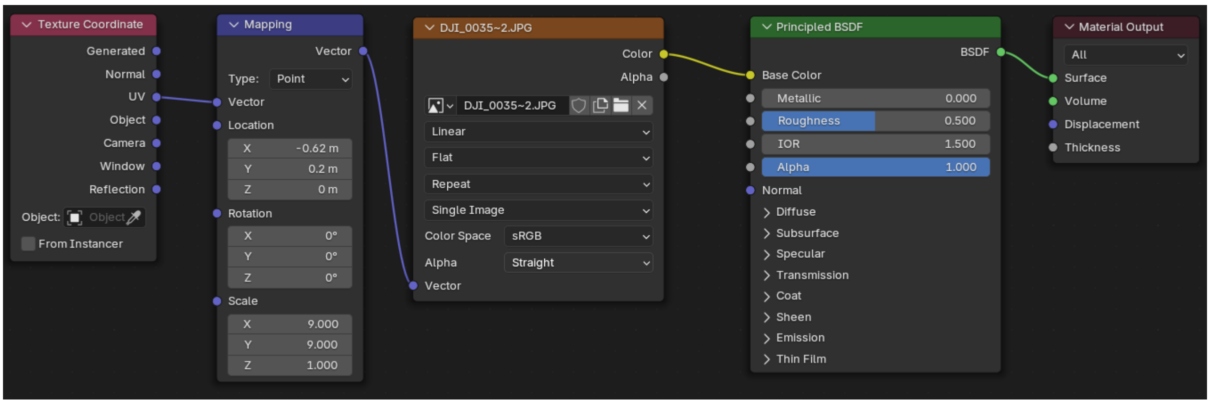

Figure 52- Texture Tiling Node Group [author's collection]

With the image mapped into the elements, final retouching must be done in the UV Editor view to correctly position the texture to each element, this is done by tweaking the mesh in this view until the texture has the right scale and alignment (the geometric mesh isn't altered in the 3D Viewport). To demonstrate the result of the implementation of these nodes, the material developed was assigned to a wall from room B003 while the rest of the elements remained with the default white material to clearly highlight the effect of the texture mapping and facilitate visual comparison, as shown in *Figure 53*.

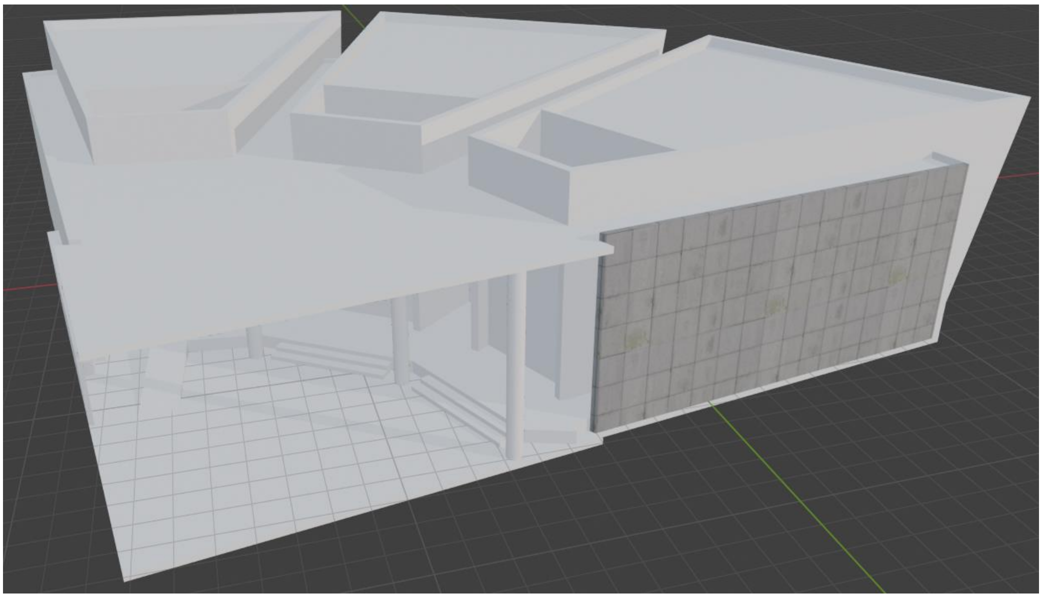

Figure 53- Demonstration of Texture Mapping on a Wall [author's collection]

The wall from room B003 stands out with the applied tiled texture, showcasing both the effectiveness and visual quality of the mapping technique. The grid-like pattern created from the warped image aligns reasonably well across the surface, preserving the architectural rhythm of the façade. Even though the final product is not entirely accurate and does not fully convey the visual complexity of the actual building, this workflow is still helpful for producing quick, rough representations, which are especially helpful in early design stages, visualizations, or situations where time and resources are limited.

For instance, the aerial surveys may not always be able to get a full or orthogonal image of the elements texture, because of existing obstacles, limiting their reach. *Figure 54* illustrates this by using a non-orthogonal image of the wall as a texture, exposing the unusable warped result.

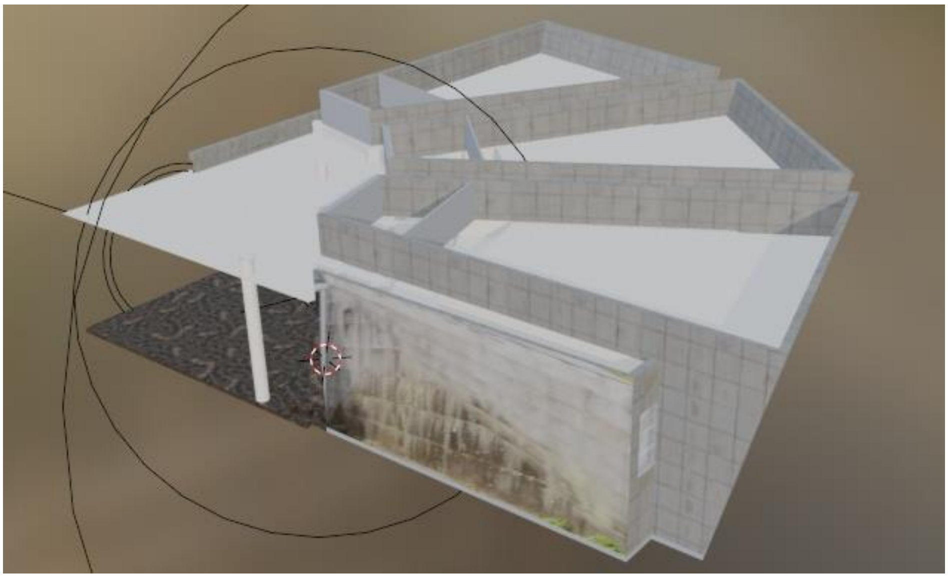

Figure 54- Non-Orthogonal Texture Mapping [author's collection]

The same UV principle was applied for thermal texturing, by repeating the previous stablished steps, without the tiling function, various infrared images from the UAV surveys were mapped in some elements to demonstrate how thermal evaluations can be performed inside this software. This way just by changing the material on the studied element, the RGB and thermal texture can be toggled at any time to perform thermal evaluations. *Figure 55* illustrates this, by using a complete RGB and thermal wall images from room B003, simultaneously taken by the DJI Mavic Enterprise Dual. This integrated approach facilitates comprehensive analysis by allowing easy comparison between visual and thermal data directly within the 3D environment.

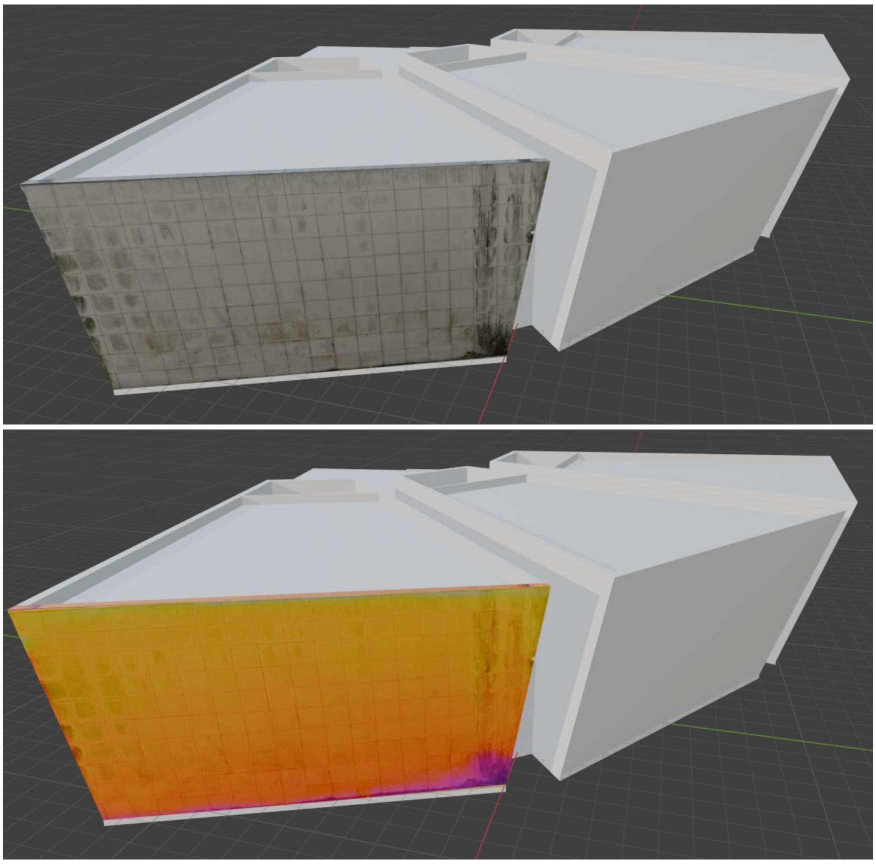

Figure 55- Thermal and RGB texture comparison [author's collection]

Thermal images, as opposed to the earlier RGB texture, have precise temperature-related information linked to the precise location and time of capture. For this reason, applying a tiling process to thermal textures is not recommended, as it would distort the spatial accuracy of the thermal readings and lead to misleading interpretations. Duplicating this data across a surface would distort the true thermal distribution because each thermal image represents actual conditions. Therefore, in this workflow, thermal textures were mapped using complete, untiled images to preserve the integrity of the data and ensure meaningful thermal evaluation.

To thermally texture the whole BIM model, orthomosaic generating software are recommended to patch together the UAV gathered image, since getting a complete uninterrupted image of every surface is often impractical due to occlusions, perspective limitations, and the need for consistent scale and alignment. Matching the generated images to each element may result in a complex and time-consuming task, which highlights the need for future research focused on thermal analysis and the exploration of open-source software capabilities aimed at automating and streamlining this process. An alternative is to "bake in" the textures after being matched together, as explored in Angheluță et al. (2023).

The remaining project components were subjected to a methodical application of this approach. To get the desired look for elements like the pillars and hanging ceilings, Blender's built-in material and texture settings were used. For other elements, including the roof and hall floor, a process similar to that used for the walls was followed; however, textures were sourced from free online resources like sketchuptextureclub.com to enhance realism. *Figure 56* showcases these applied textures, providing a clear view of the final surface finishes. Additionally, this figure summarizes the overall workflow from initial scanning to BIM modeling (Scan-to-BIM), highlighting how the integration of textures complements the digital reconstruction process.

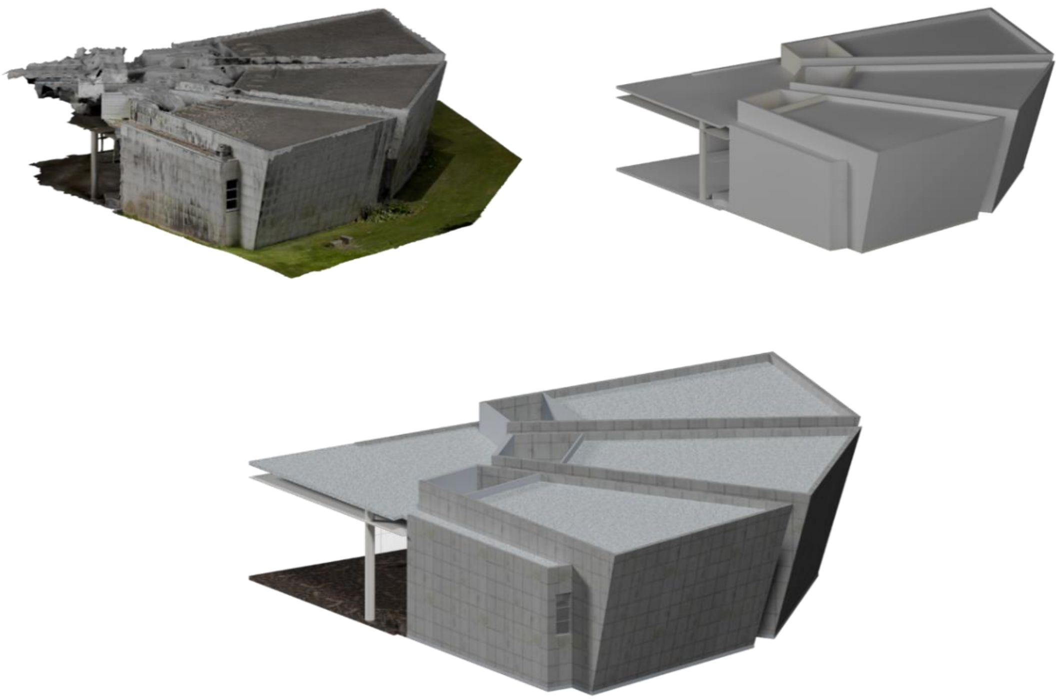

Figure 56- Overview of the Scan-to-BIM Modeling Process with Applied Textures [author's collection]

4.5. DISCUSSION

The execution of this study revealed a series of important findings. Firstly, it's clearly proven that an affordable open-source Scan-to-BIM workflow is completely feasible, enabling educational institutions, small businesses, enthusiasts and projects with limited resources to access high-quality 3D documentation and diagnostic capabilities without depending on proprietary software or expensive professional grade equipment. Secondly, photogrammetry demonstrated millimetric-level accuracy relative to the real building, and little to no requirement for scale adjustment was needed to match and align the datasets acquired from the photogrammetry and LiDAR surveys, making the developed workflow both efficient and reliable for multi-sensor integration. Third, during the BIM data integration, the open-source software Blender, with the Bonsai add-on, establishes itself as a complete and versatile platform capable of managing complex Scan-to-BIM workflows efficiently.

Prior to further interpreting the findings, it's worth noting that several limitations were identified throughout the study's progression. Firstly, although the study successfully developed an accessible Scan-to-BIM workflow, and even if professional equipment wasn't needed, nonetheless, it depended on the use of specialized high-end devices, such as a UAV with RGB and thermal cameras, and an iPad Pro 11 with advanced sensors, whose cost and technical specifications may limit the widespread adoption of the methodology. Secondly, the surveys performed only capture superficial (mainly geometrical) data, whereas, to obtain a thorough BIM model to assess the as-built conditions, internal layer data is indispensable. Thirdly, in the case of the LiDAR surveys, a significant amount of manual stitching was needed to accurately align and integrate the individual point clouds into a coherent and continuous model, and since the built-in sensor is not professional grade, lower quality is expected from those realized with actual professional grade equipment, still geometry remained accurate.

In the other hand, various setbacks were also identified in the processing and modeling stages. Especially from the photogrammetry point cloud data processing, since at first instance, a resource-limited portable computer was used to carry out this task, and ended up being unfeasible, hence a computer with better CPU and GPU specs was used instead. Additionally, 3D modeling, editing, texturing, and rendering of detailed models in Blender also required significant processing power. Furthermore, Blender Bonsai, by dividing the project into two files (.ifc and .blend) was not as user-friendly as anticipated, especially when compared to standard Blender, which is generally considered intuitive and more accessible to new users. Lastly, while Blender allows for detailed texturing, the sole export of IFC files didn't reflect this asset (additional steps using non-IFC files must be carried out), diminishing the interoperability of the workflow.

Regardless of these limitations, this study provides a replicable workflow where all the processing is done using accessible open-source software, yielding promising results that are compatible with other BIM platforms. A significant strength worth noting from this workflow, given that Blender is a widely popular open-source tool, it counts with a big online community, which makes it easy to find solutions to potential problems without the need to pay for formal courses. Along with its many features, the Blender platform also includes a Python scripting tab that enables advanced workflow customization and automation; visual programming that uses nodes for procedural modeling and material creation further enhances its flexibility and efficiency; and add-ons created by the community or the company allow the software to be tailored to the needs of specific users. This flexibility allowed for the seamless integration of multi-sensor survey data, facilitating a comprehensive and efficient Scan-to-BIM workflow.

Although the literature currently in publication shows notable progress in UAV-based data collection technologies for 3D façade modeling and building diagnostics, it is still very dispersed in terms of methodology and integration. While there is substantial research on individual sensing technologies, such as photogrammetry for high-resolution texture capture, LiDAR for geometric accuracy, and thermography for diagnostic analysis, very few studies attempt to merge all three within a coherent workflow, particularly using open-source tools. By putting forth a unified, open-source multi-sensor Scan-to-BIM methodology that capitalizes on the complementary advantages of each sensing modality, this dissertation critically expands and builds upon these discrete contributions. In doing so, it responds to documented gaps concerning interoperability, open-access processing, and practical fusion challenges. The literature reviewed supports the feasibility and benefits of combining these technologies, yet also underscores the absence of standardized, reproducible workflows, especially in resource-constrained or academic environments. Regarding open-source BIM modeling from UAV-based surveys, the current study thus not only supports earlier findings but also offers a fresh, integrative viewpoint that improves methodological coherence and usefulness.

Several potential directions for future investigation are identified in the study, mainly focusing on Blender's complementing features. For instance, the animation panel built-in into blender can further explore the potential of use of this software as a Scan-to-BIM platform, by using keyframes and multiple scans taken across periods of time of a determined building, a progressive visualization comparing eventual deterioration/improvement can be developed. Future research should also focus on carrying out deeper thermal analysis inside Blender and enhance it using the animation feature to illustrate gradual thermal behavior during different times of day or different seasons. Building on this, Blender Bonsai also offers distinct BIM features such as structural analysis, costing and scheduling, and facility management, which could be integrated to enhance the functionality and applicability of the open-source Scan-to-BIM workflow. Furthermore, Blender's capacity to simulate physical events, including complex ones like explosions, could have practical uses in safety evaluations and controlled demolition. Lastly, incorporating nondestructive survey methods for internal data collection could further enhance the Scan-to-BIM workflow by offering a more comprehensive insight into building conditions, warranting additional investigation.

5
CONCLUSIONS

This study aimed to develop an open-source Scan-to-BIM workflow, based on multi-sensor surveying. By gathering spatial and thermal data from the "B" building at FEUP, to then process it and develop a BIM model, solely using open-source software. The findings of this study show that it is possible to develop an accurate 3D reconstruction of a building section by integrating spatial and thermal data through an entirely open-source Scan-to-BIM workflow.

The main findings of the study prove that an affordable open-source Scan-to-BIM workflow is fully achievable. That means that entities such as educational institutions, small businesses, enthusiasts and projects with limited resources, can have access to high-quality 3D documentation and diagnostic capabilities. Additionally, when aligning the different datasets from the multi-sensor surveys, the photogrammetry demonstrated millimetric-level accuracy relative to the real building, and with LiDAR's case, little to no requirement for scale adjustment was needed to match and align them, indicating that the integration of diverse data sources within the workflow is reliable and produces coherent, spatially accurate 3D models. During the BIM data integration, the open-source software Blender, with the Bonsai add-on, established itself as a complete and versatile platform capable of managing complex Scan-to-BIM processes efficiently, demonstrating that open-source tools can effectively support advanced BIM tasks, offering a practical and cost-effective alternative to proprietary software solutions.

This study makes a valuable contribution to the field of Scan-to-BIM research, by proving that completely open-source workflows that incorporate multi-sensor data collection are entirely possible and able to provide precise, affordable, and expandable building documentation solutions. Notably, it addresses a significant gap in the existing literature, as a lack of studies that have explored the combined use of these three technologies within a fully open-source Scan-to-BIM workflow can be found.

The study's practical implications demonstrate the potential advantages and uses of a multi-sensor, fully open-source Scan-to-BIM workflow in a range of industries and project sizes. Since it relies solely on open-source software and affordable multi-sensor data collection methods, the developed workflow reduces financial barriers to accurate building surveying and modeling, enabling cost effective documentation. The applied methodology is also applicable outside of the original case study due to its scalability, which enables it to be modified to suit various project sizes and levels of complexity. With the creation of this workflow, the essential benefits of Scan-to-BIM, such as facilitating accurate digital representation and enhancing collaboration across architectural, engineering, and construction disciplines, are made accessible through a fully open-source and cost-effective approach.

Several limitations were identified throughout the study's progression. Professional equipment wasn't needed, nonetheless, the study heavily depended on the use of specialized high-end devices, such as a UAV with RGB and thermal cameras, and an iPad Pro 11 with advanced sensors. The surveys performed only capture superficial data, whereas, to obtain a thorough BIM model to assess the as-built conditions, internal layer data is indispensable. Significant amount of manual stitching was needed to accurately align and integrate the individual LiDAR point clouds into a coherent and continuous model, additionally, lower quality is expected from those realized with actual professional grade equipment, still geometry remained accurate. A computer with significant processing power was needed for the processing stage, since several of the tasks required high CPU and GPU capabilities. Finally, there are export limitations regarding texturing and modeling, since Bonsai divides the project into two files (.ifc and .blend), but these issues can be mitigated through additional processing steps and manual adjustments during the export workflow.

The study's findings support the potential of open-source tools to facilitate precise and economical scan-to-BIM workflows. It creates new prospects for wider adoption across a range of industries by proving that integrating multi-sensor data without proprietary software is feasible. Despite certain technical limitations, the workflow proves to be adaptable, scalable, and capable of delivering meaningful results, paving the way for future improvements and wider implementation.

Bibliography

Aicardi, I. *et al.* (2016) 'UAV photogrammetry with oblique images: First analysis on data acquisition and processing', in *International Archives of the Photogrammetry, Remote Sensing and Spatial Information Sciences - ISPRS Archives*. International Society for Photogrammetry and Remote Sensing, pp. 835–842. Available at: https://doi.org/10.5194/isprsarchives-XLI-B1-835-2016.

Aksu, K., Günaydın, E. and Duran, Z. (2024) 'Comparative analysis of 3D models generated by close range photogrammetry and smartphone-based LiDAR sensor', in. Available at: https://www.researchgate.net/publication/384264181.

Albertz, J. (2007) 'A Look Back; 140 Years of Photogrammetry', *Photogrammetric Engineering and Remote Sensing*, 73. Available at: https://www.asprs.org/wp-content/uploads/pers/2007journal/may/lookback.pdf (Accessed: 26 April 2025).

Alshawabkeh, Y., Baik, A. and Miky, Y. (2021) 'Integration of laser scanner and photogrammetry for heritage BIM enhancement', *ISPRS International Journal of Geo-Information*, 10(5). Available at: https://doi.org/10.3390/ijgi10050316.

Andaru, R. *et al.* (2019) 'The combination of terrestrial Lidar and UAV photogrammetry for interactive architectural heritage visualization using unity 3D game engine', in *International Archives of the Photogrammetry, Remote Sensing and Spatial Information Sciences - ISPRS Archives*. International Society for Photogrammetry and Remote Sensing, pp. 39–44. Available at: https://doi.org/10.5194/isprs-archives-XLII-2-W17-39-2019.

Angheluță, L.M., Popovici, A.I. and Ratoiu, L.C. (2023) 'A Web-Based Platform for 3D Visualization of Multimodal Imaging Data in Cultural Heritage Asset Documentation', *Heritage*, 6(12), pp. 7381–7399. Available at: https://doi.org/10.3390/heritage6120387.

Apple Inc. (2022) *iPad Pro 11-inch (4th generation) - Technical Specifications - Apple Support*. Available at: https://support.apple.com/en-us/111842 (Accessed: 13 June 2025).

Azari, P. *et al.* (2025) 'Georeferencing Building Information Models for BIM/GIS Integration: A Review of Methods and Tools', *ISPRS International Journal of Geo-Information*. 2024: Multidisciplinary Digital Publishing Institute (MDPI). Available at: https://doi.org/10.3390/ijgi14050180.

Balaras, C.A. and Argiriou, A.A. (2002) 'Infrared thermography for building diagnostics', *Energy and Buildings*, 34(2), pp. 171–183. Available at: https://doi.org/https://doi.org/10.1016/S0378-7788(01)00105-0.

Blender Foundation (2025) *About Blender - Blender 4.4 Manual*. Available at: https://docs.blender.org/manual/en/4.4/getting_started/about/index.html (Accessed: 12 June 2025).

Chandler, J.H. *et al.* (2005) 'Metric capabilities of low-cost digital cameras for close-range surface measurement', *The Photogrammetric Record*, 20(109), pp. 12–26. Available at: https://doi.org/10.1111/j.1477-9730.2005.00302.x.

Chen, Z. *et al.* (2022) '3D model-based terrestrial laser scanning (TLS) observation network planning for large-scale building facades', *Automation in Construction*, 144. Available at: https://doi.org/10.1016/j.autcon.2022.104594.

Collier, P. (2018) 'The development of photogrammetry in World War 1', *International Journal of Cartography*, 4(3), pp. 285–295. Available at: https://doi.org/10.1080/23729333.2018.1497439.

Crawford, A. (2019) *Interview with Vaughan Ling of Love, Death + Robots 'The Witness' - BlenderNation*. Available at: https://www.blendernation.com/2019/11/18/interview-with-vaughan-ling-of-love-death-robots-the-witness/ (Accessed: 22 June 2025).

Datacomp IT Sp. z o.o. (no date) *BIMvision - freeware IFC model viewer*. Available at: https://bimvision.eu/ (Accessed: 23 June 2025).

DJI (2021) *Mavic 2 Enterprise Series User Manual*. Available at: https://www.dji.com/global/downloads/products/mavic-2-enterprise#doc (Accessed: 24 June 2025).

EASA (2021) *Easy Access Rules for Unmanned Aircraft Systems (Regulations (EU) 2019/947 and (EU) 2019/945)*. Available at: http://eur-lex.europa.eu/, (Accessed: 25 April 2025).

Eastman *et al.* (2018) *BIM Handbook*. Hoboken, NJ: John Wiley & Sons. Available at: https://doi.org/10.1002/9781119287568.

European Parliament & Council of the European Union (2018) *Regulamento (UE) N 2018_1139, do Parlamento e do Conselho Europeu, de 4 de julho, rela*. Available at: https://eur-lex.europa.eu/legal-content/PT/TXT/PDF/?uri=CELEX:32018R1139&from=PT (Accessed: 25 April 2025).

FEUP (no date) *FEUP - Aulas i (B), piso 0*. Available at: https://sigarra.up.pt/feup/pt/instal_geral.edificio_view?pv_id=1404&pv_num_piso=0 (Accessed: 13 June 2025).

Fobiri, G., Musonda, I. and Muleya, F. (2022) 'Reality Capture in Construction Project Management: A Review of Opportunities and Challenges', *Buildings*, 12(9). Available at: https://doi.org/10.3390/buildings12091381.

Gao, J. (2002) 'Integration of GPS with Remote Sensing and GIs: Reality and Prospect', *Photogrammetric Engineering & Remote Sensing*, 68(1), pp. 31–35.

Garnero, G., Godone, D. and Bacciocchi, M. (2010) 'The employment of terrestrial laser scanner in cultural heritage conservation: The case study of Vallinotto Chapel in Carignano-Italy', *Applied Geomatics*, 2(2), pp. 59–63. Available at: https://doi.org/10.1007/s12518-010-0018-9.

Gil-Docampo, M. *et al.* (2023) 'UAS IR-Thermograms Processing and Photogrammetry of Thermal Images for the Inspection of Building Envelopes', *Applied Sciences (Switzerland)*, 13(6). Available at: https://doi.org/10.3390/app13063948.

Guan, S., Zhu, Z. and Wang, G. (2022) 'A Review on UAV-Based Remote Sensing Technologies for Construction and Civil Applications', *Drones*. Multidisciplinary Digital Publishing Institute (MDPI). Available at: https://doi.org/10.3390/drones6050117.

Hoffmann, M., Nagle, F. and Zhou, Y. (2024) *The Value of Open Source Software*. Available at: https://papers.ssrn.com/sol3/papers.cfm?abstract_id=4693148 (Accessed: 13 June 2025).

Hou, Y. *et al.* (2021) 'Fusing tie points' RGB and thermal information for mapping large areas based on aerial images: A study of fusion performance under different flight configurations and experimental conditions', *Automation in Construction*, 124. Available at: https://doi.org/10.1016/j.autcon.2021.103554.

IfcOpenShell (2024) *Bonsai — Blender Extensions*. Available at: https://extensions.blender.org/add-ons/bonsai/ (Accessed: 14 June 2025).

Irizarry, J., Gheisari, M. and Walker, B.N. (2012) *Usability assessment of drone technology as safety inspection tools*, *Journal of Information Technology in Construction (ITcon)*. Available at: http://www.itcon.org/2012/12.

Kozera, C.A. (2018) *Military Use of Unmanned Aerial Vehicles-A Historical Study*, *Scientific and Technical Journal Safety & Defense*. Available at: http://www.ctie.monash.edu.au/hargrave/rpav_home.html.

Liu, W. (2022) *Analysis of the External Environment of the Civil Drone Industry: A Case Study of DJI*, *Proceedings of the 2022 7th International Conference on Social Sciences and Economic Development (ICSSED 2022)*. Atlantis Press. Available at: https://doi.org/10.2991/aebmr.k.220405.144.

Lombardi, M. and Rizzi, D. (2024) 'Semantic modelling and HBIM: A new multidisciplinary workflow for archaeological heritage', *Digital Applications in Archaeology and Cultural Heritage*, 32. Available at: https://doi.org/10.1016/j.daach.2024.e00322.

Ma, L. *et al.* (2024) 'Impact of multiple factors on the use of an UAV-mounted infrared thermography method for detection of debonding in facade tiles', *Journal of Building Engineering*, 96. Available at: https://doi.org/10.1016/j.jobe.2024.110592.

Mueller, M.M. *et al.* (2023) 'Novel UAV Flight Designs for Accuracy Optimization of Structure from Motion Data Products', *Remote Sensing*, 15(17). Available at: https://doi.org/10.3390/rs15174308.

Nelson, R. (2013) 'How did we get here? An early history of forestry lidar', *Canadian Journal of Remote Sensing*, 39(SUPPL.1). Available at: https://doi.org/10.5589/m13-011.

Nex, F. and Remondino, F. (2014) 'UAV for 3D mapping applications: A review', *Applied Geomatics*, 6(1), pp. 1–15. Available at: https://doi.org/10.1007/s12518-013-0120-x.

Norouzi Ghazbi, S. *et al.* (2016) 'Quadrotors unmanned aerial vehicles: A review', *International Journal on Smart Sensing and Intelligent Systems*, 9(1), pp. 309–333. Available at: https://doi.org/10.21307/ijssis-2017-872.

Oostwegel, L.J.N. *et al.* (2022) 'Digitalization of culturally significant buildings: ensuring high-quality data exchanges in the heritage domain using OpenBIM', *Heritage Science*, 10(1). Available at: https://doi.org/10.1186/s40494-021-00640-y.

Open Source Initiative (2024) *The Open Source Definition – Open Source Initiative*. Available at: https://opensource.org/osd (Accessed: 13 June 2025).

OSArch Community (2025) *BlenderBIM Add-on*. Available at: https://wiki.osarch.org/index.php/BlenderBIM_Add-on#Bonsai_Add-on (Accessed: 14 June 2025).

Palik, M. and Nagy, M. (2019) 'Brief history of UAV development', *Repüléstudományi Közlemények*, 31(1), pp. 155–166. Available at: https://doi.org/10.32560/rk.2019.1.13.

Parracho, D.F.R. (2021) *Processos Digitais Para A Realização De Levantamentos Fotogramétricos E Termográficos Com Veículos Aéreos Não Tripulados (VANT)*. MSc Dissertation, Faculdade de Engenharia da Universidade do Porto (FEUP). Available at: https://repositorio-aberto.up.pt/handle/10216/135199 (Accessed: 16 May 2025).

Parracho, D.F.R., Martins, J.P. and Barreira, E. (2022) 'Metodologia digital para a realização de levantamentos fotogramétricos e termográficos de edifícios existentes com drones – Caso de estudo', in *4º congresso português de 'Building Information Modelling' vol. 2 - ptBIM*. UMinho Editora, pp. 395–406. Available at: https://doi.org/10.21814/uminho.ed.77.34.

Quagliati, N. (2020) 'Training the eye: Production and reception of aerial photography during the World Wars', *Acta Universitatis Carolinae, Geographica*, 55(1), pp. 93–111. Available at: https://doi.org/10.14712/23361980.2020.6.

Rashidi, M. *et al.* (2020) ‘A decade of modern bridge monitoring using terrestrial laser scanning: Review and future directions’, *Remote Sensing*, 12(22), pp. 1–34. Available at: https://doi.org/10.3390/rs12223796.

Rebelo, C. *et al.* (2015) *Building 3D city models: Testing and comparing laser scanning and low-cost UAV data using FOSS technologies*. Edited by O. Gervasi et al. Lisbon, Portugal: Springer International Publishing. Available at: https://doi.org/10.1007/978-3-319-21470-2_26.

Silva, R. (2024) *Granito do Porto é Pedra Património Mundial da UNESCO – Notícias da Faculdade de Ciências*. Available at: https://noticias.up.pt/fcup/granito-do-porto-e-pedra-patrimonio-mundial-da-unesco/ (Accessed: 19 June 2025).

Rogalski, A. (2012) ‘History of infrared detectors’, *Opto-Electronics Review*, 20(3), pp. 279–308. Available at: https://doi.org/10.2478/s11772−012−0037−7.

Salzano, A. *et al.* (2023) *Systematic Literature Review of Open Infrastructure BIM*. Available at: https://doi.org/10.3390/buildings13071593.

Scaniverse (2024) *How to use Scaniverse 3D Scanner for iOS and Android*. Available at: https://scaniverse.com/support (Accessed: 18 June 2025).

Schenk, T. (2005) *Introduction to Photogrammetry*. The Ohio State University. Available at: https://www.mat.uc.pt/~gil/downloads/IntroPhoto.pdf (Accessed: 26 April 2025).

Shaw, I.G.R. (2013) ‘Predator empire: The geopolitics of US drone warfare’, *Geopolitics*, 18(3), pp. 536–559. Available at: https://doi.org/10.1080/14650045.2012.749241.

Siddi, F. (2025) *Making Flow – Interview with director Gints Zilbalodis — blender.org*. Available at: https://www.blender.org/user-stories/making-flow-an-interview-with-director-gints-zilbalodis/ (Accessed: 22 June 2025).

Skrzypietz, T. (2012) *Unmanned Aircraft Systems for civilian Missions md4-1000/ © microdrones GmbH*, *Perception*. Available at: https://www.bigs-potsdam.org/app/uploads/2020/06/PolicyPaper-No.1_Civil-Use-of-UAS_Bildschirmversion-interaktiv.pdf (Accessed: 24 April 2025).

Spreafico, A. *et al.* (2021) ‘The ipad pro built-in lidar sensor: 3D rapid mapping tests and quality assessment’, in *International Archives of the Photogrammetry, Remote Sensing and Spatial Information Sciences - ISPRS Archives*. International Society for Photogrammetry and Remote Sensing, pp. 63–69. Available at: https://doi.org/10.5194/isprs-archives-XLIII-B1-2021-63-2021.

Thompson, M.M. and Mikhail, E.M. (1976) ‘Automation in Photogrammetry: Recent Developments and Applications (1972–1976)’, *Photogrammetric Engineering and Remote Sensing*, 42, pp. 329–329–336.

Vacca, G., Dessì, A. and Sacco, A. (2017) ‘The use of nadir and oblique UAV images for building knowledge’, *ISPRS International Journal of Geo-Information*, 6(12). Available at: https://doi.org/10.3390/ijgi6120393.

Vetrivel, A. *et al.* (2015) ‘Identification of damage in buildings based on gaps in 3D point clouds from very high resolution oblique airborne images’, *ISPRS Journal of Photogrammetry and Remote Sensing*, 105, pp. 61–78. Available at: https://doi.org/10.1016/j.isprsjprs.2015.03.016.

Vetrivel, A. *et al.* (2018) ‘Disaster damage detection through synergistic use of deep learning and 3D point cloud features derived from very high resolution oblique aerial images, and multiple-kernel-learning’, *ISPRS Journal of Photogrammetry and Remote Sensing*, 140, pp. 45–59. Available at: https://doi.org/10.1016/j.isprsjprs.2017.03.001.

Wade, N.J. (1987) *On the late invention of the stereoscope*, *Perception*. Available at: https://doi.org/10.1068/p160785.

Wehr, A. and Lohr, U. (1999) 'Airborne laser scanning-an introduction and overview', *ISPRS Journal of Photogrammetry & Remote Sensing*, 54(2–3), pp. 68–82. Available at: https://doi.org/10.1016/S0924-2716(99)00011-8.

Wu, B. *et al.* (2018) 'Integration of aerial oblique imagery and terrestrial imagery for optimized 3D modeling in urban areas', *ISPRS Journal of Photogrammetry and Remote Sensing*, 139, pp. 119–132. Available at: https://doi.org/10.1016/j.isprsjprs.2018.03.004.

Yucel, B., Liu, J. and Alathamneh, S. (2024) 'A Comparative Analysis of Point Clouds Acquired from UAV Photogrammetry and UAV-based LiDAR in Built Environment', in. EasyChair, pp. 584–574. Available at: https://doi.org/10.29007/hr8w.

Zhang, C., Wang, F., *et al.* (2023) 'Automated UAV image-to-BIM registration for building façade inspection using improved generalised Hough transform', *Automation in Construction*, 153. Available at: https://doi.org/10.1016/j.autcon.2023.104957.

Zhang, C., Zou, Y., *et al.* (2023) 'Thermal-textured BIM generation for building energy audit with UAV image fusion and histogram-based enhancement', *Energy and Buildings*, 301. Available at: https://doi.org/10.1016/j.enbuild.2023.113710.